Silverman, Sean M., Pathological Mechanisms of Retinal Ischemia/Reperfusion Injury and Potential Targets of Neuroprotection. Doctor of Philosophy (Visual Sciences), November, 2015, 123pp., 23 illustrations, bibliography, 206 titles.

Neurodegenerative diseases trigger a cascade of pathological mediators including significant accumulation of reactive oxygen species (ROS) and chronic neuroinflammation resulting in widespread neuronal loss. We can effectively mimic these changes in a mouse model of retinal ischemia/reperfusion (I/R) injury. Herein we demonstrate retinal I/R leads to chronic upregulation of C1q expression accompanied by similar long-term activation of microglia and astrocytes, as well as a significant increase in retinal ROS. These changes resulted in morphological and functional degeneration. In addition, we identified the neuroprotective potential of modulating changes in C1q and superoxide by genetic and pharmacological methods. In the retina I/R injury resulted in significant increases in C1q expression, glial activation and cell density by day 3 compared to controls. These changes continued to increase and were sustained through our entire 28 day time course. Similar effects from injury were observed in the superior colliculus (SC), one of the primary visual centers in the brain of rodents. Surprisingly, hemispheres corresponding to both injured and noninjured eyes displayed signs of chronic neuroinflammation by day 21. Using the chemilluminescent compound L-012 we demonstrated a novel method for non-invasive *in vivo* detection of superoxide in the eye as early as 24 hours post injury. These findings were confirmed with dihydroethidium (DHE) in the retina. Our previous work has characterized inner retinal thinning, loss of retinal ganglion cells

(RGCs), and suppression of b-wave amplitudes due to I/R injury. Using *C1qa*-deficient mice, we show complete morphological protection and ablation of reactive microgliosis. However, astrocytes were unaffected by deletion of *C1q*, and retinal function was only partially preserved. Two superoxide inhibitors, Apocynin and Tempol, significantly reduced L-012 chemilluminescence 24 and 48 hours after injury. Further, Apocynin treatment completely protected against morphological degeneration in the retina and significantly rescued functional deficits. In conclusion, this study demonstrates the therapeutic potential of modulating either C1q or superoxide for neuroprotection following injury or diseases where they are implicated in pathological loss.

PATHOLOGICAL MECHANISMS OF RETINAL ISCHEMIA/REPERFUSION INJURY AND POTENTIAL TARGETS OF NEUROPROTECTION

Sean M. Silverman, B.S.

APPROVED:

_____

Abbot F. Clark, PhD, Major Professor

_____

Iok-Hou Pang, PhD, Committee Member

_____

Raghu Krishnamoorthy, PhD, Committee Member

_____

Weiming Mao, PhD, Committee Member

_____

Harlan Jones, PhD, University Member

_____

Abbot F. Clark, Director, North Texas Eye Research Institute

_____

Meharvan Singh, PhD, Dean, Graduate School of Biomedical Sciences

PATHOLOGICAL MECHANISMS OF RETINAL ISCHEMIA/REPERFUSION INJURY AND POTENTIAL TARGETS OF NEUROPROTECTION

DISSERTATION

Presented to the Graduate Council of the

Graduate School of Biomedical Sciences

University of North Texas Health Science Center at Fort Worth

In Partial Fulfillment of the Requirements

For the Degree of

DOCTOR OF PHILOSOPHY

By

Sean M. Silverman, B.S.

Fort Worth, Texas

November 2015

ACKNOWLEDGEMENTS

First and foremost I would like to express my deepest gratitude to my mentor Dr. Abe Clark. Without your support, insight, patience, and belief in me none of this would have been possible. It has been a long and at times difficult journey through my doctoral program. At times I questioned or doubted my ability to complete my doctoral training, and you were always there for reassurance. I can only hope to attain the levels of success you have reached in your scientific career, but more importantly I hope maintain the same family-centered values I see you uphold during my own professional development. I could not have found a better mentor in every sense of the word, and I will never forget everything I have learned under your guidance.

I also express my thanks to Dr. Iok-Hou Pang, who has served as a co-mentor to me the last couple years. You have held me to the highest standards and allowed me the freedom to design and conduct many these studies with seemingly absolute trust in my knowledge and skill. Special thanks to my advisory committee members Drs. Raghu Krishnamoorthy, Weiming Mao, Harlan Jones, and especially the late Robert Wordinger for their advice and guidance through each step of the doctoral training process.

I would also like to take time to thank past and current lab members who have provided their knowledge and advice that helped shaped my development behind the bench. Dr. Byung-Jin Kim for his teachings in attention to detail, animal procedure, and most importantly learning the balance between critiquing and being overly critical. Dr. Yang Liu for her expertise in teaching *in vivo* animal protocols, assistance in the L-012 studies, and overall scientific intellect. Dr. Colleen McDowell for her early training and knowledge in mouse procedures and genetics. Drs.

Tasneem Sharma and Ankur Jain for their scientific discussions and insight, and entertainment and friendship both inside and outside the lab. Special thanks to Drs. Yong Park and Morgan Brooks for all the time and late nights spent in the library from studying to core exams to writing the dissertation. Without you guys as support along the entire way graduate school would not have been the same experience.

Last but certainly not least, I wish to thank my family and friends. My deepest appreciation goes to my loving and understanding wife Laura. You were always by my side for the entirety of my PhD training, despite the pressure and hardship the program placed on our relationship over the years. To my parents and Chad, thank you for always believing in me to finish and constantly asking for updates, even though you often had no idea what I was talking about. Thank you to Sarah and Joe, for all your encouragement and prayers along the way. And finally, thank you to Matt C., Jeremy F., Matt D., Jake K., Scott, Mark M., and all the other guys who helped me maintain my sanity and enjoy some much needed time out of lab. You will all be missed as I move on to the next stage of my career.

TABLE OF CONTENTS

Page

LIST OF ILLUSTRATIONS

CHAPTER I

CHAPTER II

CHAPTER III

CHAPTER IV

CHAPTER I

INTRODUCTION

Ischemia in the CNS and retina

According to the Centers for Disease Control (CDC), in 2008 stroke was the fourth leading cause of death in the United States and a leading cause of disability. Cost of care associated with stroke survivors has reached nearly $20 billion per year. Stroke, or ischemic attacks, is the lack of adequate blood flow to a tissue resulting in deprivation of oxygen and metabolic substrates, energy depletion, and ultimately causing cell and tissue death. Leading risk factors associated with stroke include age, comorbidities, and lifestyle choices including lack of physical activity, weight management, diet, and smoking (Goldstein et al. 2011).

The metabolic demands of the retina are among the highest of any tissue within the body, receiving blood from both the choriocapillaris which feeds the outer retina and the central retinal artery (CRA) for the inner neural layers (Kaur et al. 2008). Occlusion of a terminal artery such as the CRA in a complex highly vascularized tissue like the retina results in progressive and permanent damage. As such the degree of damage is dependent on the time and severity of the obstruction. These changes are mediated by a cascade of biological factors (Figure 1) including but not limited to excess ion influx, excitatory neurotransmitter release, free radical formation, and inflammation (D'Onofrio and Koeberle 2013; Osborne et al. 2004). Retinal ischemia is a characteristic of several clinical disorders including ischemic optic neuropathy, carotid occlusive disorders, retinopathy of prematurity, diabetic retinopathy, and glaucoma (D'Onofrio and Koeberle 2013).

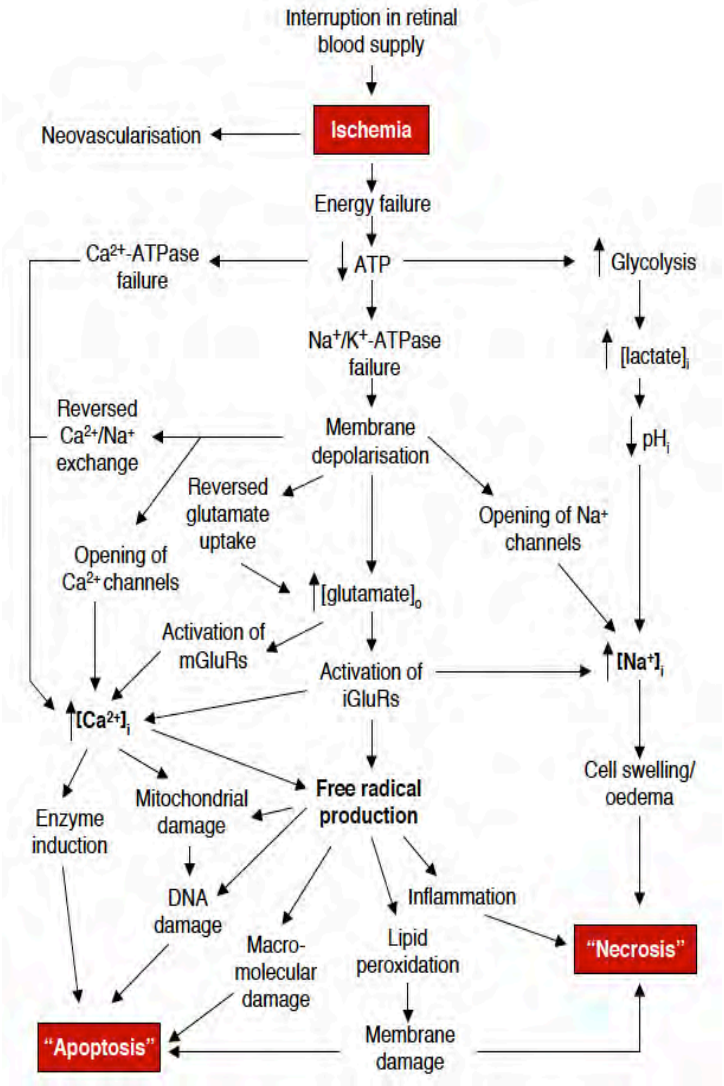

Figure 1. Mediators of ischemic pathology. Ischemia and reperfusion injury results in a cascade of biological events each resulting in a progressive downstream change with an end result of apoptosis or necrosis of the affected tissue. **Adopted from Obsborne et al. 2004.**

Animal Models of Retinal Ischemia

Several models of retinal ischemia have been developed for purposes of clinical disease modeling for the aforementioned conditions. While a wide host of species have been used for *in*

vivo and *ex vivo* ischemia/reperfusion (I/R), small rodents including rats and mice, are the preferred modeling system due to the similarity of their vasculature pattern with higher primates and humans (Minhas et al. 2012). In addition, inbred mice are genetically homogenous and are routinely genetically modified using transgenic technologies to overexpress or remove genes of interest, on top of the fact they share a genetic similarity to humans (Traystman 2003). Likewise, a variety of approaches for occlusion have been described using methodologies of elevating intraocular pressure (IOP), ligation of arteries, photocoagulation, and constriction using endothelin-1 (Block et al. 1992; Buchi et al. 1994; Takei et al. 1993). However, the high IOP model appears to be the most commonly used method.

The high IOP model, first described in 1952 by Smith and Baird (Smith and Baird 1952), is accomplished through the cannulation of the anterior chamber connected to an elevated pressure reservoir. The addition of liquid to the chamber increases the IOP above systolic blood pressure to match that of the pressure height of the reservoir, causing compression of the vasculature in the optic disc cutting off blood supply to the inner retina (Osborne et al. 2004). Earlier work has identified time dependent changes associated with retinal ischemia, suggesting at least 25 minutes is necessary for permanent loss of visual function, 35 minutes for immunologic response, and 45 minutes for histo-pathological changes (Foulds and Johnson 1974; Osborne and Larsen 1996; Selles-Navarro et al. 1996). Pathological effects of this model are manifested both histologically and physiologically in the inner retina. This is evidenced by significant thinning of the inner plexiform (IPL) and inner nuclear (INL) layers, loss of ganglion cells (RGCs), and reduced electroretinography (ERG) b-wave amplitude and latency (Kim et al. 2013). Additionally, there are a host of changes in gene expression that accompany and likely induce the observed pathologies including an upregulation in inflammatory and immune

response, eye development, cell-cell signaling, and cell death and apoptotic genes (Kim et al. 2013). Furthermore, loss of RGCs following injury results in detrimental changes at their post-synaptic termination sites in the visual centers of the brain (Figure 2), specifically in the superficial layers of the superior colliculus (SC) and lateral geniculate nucleus (LGN) in the mouse (Kim et al; unpublished). This leads to loss of relay neurons, defects in anterograde transport, and decreased innervation (Aviles-Trigueros et al. 2003; Ito et al. 2009; Mayor-Torroglosa et al. 2005).

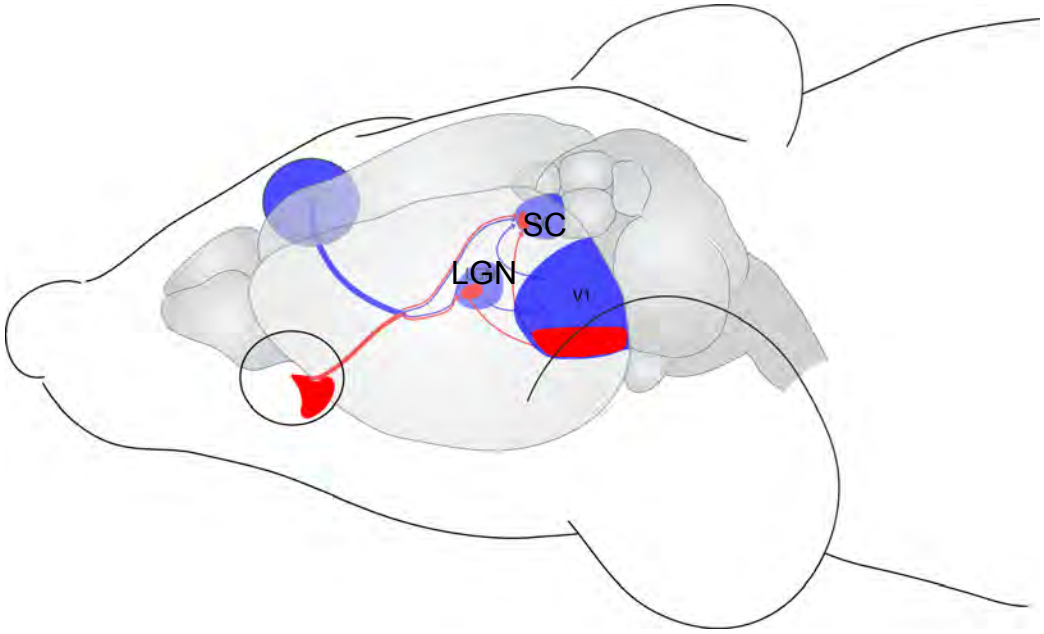

Figure 2. The retinogeniculate pathway in the rodent. Retinal ganglion cell axons exit the eye through the optic nerve converging with axons from the contralateral eye at the optic chiasm. The majority of axons will cross over at the chiasm and project to their post-synaptic targets at the SC or LGN in the contralateral side of the brain, which will further relay visual information to the primary visual cortex (V1). **Modified from Wilks et al. 2013.**

Neuroinflammation

It was once believed that the CNS, including the eye, was immunoprivileged due to the inability of circulating immune cells to penetrate the blood-brain (BBB) and blood-retinal barrier (BRB). However, cytokines such as TNFα and IL-6 have been observed to be actively transported across the BBB (Lyman et al. 2014). There also exists specialized resident immune response cells, including astrocytes and microglia collectively termed the glia (Figure 3). These cells play critical roles not only during an inflammatory response in their activated state, but also actively maintain homeostasis in a resting cell state. Neuroinflammation is often viewed as a double-edged sword contributing to both beneficial and detrimental effects on biological processes occurring in the CNS. An acute response is designed to remove harmful pathogens and cellular debris in order to protect cells and tissues (Saijo and Glass 2011). However, a chronic response has been associated with several neurodegenerative diseases such as Alzheimer's disease (AD), Amoyotrophic Lateral Sclerosis (ALS), and glaucoma, and is implicated in the progression of pathology and neuronal loss in these disorders (Harvey and Durant 2014; Soto and Howell 2014).

Microglia are derived from hematopoietic stem cells in the extra-embryonic yolk sac, sharing a myeloid lineage and requiring many of the same transcription factors for differentiation as tissue macrophages (Ginhoux et al. 2010). As such, they are classified as and express the macrophage-specific markers CD11b, CD14, and F4/80 (Saijo and Glass 2011). In their resting state, microglial processes are constantly in motion surveying the surrounding tissue of the CNS (Nimmerjahn et al. 2005). This resting phenotype can be identified experimentally by their ramified morphology.

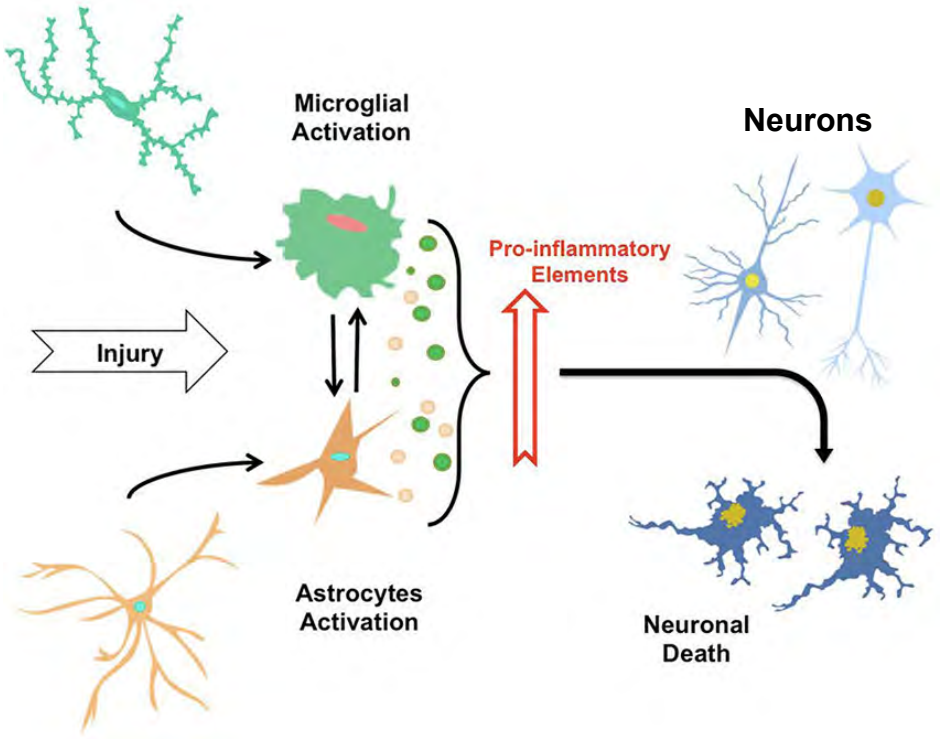

Figure 3. The basics of the neuroinflammatory response. An injury or stimulus to tissue in the CNS leads to morphological changes associated with activation of astrocytes and microglia. After which, there is a dramatic increase in production pro-inflammatory factors, amongst other biological processes, all resulting in cell death. **Modified from (Morales et al. 2014)**

In the presence of a stimulus microglia transition into an activated state, changing from a ramified to an amoeboid morphology and exhibit characteristics of their macrophage lineage. In this activated state, microglia actively phagocytose surrounding cells, produce pro-inflammatory cytokines and neurotrophic factors, and undergo active proliferation (Davalos et al. 2005; Glass et al. 2010). Recent studies have also demonstrated a role for microglial synaptic engulfment in the removal of unnecessary connections during development of the retinogeniculate system (Schafer et al. 2012).

Astrocytes differ from microglia in that they make direct contact with the neurons, blood vessels, and other glial cells, provide metabolic support, modulate synaptic activity, and maintain the blood-brain barrier (Harvey and Durant 2014). This close relationship in the CNS makes astrocytes essential for development and survival. Complete elimination of astrocytes unsurprisingly is embryonic lethal in mice (Delaney et al. 1996). Like microglia, astrocytes have a key role in controlling the extent of damage and aiding in the repair and recovery process. To a certain extent, astrocytes are thought to reduce pathology in disorders such as AD and Parkinson disease (PD) (Pekny et al. 2014). Activated astrocytes, termed reactive astrogliosis, are often identified experimentally through increased expression of their intermediate filament (IF) proteins glial fibrillary acidic protein (GFAP) and vimentin, and hypertrophy of their cellular processes (Hol and Pekny 2015). Additionally, gene profiling studies have identified a dramatic shift in gene expression clusters between resting and reactive astrocytes. While singularly termed reactive astrocytes, these astrocytes are in fact a heterogeneous population of cells, demonstrating varying reactions to different insults (Anderson et al. 2014; Zamanian et al. 2012). The most notable and permanent result from reactive gliosis is formation of glial scarring. Scars represent complex intertwinement of newly proliferated astrocytic processes resulting in permanent tissue reorganization (Wanner et al. 2013).

Complement and C1q

The complement cascade consists of over 30 cytoplasmic and membrane-associated proteins, which can be activated through three independent pathways: the classical, alternative, or lectin, which proceed through a series of sequential proteolytic cleavages (Figure 4). Activation of complement components can initiate inflammation, leukocyte migration, and

phagocytosis of debris and cells (Mastellos et al. 2004). While the liver acts as the main site of compelement biosynthesis, several studies indicate local production of the full range of complement proteins, receptors, and inhibitors in the CNS. Neurons, astrocytes, microglia, and oligodendrocytes all have the capacity to synthesize complement proteins (Barnum 1995; Gasque et al. 2000; Levi-Strauss and Mallat 1987; Thomas et al. 2000). C1q, the initiating protein of the classical complement cascade, is a large complex comprised of six A, six B, and six C chains. Each chain contains a globular region at the carboxyl terminal, and a collagen-like stem region at the amino-terminal (Kishore and Reid 2000). C1q is best known for its ability to identify and bind structures such as IgG, IgM, phosphatidylserine, and C-reactive protein (CRP) via its globular (gC1q) domain (Kouser et al. 2015).

However, recent evidence demonstrates classical complement proteins contribute to various neurodegenerative and age-related diseases, in tissues once considered immunoprivileged (Bonifati and Kishore 2007; Ricklin et al. 2010; Ricklin and Lambris 2007). C1q deposits have been observed in *post mortem* brain samples in areas of primary pathology, with mRNA expression levels increased up to 80-fold in comparison to age-matched controls (Singhrao et al. 1999; Walker and McGeer 1992; Yasojima et al. 1999). A role for C1q was recently discovered in the developing mouse retinogeniculate system. In the dorsal lateral geniculate nucleus (dLGN), C1q colocalized with markers of immature synapses, and either *C1qa* or *C3*-deficiency resulted in retention of overlapping inappropriate connections (Fourgeaud and Boulanger 2007; Stevens et al. 2007). Interestingly, these excessive excitatory synaptic connections are associated with increased epileptogenesis compared with WT mice (Brennan et al. 2012; Chu et al. 2010). Furthermore, C1q expression increased more than 300-fold during

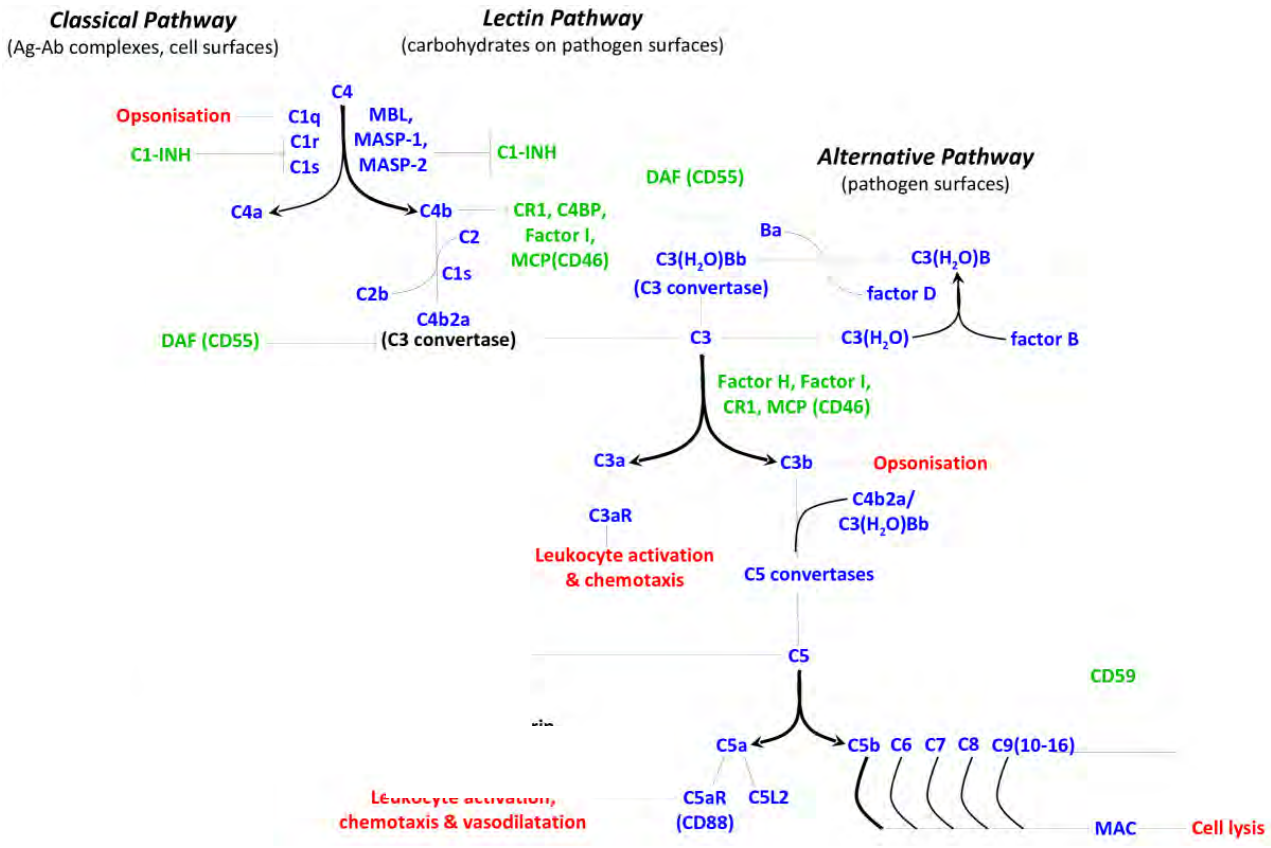

Figure 4. Diagram of the complement cascade. Depiction of the three independent pathways involved in complement activation, including initiating proteins, sites of cleavage for downstream activation, endogenous inhibitors (green) essential for pathway regulation, and the functional activation steps (red). **Modified from (Brennan et al. 2012).**

normal brain aging in the mouse, and *C1qa*-deficiency reduced levels of age-related cognitive and memory decline (Stephan et al. 2013).

Reactive Oxygen Species

Increased generation of free radicals leading to oxidative stress represents one of the earliest responses of cells upon reperfusion of blood flow following an ischemic attack

(Kuriyama et al. 2001; Love 1999). Despite the endogenous mechanisms designed to eliminate reactive oxygen species (ROS) and reactive nitrogen species (RNS) (Figure 5), injury such as ischemia overwhelms the neutralizing enzymes and scavenger molecules ultimately leading to DNA damage and apoptosis (Bonne et al. 1998; Manzanero et al. 2013; Osborne et al. 2004). The mitochondria are an important source of free radicals, wherein the reduction of oxygen in the electron transport chain results in formation of the superoxide anion ($O^{\bullet}_2{}^{-}$).

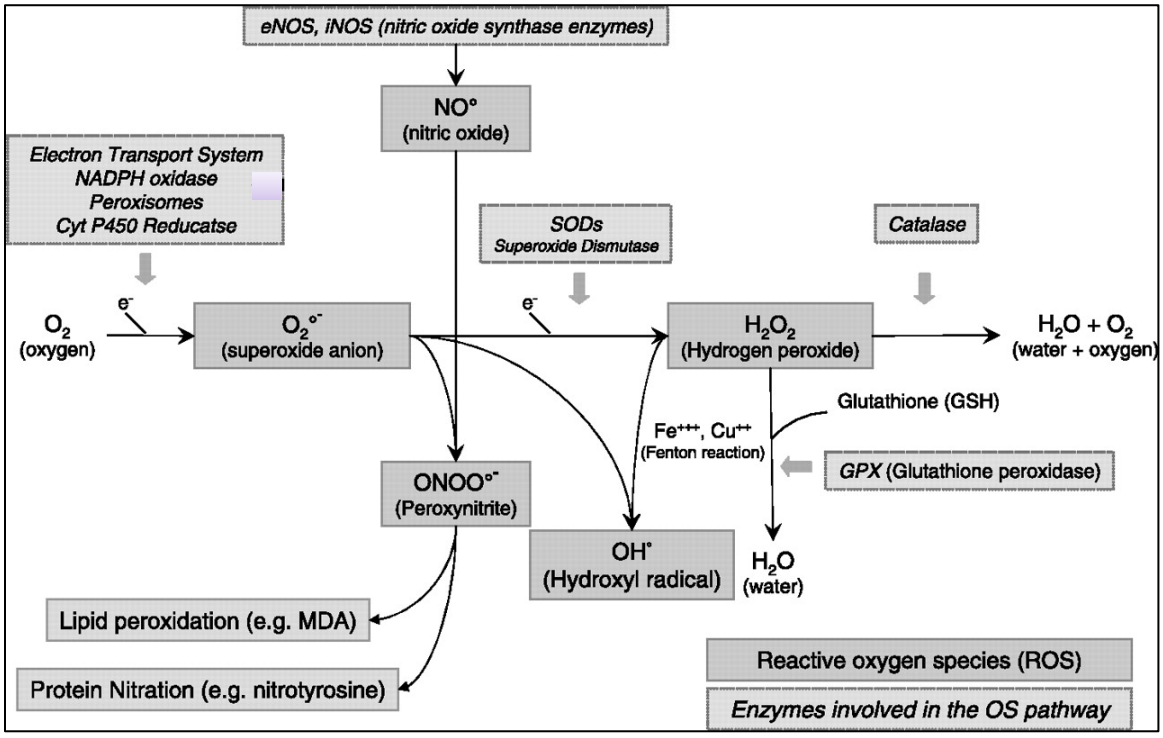

Figure 5. Generation of reactive oxygen species. The superoxide free radical is highly unstable and is rapidly converted to reactive oxygen or reactive nitrogen species by endogenous enzymes. Defense peroxidases present in cells are capable of reducing these species into reusable molecules by the cells. **Modified from (Djamali 2007).**

The instability of superoxide allows for the rapid conversion to other ROS or RNS such as hydroxyl free radical ($OH^{\bullet}$), hydrogen peroxide (H_2O_2), or peroxynitrite ($ONOO^-$) (Murphy

2009). Therefore, superoxide represents a prime therapeutic target when the intrinsic antioxidant enzymes including superoxide dismutase (SOD) or glutathione can no longer manage the increased free radical load. Several antioxidant treatment approaches either pre or post-injury have been utilized with relative success in animal models of cerebral and retinal ischemia (Bonne et al. 1998; Hein et al. 2012; Olmez and Ozyurt 2012; Osborne et al. 2004; Roh et al. 2011).

Despite the advances made in understanding and protecting against oxidative damage, there still exists an unmet need for the ability non-invasively to detect *in vivo* expression levels of ROS following ischemic events. Traditional measures rely fluorescent probes, electron spin resonance, and markers of oxidation, nitration, lipid peroxidation, and DNA damage. All of which are performed *in vitro* or in *ex vivo* tissue samples requiring sacrifice of animals (Halliwell and Whiteman 2004). This challenge is being approached with the use of ROS-oxidizing probes that produce a chemiluminescent signal upon reaction. Compounds such as luminol, lucigenin, and MCLA have been successfully demonstrated to detect free radical formation in the mouse (Gross et al. 2009; Lee et al. 2007). L-012 (8-amino-5-chloro-7-phenylpyrrido [3,4-*d*]-pyridazine-1, 4 (2*H,*3*H*) dione), a derivative of luminol, is emerging as a more viable candidate as it shows greater sensitivity, it is non-toxic, and is not subject to redox cycling (Kielland et al. 2009; Nishinaka et al. 1993; Zielonka et al. 2013). L-012 was observed to detect significant subcutaneous changes in ROS due to stimulation with LPS, ethanol, nanoparticles, and even in the colon in a genetic mouse model of colitis (Asghar et al. 2014; Hu et al. 2015; Kielland et al. 2009; Zhou et al. 2012). These studies demonstrate the potential for *in vivo* ROS detection in animal injury models including I/R.

Hypothesis

Although several groups have used various approaches to reduce the extent of damage due to I/R injury, there remain multiple novel avenues that could be explored for development of improved neuroprotective treatment strategies. Many studies have looked at I/R in the context cerebral or cardiovascular animal models, and retinal I/R appears to reproduce these findings. Our study will present a unique neuroprotective outlook targeting neuroinflammation and ROS following an ischemic insult in the eye. Only one previous study has evaluated the effect of retinal ischemia in complement knockout mice, for which they demonstrated a delay in damage to the RGC somas and axons in the absence of *C3* (Kuehn et al. 2008). Yet, this study failed to comprehensively examine the vast changes that occur in the retina and extensions of the visual system due to ischemic injury. $C3^{-/-}$ mice were only evaluated for prevention of death in RGCs, a characterization of glaucomatous injury while retinal ischemia destroys additional neurons in the inner retina. Additionally, our work will be the first to demonstrate the potential for *in* vivo ROS detection in the eye of a live mouse. Our goal is to temporally demonstrate and visualize the changes in expression of C1q and ROS, and to better understand their pathological mechanisms in the visual system after retinal I/R. In addition, we will identify neuroprotection mediated through the disruption of these signaling pathways. Based on this we have developed a central hypothesis that **retinal ischemia/reperfusion (I/R) injury upregulates expression of C1q and ROS, which mediate pathological changes in the retina and SC.**

Specific Aims and Rationale

Specific Aim 1: Determine the pathogenic role of C1q in the visual pathway of mice receiving retinal I/R injury

1A Determine temporal expression patterns of C1q in the retina and SC following I/R injury, as well as identify cells responsible for their expression.

1B Measure I/R induced loss of visual function and signaling in *C1qa*$^{+/+}$ (WT), *C1qa*$^{+/-}$, and *C1qa*$^{-/-}$ mice

1C Quantify degree of neurodegeneration in WT, *C1qa*$^{+/-}$, and *C1qa*$^{-/-}$ mice retinas and SC

Rationale: Increased expression of complement proteins has been observed in several neurodegenerative disorders both experimentally and clinically, including Alzheimer's disease, Multiple Sclerosis, Parkinson's, and glaucoma (Bonifati and Kishore 2007; Ren and Danias 2010). Ischemic injury has been shown to upregulate several key complement proteins, such as C1q, C3, C5, and the terminal membrane attack complex (MAC) (Arumugam et al. 2004; D'Ambrosio et al. 2001). Our work will focus on the changes in spatiotemporal activity of C1q following retinal ischemia in neurons at local (retina) and distal (SC) tissue sites affected by injury over an extended time course. In the retina, several different cells are known to synthesize C1q, including microglia, astrocytes, Müller cells, and even RGCs (Barnum 1995; Stasi et al. 2006). Therefore, it is important to establish which cells are primarily responsible for upregulation of C1q production, and the effect that increased C1q levels have on the activity of these cells. This can best be demonstrated using fluorescent *in situ* hybridization (FISH), colocalizing *C1qa* mRNA with cell-specific markers. We aim to identify the classical complement cascade as the primary effector pathway following retinal I/R through elimination of initiating protein, C1q. To establish the role of C1q in ischemic neurodegeneration, we will perform retinal I/R in WT and *C1qa*-deficient mice. Through the use of histological, physiological, and molecular techniques, we will identify how the failure of C1q to initiate activation of the classical cascade protects the visual system from the known degenerative effects

of retinal I/R (Kim et al. 2013). Additionally, by examining the retina and SC, we can begin to understand the deficits a chronic neuroinflammatory response in the retina has on post-synaptic targets in the brain.

Specific Aim 2: Determine changes in ROS levels following retinal I/R and protection of the retina through their abatement

2A Use L-012 to observe and quantify *in vivo* expression of ROS in the mouse eye following retinal I/R injury

2B *Post mortem* confirmation and characterization of ROS in the retina

2C Assess L-012 luminescence and protection in the retina from the use of compounds that reduce ROS

Rationale: ROS accumulation occurs within hours after ischemic injury following the release of excess glutamate (Bonne et al. 1998; Olmez and Ozyurt 2012; Osborne et al. 2004). However, despite the wealth of research on ROS, there remains an unmet need for a non-invasive *in vivo* method of detection. Current assays are performed either *in vitro* or using *post mortem* tissue, requiring sacrifice of experimental animals. L-012, a derivative of the chemiluminescent compound luminol, has recently been shown to quantify superoxide and other ROS in the mouse abdomen following LPS-mediated inflammation (Kielland et al. 2009; Zhou et al. 2012). Our aim is to further determine whether L-012 is a viable tool for *in vivo* detection of ROS, and be the first to identify this potential in a retinal I/R injury model. To confirm L-012 accurately detects ROS, *ex vivo* assays will be used allowing us to identify more specifically which free radicals are being detected. Lastly, to establish L-012 as a diagnostic measurement of ROS, we

will administer superoxide-reducing compounds together with L-012, showing a positive correlation between reduction of ROS and chemiluminescent intensity. Apocynin (4-hydroxy-3-methoxy-acetophenone) a selective inhibitor of NADPH oxidase (NOX) and Tempol (4-hydroxy-2,2,6,6-tetramethylpiperidine-1-oxyl) a superoxide dismutase (SOD) mimetic will both be tested. After evaluating the ability of L-012 to detect changes in ROS, we further aim to identify whether reduction of ROS mediates protection of the retina through a variety of histological, functional, and biochemical assays.

Significance

Following ischemic conditions and reperfusion in the CNS, there is a significant and detrimental upregulation of free radical formation and neuroinflammation that occurs from minutes to days after reperfusion. Our study will be the first to correlate the temporal changes in ROS production and neuroinflammation occurring after a transient retinal I/R injury. This will allow us to elucidate the mechanisms responsible for early changes in the tissue post injury, and those causing long-term irreversible damage. Following this approach, we will use different methods of controlling these mediators of degeneration to determine if they demonstrate neuroprotective effects to the visual system. Finally, this study will establish a novel method for detecting changes in ROS production in the retina. Our work will be the first to utilize the chemiluminescent probe L-012 for the detection of ROS following retinal I/R, fulfilling the unmet need for a non-invasive *in vivo* application, thereby saving investigators time, animals, and money.

References

Anderson MA, Ao Y, Sofroniew MV. 2014. Heterogeneity of reactive astrocytes. Neurosci Lett 565:23-9.

Arumugam TV, Shiels IA, Woodruff TM, Granger DN, Taylor SM. 2004. The role of the complement system in ischemia-reperfusion injury. Shock 21:401-9.

Asghar MN, Emani R, Alam C, Helenius TO, Gronroos TJ, Sareila O, Din MU, Holmdahl R, Hanninen A, Toivola DM. 2014. In vivo imaging of reactive oxygen and nitrogen species in murine colitis. Inflamm Bowel Dis 20:1435-47.

Aviles-Trigueros M, Mayor-Torroglosa S, Garcia-Aviles A, Lafuente MP, Rodriguez ME, Miralles de Imperial J, Villegas-Perez MP, Vidal-Sanz M. 2003. Transient ischemia of the retina results in massive degeneration of the retinotectal projection: long-term neuroprotection with brimonidine. Exp Neurol 184:767-77.

Barnum SR. 1995. Complement biosynthesis in the central nervous system. Crit Rev Oral Biol Med 6:132-46.

Block F, Schwarz M, Sontag KH. 1992. Retinal ischemia induced by occlusion of both common carotid arteries in rats as demonstrated by electroretinography. Neurosci Lett 144:124-6.

Bonifati DM, Kishore U. 2007. Role of complement in neurodegeneration and neuroinflammation. Mol Immunol 44:999-1010.

Bonne C, Muller A, Villain M. 1998. Free radicals in retinal ischemia. Gen Pharmacol 30:275-80.

Brennan FH, Anderson AJ, Taylor SM, Woodruff TM, Ruitenberg MJ. 2012. Complement activation in the injured central nervous system: another dual-edged sword? J Neuroinflammation 9:137.

Buchi ER, Lam TT, Suvaizdis I, Tso MO. 1994. Injuries induced by diffuse photodynamic action in retina and choroid of albino rats. Morphologic study of an experimental model. Retina 14:370-8.

Chu Y, Jin X, Parada I, Pesic A, Stevens B, Barres B, Prince DA. 2010. Enhanced synaptic connectivity and epilepsy in C1q knockout mice. Proc Natl Acad Sci U S A 107:7975-80.

D'Ambrosio AL, Pinsky DJ, Connolly ES. 2001. The role of the complement cascade in ischemia/reperfusion injury: implications for neuroprotection. Mol Med 7:367-82.

D'Onofrio PM, Koeberle PD. 2013. What can we learn about stroke from retinal ischemia models? Acta Pharmacol Sin 34:91-103.

Davalos D, Grutzendler J, Yang G, Kim JV, Zuo Y, Jung S, Littman DR, Dustin ML, Gan WB. 2005. ATP mediates rapid microglial response to local brain injury in vivo. Nat Neurosci 8:752-8.

Delaney CL, Brenner M, Messing A. 1996. Conditional ablation of cerebellar astrocytes in postnatal transgenic mice. J Neurosci 16:6908-18.

Djamali A. 2007. Oxidative stress as a common pathway to chronic tubulointerstitial injury in kidney allografts. Am J Physiol Renal Physiol 293:F445-55.

Foulds WS, Johnson NF. 1974. Rabbit electroretinogram during recovery from induced ischaemia. Trans Ophthalmol Soc U K 94:383-93.

Fourgeaud L, Boulanger LM. 2007. Synapse remodeling, compliments of the complement system. Cell 131:1034-6.

Gasque P, Dean YD, McGreal EP, VanBeek J, Morgan BP. 2000. Complement components of the innate immune system in health and disease in the CNS. Immunopharmacology 49:171-86.
Ginhoux F, Greter M, Leboeuf M, Nandi S, See P, Gokhan S, Mehler MF, Conway SJ, Ng LG, Stanley ER and others. 2010. Fate mapping analysis reveals that adult microglia derive from primitive macrophages. Science 330:841-5.
Glass CK, Saijo K, Winner B, Marchetto MC, Gage FH. 2010. Mechanisms underlying inflammation in neurodegeneration. Cell 140:918-34.
Goldstein LB, Bushnell CD, Adams RJ, Appel LJ, Braun LT, Chaturvedi S, Creager MA, Culebras A, Eckel RH, Hart RG and others. 2011. Guidelines for the primary prevention of stroke: a guideline for healthcare professionals from the American Heart Association/American Stroke Association. Stroke 42:517-84.
Gross S, Gammon ST, Moss BL, Rauch D, Harding J, Heinecke JW, Ratner L, Piwnica-Worms D. 2009. Bioluminescence imaging of myeloperoxidase activity in vivo. Nat Med 15:455-61.
Halliwell B, Whiteman M. 2004. Measuring reactive species and oxidative damage in vivo and in cell culture: how should you do it and what do the results mean? Br J Pharmacol 142:231-55.
Harvey H, Durant S. 2014. The role of glial cells and the complement system in retinal diseases and Alzheimer's disease: common neural degeneration mechanisms. Exp Brain Res 232:3363-77.
Hein TW, Ren Y, Potts LB, Yuan Z, Kuo E, Rosa RH, Jr., Kuo L. 2012. Acute retinal ischemia inhibits endothelium-dependent nitric oxide-mediated dilation of retinal arterioles via enhanced superoxide production. Invest Ophthalmol Vis Sci 53:30-6.
Hol EM, Pekny M. 2015. Glial fibrillary acidic protein (GFAP) and the astrocyte intermediate filament system in diseases of the central nervous system. Curr Opin Cell Biol 32:121-30.
Hu XT, Ding C, Zhou N, Xu C. 2015. Quercetin protects gastric epithelial cell from oxidative damage in vitro and in vivo. Eur J Pharmacol 754:115-24.
Ito Y, Shimazawa M, Chen YN, Tsuruma K, Yamashima T, Araie M, Hara H. 2009. Morphological changes in the visual pathway induced by experimental glaucoma in Japanese monkeys. Exp Eye Res 89:246-55.
Kaur C, Foulds WS, Ling EA. 2008. Blood-retinal barrier in hypoxic ischaemic conditions: basic concepts, clinical features and management. Prog Retin Eye Res 27:622-47.
Kielland A, Blom T, Nandakumar KS, Holmdahl R, Blomhoff R, Carlsen H. 2009. In vivo imaging of reactive oxygen and nitrogen species in inflammation using the luminescent probe L-012. Free Radic Biol Med 47:760-6.
Kim BJ, Braun TA, Wordinger RJ, Clark AF. 2013. Progressive morphological changes and impaired retinal function associated with temporal regulation of gene expression after retinal ischemia/reperfusion injury in mice. Mol Neurodegener 8:21.
Kishore U, Reid KB. 2000. C1q: structure, function, and receptors. Immunopharmacology 49:159-70.
Kouser L, Madhukaran SP, Shastri A, Saraon A, Ferluga J, Al-Mozaini M, Kishore U. 2015. Emerging and Novel Functions of Complement Protein C1q. Front Immunol 6:317.
Kuehn MH, Kim CY, Jiang B, Dumitrescu AV, Kwon YH. 2008. Disruption of the complement cascade delays retinal ganglion cell death following retinal ischemia-reperfusion. Exp Eye Res 87:89-95.

Kuriyama H, Waki M, Nakagawa M, Tsuda M. 2001. Involvement of oxygen free radicals in experimental retinal ischemia and the selective vulnerability of retinal damage. Ophthalmic Res 33:196-202.
Lee D, Khaja S, Velasquez-Castano JC, Dasari M, Sun C, Petros J, Taylor WR, Murthy N. 2007. In vivo imaging of hydrogen peroxide with chemiluminescent nanoparticles. Nat Mater 6:765-9.
Levi-Strauss M, Mallat M. 1987. Primary cultures of murine astrocytes produce C3 and factor B, two components of the alternative pathway of complement activation. J Immunol 139:2361-6.
Love S. 1999. Oxidative stress in brain ischemia. Brain Pathol 9:119-31.
Lyman M, Lloyd DG, Ji X, Vizcaychipi MP, Ma D. 2014. Neuroinflammation: the role and consequences. Neurosci Res 79:1-12.
Manzanero S, Santro T, Arumugam TV. 2013. Neuronal oxidative stress in acute ischemic stroke: sources and contribution to cell injury. Neurochem Int 62:712-8.
Mastellos D, Morikis D, Strey C, Holland MC, Lambris JD. 2004. From atoms to systems: a cross-disciplinary approach to complement-mediated functions. Mol Immunol 41:153-64.
Mayor-Torroglosa S, De la Villa P, Rodriguez ME, Lopez-Herrera MP, Aviles-Trigueros M, Garcia-Aviles A, de Imperial JM, Villegas-Perez MP, Vidal-Sanz M. 2005. Ischemia results 3 months later in altered ERG, degeneration of inner layers, and deafferented tectum: neuroprotection with brimonidine. Invest Ophthalmol Vis Sci 46:3825-35.
Minhas G, Morishita R, Anand A. 2012. Preclinical models to investigate retinal ischemia: advances and drawbacks. Front Neurol 3:75.
Morales I, Guzman-Martinez L, Cerda-Troncoso C, Farias GA, Maccioni RB. 2014. Neuroinflammation in the pathogenesis of Alzheimer's disease. A rational framework for the search of novel therapeutic approaches. Front Cell Neurosci 8:112.
Murphy MP. 2009. How mitochondria produce reactive oxygen species. Biochem J 417:1-13.
Nimmerjahn A, Kirchhoff F, Helmchen F. 2005. Resting microglial cells are highly dynamic surveillants of brain parenchyma in vivo. Science 308:1314-8.
Nishinaka Y, Aramaki Y, Yoshida H, Masuya H, Sugawara T, Ichimori Y. 1993. A new sensitive chemiluminescence probe, L-012, for measuring the production of superoxide anion by cells. Biochem Biophys Res Commun 193:554-9.
Olmez I, Ozyurt H. 2012. Reactive oxygen species and ischemic cerebrovascular disease. Neurochem Int 60:208-12.
Osborne NN, Casson RJ, Wood JP, Chidlow G, Graham M, Melena J. 2004. Retinal ischemia: mechanisms of damage and potential therapeutic strategies. Prog Retin Eye Res 23:91-147.
Osborne NN, Larsen AK. 1996. Antigens associated with specific retinal cells are affected by ischaemia caused by raised intraocular pressure: effect of glutamate antagonists. Neurochem Int 29:263-70.
Pekny M, Wilhelmsson U, Pekna M. 2014. The dual role of astrocyte activation and reactive gliosis. Neurosci Lett 565:30-8.
Ren L, Danias J. 2010. A role for complement in glaucoma? Adv Exp Med Biol 703:95-104.
Ricklin D, Hajishengallis G, Yang K, Lambris JD. 2010. Complement: a key system for immune surveillance and homeostasis. Nat Immunol 11:785-97.
Ricklin D, Lambris JD. 2007. Complement-targeted therapeutics. Nat Biotechnol 25:1265-75.

Roh MI, Murakami Y, Thanos A, Vavvas DG, Miller JW. 2011. Edaravone, an ROS scavenger, ameliorates photoreceptor cell death after experimental retinal detachment. Invest Ophthalmol Vis Sci 52:3825-31.
Saijo K, Glass CK. 2011. Microglial cell origin and phenotypes in health and disease. Nat Rev Immunol 11:775-87.
Schafer DP, Lehrman EK, Kautzman AG, Koyama R, Mardinly AR, Yamasaki R, Ransohoff RM, Greenberg ME, Barres BA, Stevens B. 2012. Microglia sculpt postnatal neural circuits in an activity and complement-dependent manner. Neuron 74:691-705.
Selles-Navarro I, Villegas-Perez MP, Salvador-Silva M, Ruiz-Gomez JM, Vidal-Sanz M. 1996. Retinal ganglion cell death after different transient periods of pressure-induced ischemia and survival intervals. A quantitative in vivo study. Invest Ophthalmol Vis Sci 37:2002-14.
Singhrao SK, Neal JW, Morgan BP, Gasque P. 1999. Increased complement biosynthesis by microglia and complement activation on neurons in Huntington's disease. Exp Neurol 159:362-76.
Smith GG, Baird CD. 1952. Survival time of retinal cells when deprived of their blood supply by increased intraocular pressure. Am J Ophthalmol 35:133-6.
Soto I, Howell GR. 2014. The complex role of neuroinflammation in glaucoma. Cold Spring Harb Perspect Med 4.
Stasi K, Nagel D, Yang X, Wang RF, Ren L, Podos SM, Mittag T, Danias J. 2006. Complement component 1Q (C1Q) upregulation in retina of murine, primate, and human glaucomatous eyes. Invest Ophthalmol Vis Sci 47:1024-9.
Stephan AH, Madison DV, Mateos JM, Fraser DA, Lovelett EA, Coutellier L, Kim L, Tsai HH, Huang EJ, Rowitch DH and others. 2013. A dramatic increase of C1q protein in the CNS during normal aging. J Neurosci 33:13460-74.
Stevens B, Allen NJ, Vazquez LE, Howell GR, Christopherson KS, Nouri N, Micheva KD, Mehalow AK, Huberman AD, Stafford B and others. 2007. The classical complement cascade mediates CNS synapse elimination. Cell 131:1164-78.
Takei K, Sato T, Nonoyama T, Miyauchi T, Goto K, Hommura S. 1993. A new model of transient complete obstruction of retinal vessels induced by endothelin-1 injection into the posterior vitreous body in rabbits. Graefes Arch Clin Exp Ophthalmol 231:476-81.
Thomas A, Gasque P, Vaudry D, Gonzalez B, Fontaine M. 2000. Expression of a complete and functional complement system by human neuronal cells in vitro. Int Immunol 12:1015-23.
Traystman RJ. 2003. Animal models of focal and global cerebral ischemia. ILAR J 44:85-95.
Walker DG, McGeer PL. 1992. Complement gene expression in human brain: comparison between normal and Alzheimer disease cases. Brain Res Mol Brain Res 14:109-16.
Wanner IB, Anderson MA, Song B, Levine J, Fernandez A, Gray-Thompson Z, Ao Y, Sofroniew MV. 2013. Glial scar borders are formed by newly proliferated, elongated astrocytes that interact to corral inflammatory and fibrotic cells via STAT3-dependent mechanisms after spinal cord injury. J Neurosci 33:12870-86.
Yasojima K, Schwab C, McGeer EG, McGeer PL. 1999. Up-regulated production and activation of the complement system in Alzheimer's disease brain. Am J Pathol 154:927-36.
Zamanian JL, Xu L, Foo LC, Nouri N, Zhou L, Giffard RG, Barres BA. 2012. Genomic analysis of reactive astrogliosis. J Neurosci 32:6391-410.

Zhou J, Tsai YT, Weng H, Tang L. 2012. Noninvasive assessment of localized inflammatory responses. Free Radic Biol Med 52:218-26.
Zielonka J, Lambeth JD, Kalyanaraman B. 2013. On the use of L-012, a luminol-based chemiluminescent probe, for detecting superoxide and identifying inhibitors of NADPH oxidase: a reevaluation. Free Radic Biol Med 65:1310-4.

CHAPTER II

C1Q PROPAGATES MICROGLIAL ACTIVATION AND NEURODEGENERATION IN THE VISUAL AXIS FOLLOWING RETINAL ISCHEMIA/REPERFUSION INJURY

Sean M Silverman, Byung-Jin Kim, Gareth R. Howell, Joselyn Miller,

Simon W.M. John, Robert J. Wordinger, and Abbot F. Clark

Abstract

Background: C1q represents the initiating protein of the classical complement cascade, however recent findings indicate pathway independent roles such as developmental pruning of retinal ganglion cell (RGC) axons. Furthermore, chronic neuroinflammation, including increased expression of C1q and activation of microglia and astrocytes, appears to be a common finding among many neurodegenerative disease models. Here we compare the effects of a retinal ischemia/reperfusion (I/R) injury on glial activation and neurodegeneration in wild type (WT) and *C1qa*-deficient mice in the retina and superior colliculus (SC). Retinal I/R was induced in mice through elevation of intraocular pressure to 120 mmHg for 60 min followed by reperfusion. Glial cell activation and population changes were assessed using immunofluorescence. Neuroprotection was determined using histological measurements of retinal layer thickness, RGC counts, and visual function by flash electroretinography (ERG).

Results: Retinal I/R injury significantly upregulated C1q expression in the retina as early as 72 hours and within 7 days in the superficial SC, and was sustained as long as 28 days. Accompanying increased C1q expression was activation of microglia and astrocytes as well as a significantly increased glial population density observed in the retina and SC. Microglial activation and changes in density were completely ablated in *C1qa*-deficient mice, interestingly however there was no effect on astrocytes. Furthermore, loss of *C1qa* significantly rescued I/R-induced loss of RGCs and protected against retinal layer thinning in comparison to WT mice. ERG assessment revealed early preservation of b-wave amplitude deficits from retinal I/R injury due to *C1qa*-deficiency that was lost by day 28.

Conclusions: Our results for the first time demonstrate the spatiotemporal changes in the neuroinflammatory response following retinal I/R injury at both local and distal sites of injury. In

addition, we have shown a role for C1q as a primary mediator of microglial activation and pathological damage. This suggests developmental mechanisms of C1q may be re-engaged during injury response, modulation of which may be beneficial for neuroprotection.

Key Words:

Retinal ischemia; C1q; neuroinflammation; microglia; astrocytes; neuroprotection

Background

Ischemic events in the CNS cause traumatic tissue damage and irreversible loss of neurons present at the ischemic core and surrounding areas. The metabolic demands of the retina are among the highest of any tissue within the body, receiving a dual blood supply from both the choriocapillaris and the central retinal artery (CRA) [1]. Thus, transient retinal ischemic attacks often cause permanent tissue damage resulting in irreversible vision loss. Following ischemic events in the CNS, there is a significant and detrimental upregulation of biological factors including excess ion influx, excitatory neurotransmitter release, free radical formation, and inflammation [2-4]. Neuroinflammation represents a complex event in the CNS, often involving an activated cellular response from resident immune cells. Once activated, these glial cells secrete a host of pro-inflammatory proteins propagating a chronic cascade of apoptotic or phagocytic events [4].

Two of the primary effector cells during neuroinflammation are the microglia and astrocytes. Both constitute two of the resident immune cells of visual system (the retina, optic nerve, and visual centers of the brain). Astrocytes maintain direct contact with the neurons, blood vessels, and other glial cells, providing metabolic support, modulating synaptic activity, and maintenance of the blood-brain barrier [5, 6]. Whereas microglia represent the resident monocytes of the CNS, derived from myeloid precursors, their processes are constantly in a mode of surveillance in addition to their antigen-presenting and phagocytic capabilities [7, 8, 5, 9]. However, when glia are stimulated by disease or injury, they shift to an activation state leading to the production of inflammatory mediators such as chemokines, cytokines, and complement proteins [10-12]. Activation of brain astrocytes causes a dramatic upregulation by at

least four-fold of over 260 genes compared to of quiescent astrocytes, with some genes showing 10 to 100-fold changes in expression [13]. Accompanying these changes, reactive astrocytes undergo cell proliferation, somatic hypertrophy, overlapping of processes, and scar formation [14]. Likewise, microglia when stimulated undergo a well-defined morphological transformation, proliferation and migration, as well as expression of adhesion molecules [15]. These reactive microglia are often observed at sites of pathology in several neurodegenerative diseases including Alzheimer's disease and glaucoma [16]. Coupled with their secretion of pro-inflammatory factors such as TNF-a, IL-1B, and C1q, microglia are an ideal candidate as a primary mediator of damage.

C1q, the initiating protein of the classical Complement cascade, is a large complex comprised of six A, six B, and six C chains. Each chain contains a globular region at the carboxyl terminus and a collagen-like stem region at the amino-terminus [17]. Traditionally, the classical pathway is the antibody-dependent activation of complement, as C1q is known to bind to the surface of foreign substances and antibodies [18]. However, recent evidence demonstrates classical complement proteins contribute to various neurodegenerative and age-related diseases [19]. In the DBA/2J model of spontaneous glaucoma, *C1qa* was among the earliest differentially regulated genes not only in the retina, but also at the optic nerve head (ONH) prior to onset of a glaucomatous phenotype [20, 21]. More surprisingly, during development in the dorsal lateral geniculate nucleus (dLGN), C1q colocalized with either immature pre- or post-synaptic markers, and loss of C1q resulted in retention of overlapping inappropriate connections [21, 22]. Furthermore, C1q expression in certain areas of the brain was found to increase more than 300-fold during normal aging in the mouse. Reduced levels of cognitive and memory decline were observed in aged *C1qa*-knockout mice compared with age-matched WT mice [23].

In this study, we demonstrate the impact of the neuroinflammatory response following an ischemic event in the retina. We identify time dependent increases in cell density and morphological changes of both astrocytes and microglia not only in the retina but also the superior colliculus, a primary termination site of retinal ganglion cell (RGC) axons exiting the retina. Furthermore, we observed significant increases in C1q expression correlating with reactive gliosis. Our goal was to determine if genetic deletion of *C1qa* could morphologically and functionally protect the retina from pathological changes resulting from retinal I/R injury that we have previously characterized [24], as well as attenuate the activation of glial cells in the visual system.

Results

C1q expression in the visual axis following I/R injury

Upregulation of complement expression is well documented following ischemic injury; however, temporal changes in C1q expression after retinal I/R have not been identified. In eyes receiving one hour of ischemic injury, C1q was observed primarily in the inner neural retina, extending from the nerve fiber layer (NFL) through the inner plexiform layer (IPL) (Figures 1A-F). Quantification of fluorescence intensity revealed statistically significant differences ($p<0.01$) between ischemic ($5.5x10^6 \pm 9.6x10^5$) and uninjured eyes ($2.4x10^6 \pm 3.5x10^5$) as early as day 3, and remaining elevated as long as 28 days ($5.3x10^6 \pm 5.1x10^5$) (Figure 1G), with a peak intensity 21 days post injury. No changes were observed between uninjured eyes of experimental mice and retinas from naïve mice.

The primary termination site of a majority of RGC axons in rodents is in the superficial superior colliculus (SC) of the optic tectum. A significant majority of the axons have been shown to cross the optic chiasm and synapse with the hemisphere of the SC contralateral to the eye from which the axons are projecting [25]. The RGC axons synapse with relay neurons in order to transfer signals from the retina to the visual cortex. We investigated if a local injury to the retina caused changes in C1q expression at these distal sites in the visual axis. On day 7 the SC hemisphere contralateral to the ischemic eye, henceforth labeled the ischemic hemisphere, displayed a significant elevation in C1q expression in comparison to the ipsilateral hemisphere receiving input from the uninjured retina (Figure 2A). As in the retina, we quantified differences in C1q expression between the two hemispheres over the 28 day time course. Significant elevation of C1q expression was observed as early as day 7 between hemispheres corresponding to the ischemic ($1.8x10^7 \pm 2.4x10^6$) and uninjured ($8.5x10^6 \pm 1.9x10^6$) eyes. Interestingly by day 14, although not significant, an increase in C1q was apparent in the ipsilateral hemisphere. A second wave of C1q activity was observed at day 28 post injury, displaying peak intensity in both hemispheres. Expression of C1q in the SC on day 28 was statistically significant ($p<0.05$) compared to all earlier time points in both hemispheres (Figure 2B).

Ischemic induced gliosis in the visual axis

Ischemic attacks in the CNS are known to activate resident glial cells [4] therefore, we investigated spatiotemporal changes in both microglia and astrocytes (including Müller cells in the retina) accompanying upregulation of C1q following retinal I/R injury. As expected, representative images (Figures 3A-D) display morphological differences identified between glial

cells of uninjured (Figures 3A&C) and ischemic (Figures 3B&D) retinas. Activation of microglia is commonly identified by a change from a resting ramified morphology (Figure 3i) to an amoeboid shape (Figure 3ii). Activation of astrocytes and Müller cells is observed by upregulation of GFAP expression, as well as outward extension of their processes from the astrocyte somas and Müller cell end feet into the GCL (Figure 3D). Quantification of these changes revealed significant differences in $Iba1^+$ retinal microglia density in ischemic eyes as early as day 3 (1.73% ± 0.35,) and sustained over the entire 28 day time course ($p<0.01$) compared to contralateral retinas (0.61% ± 0.13) (Figure 3E). While GFAP does not distinguish between astrocytes and Müller cells, there was an observed increase in $GFAP^+$ cells beginning on day 3; however, a statistically significant difference between ischemic (3.56% ± 0.34) and uninjured eyes (1.74% ± 0.34) was not seen until day 7 (Figure 3F). Increased density of $GFAP^+$ cells was significantly different throughout our time course ($p<0.01$), displaying a gradual increase as pathology progressed. No significant changes were observed in any glial cell type between uninjured contralateral retinas and those of naïve mice.

Given that the upregulation of C1q in the retina was accompanied by reactive gliosis, we reasoned a similar effect would be observed in the SC. Similar to our observation of retinal C1q expression, there was a marked difference in glial cell activity in the superficial layers of the SC, correlating to regions of synaptic termination sites of RGC axons (Figures 4A-D). Both astrocytes (Figures 4-B) and microglia (Figures 4C-D) were observed in a reactive morphological state in the contralateral hemispheres from ischemic eyes in comparison to the ipsilateral hemisphere as early as 7 days post injury. Cell density of both $Iba1^+$ and $GFAP^+$ cells was quantitated in a similar method to our retinal analysis. A very statistically significant ($p<0.001$) difference in microglial density between hemispheres was seen as early as day 7

(2.56% ± 0.29 compared to 1.27% ± 0.23). Density of microglia appeared to drop by day 14, and in a biphasic manner steadily returned on day 28 to peak levels observed on day 7 (Figure 4E). No significant differences were observed in astrocyte population density between contralateral and ipsilateral hemisphere measurements (Figure 4F). Interestingly, microglia and astrocyte densities in the hemispheres ipsilateral from injured eyes began significantly increasing on day 21 ($p<0.01$) for microglia and day 28 ($p<0.05$) for astroctyes (Figures 4E-F). Whereas previously significant differences between SC hemispheres could be determined in $Iba1^+$ populations, by day 21 both hemispheres were indistinguishable. Our quantification reveals concurrent and progressive increases in C1q expression and glial cell activity in both local and distal tissue sites of the visual axis following retinal I/R.

C1q mediates morphological damage in the retina

Previously we have published morphological degeneration and altered retinal gene expression resulting from retinal I/R [24]; here we employ several of those same assays to observe these changes in WT, heterozygous, or homozygous mice null for *C1qa*. Retinal I/R caused a thinning of the inner layers of the neural retina associated with a loss in the neurons residing in the GCL, IPL, and INL, the same layers in which we observed a prolonged neuroinflammatory response. However, we observed a significant protection of all of these layers in $C1qa^{+/-}$ and $C1qa^{-/-}$ mice (Figure 5A). We further quantified these findings through caliper measurements using ImageJ. Overall, we found no statistical difference between the total thickness of uninjured retinas (327.6 ± 7.9μm) compared with the ischemic retinas of $C1qa^{+/-}$ (317.0 ± 10.9μm) and $C1qa^{-/-}$ (309.5 ± 14.5μm). Furthermore, a significant difference was

quantified in both the IPL ($p<0.05$) and INL ($p<0.001$) when comparing WT and C1qa$^{-/-}$ mice (Figure 5B). Control measurements were performed in both naïve and uninjured eyes in both *C1qa* mutant genotypes for phenotypic variation, and no significant differences in individual layer or total retinal thickness were observed (data not shown). All measurements were performed under masked conditions.

In addition to deficits in retinal layer thickness, a significant loss of RGCs occured following I/R injury. Two independent methods of cell counting were utilized to assess loss of RGCs between ischemic eyes of our three genotypes. Representative images demonstrate the differences observed in the GCL of H&E stained retinas between control and ischemic retinas of WT and *C1qa*-deficient animals (Figure 6A). Cell counts revealed a statistically significant loss ($p<0.01$) in ischemic eyes of WT mice (317 ± 23 cells per mm) in comparison to their contralateral uninjured retinas (450 ± 11 cells per mm). However, no statistical differences were determined between control retinas and those from *C1qa*$^{+/-}$ and *C1qa*$^{-/-}$ mice (401 ± 31 and 394 ± 24 cells per mm, respectively) (Figure 6B). Since H&E staining is unable to differentiate between RGCs and displaced amacrine cells, the RGC-specific marker RNA-binding protein with multiple splicing (Rbpms) was used for a more accurate characterization (Figure 6C). Again, there was a significant difference ($p<0.01$) identified between control (215 ± 8 cell per mm) and ischemic retinas (151 ± 8 cells per mm) of WT mice. This difference was ablated in C1qa$^{+/-}$ ischemic eyes (172 ± 15 cell per mm), and further a significant difference was seen when ischemic eyes of WT mice were compared with those of *C1qa*$^{-/-}$ animals (198 ± 16 cells per mm, $p<0.01$) compared to WT (Figure 6D). There were no differences in RGC counts in contralateral uninjured and naïve retinas of WT and *C1qa*-deficient strains (data not shown). All counts were performed in a masked manner.

Retinal functional deficits are delayed in absence of C1qa

Along with our characterization of morphological deficits, we also used scotopic flash ERG to assess changes in retinal function in our three genetic backgrounds. Representative traces display differences in ERG b-wave amplitudes between ischemic and control eyes in WT mice (Figure 7A). An intensity of 3000mcd.s/m^2 was chosen for quantification. We observed a significant loss in b-wave amplitudes in all animals 7 days following retinal I/R ($p<0.05$-0.01). While b-wave measurements remained statistically different in WT and *C1qa*$^{+/-}$ mice ($p<0.01$) throughout our study compared to uninjured eyes, a functional rescue was seen in our complete knockouts. *C1qa*$^{-/-}$ mice were observed not only to have significantly greater ($p<0.05$) b-wave readings at day 14 compared to WT (464.3 ± 29.3μV and 324.5 ± 27.3μV, respectively), but also there was no statistical difference in comparison to control eyes. This rescue appeared to be temporary, and by the end of our time course on day 28, no discernable differences were observed in any animals receiving I/R injury (Figure 7B).

C1q-Deficiency modulates glial response in the visual axis after injury

Our studies conducted using WT mice established the extent of reactive gliosis observed through the visual axis over a 28 day time course following retinal I/R injury (Figures 3 & 4). Given our findings of protection observed in the retina, we hypothesized C1q may be responsible for the activation and density increases observed in glial cells. The same methodology was used to perform density analysis in both the retina and SC in *C1qa*-deficient mice. Initially, significant differences were observed as early as day 7 post injury, and maximum density was measured on

day 28. Therefore, we chose these two key time points for our assessment of glial density in the absence of C1q.

In the retina, unlike the changes observed in WT animals, no statistical differences in microglial density were observed between ischemic and contralateral uninjured retinas in either *C1qa*$^{+/-}$ or *C1qa*$^{-/-}$ mice at 7 and 28 days post injury (Figure 8A). In addition, injured retinas from *C1qa*-deficient mice displayed significantly decreased ($p<0.001$) microglial density when compared with WT injured retinas at early and late time points. Likewise for SC microglia, no differences were observed between hemispheres at day 7 and no significant increases in density were measured between days 7 and 28 in either of our *C1qa*-deficient mice, as was previously seen in WT mice (Figure 8C). However, a different trend was observed in astrocyte activity and density. Although no differences were observed on day 7 in both the retina and SC of *C1q*a-deficient animals, by the end of our time course, significant changes in density were determined. Retinas of *C1qa*$^{+/-}$ and *C1qa*$^{-/-}$ mice receiving I/R injury displayed statistically significant ($p<0.05$-0.01) increases in GFAP^{+} cell density ($3.02 \pm 0.34\%$ and $3.05 \pm 0.62\%$, respectively) compared to uninjured retinas (Figure 8B). Similar to our results observed in the SC of WT mice, no difference could be determined between ipsilateral and contralateral hemispheres by day 28, and there was a statistically significant increase in astrocyte density compared to day 7 ($p<0.05 – 0.01$, Figure 8D). In both the retina and the SC no differences were determined when astrocyte density in *C1qa*$^{+/-}$ mice were compared to *C1qa*$^{-/-}$ mice. Although the density of astrocytes was reduced when astrogliosis of *C1qa*-deficient mice was compared to WT, no statistical differences were observed. Taken all together, our data indicate reactive gliosis was observed in both astrocytes and microglia in the visual axis of WT animals, but *C1qa*-deficient mice had an ablated microglial response. However, while significant changes were observed in astrocyte

density following injury, this response also was dampened prior to onset of pathology in comparison to that measured in WT mice.

Discussion

Our studies have demonstrated a significant temporal increase in C1q expression that is accompanied by an increase in reactive microglial and astrocytic retinal cell density following retinal I/R injury. Further, this response is mirrored at RGC termination sites in the visual system through increased C1q expression observed in the SC. These findings agree with previous reports indicating the involvement of both the complement system and glial response to ischemic events not only in the retina, but also areas of the brain affected by I/R Injury [4, 26, 11, 27]. The absence of C1q provided retinal neuroprotection through rescue against I/R-induced retinal thinning and neuronal loss. Additionally, attenuation of the activated microglial response in the retina and SC was observed in *C1qa*-deficient animals. To our knowledge, this is the first report to identify a time-dependent neuroinflammatory response in the visual system following retinal ischemia, and to establish C1q as a primary mediator of damage.

Given the wide variety of animal models of ischemic injury (e.g. global, cardiac, cerebral, or retinal), several methods for neuroprotection have met with mixed results [28]. The retina provides a unique target for testing of neuroprotective compounds as investigators have the option of local [29-31] or systemic [32-34] delivery of therapeutic compounds or biologics. We have demonstrated significant protection against both functional and morphological deficits in the retina and SC subjected to I/R injury using the JNK inhibitor SP600125 (Kim et al, submitted for publication). Time dependent gene profiling following retinal ischemia identifies several

members of the complement family to be among the most significant changes as early as 7 days post injury [3, 35]. Previous studies identifying protection of RGCs in a *C3*-deficient mouse following retinal I/R demonstrated a delayed loss of cells after 3 weeks; however, no difference in axonal damage was seen compared with WT mice [3]. While our endpoints differed from Kuehn et al, we were able to show a significant rescue of RGCs and cells in the GCL. While there exists sufficient evidence of activation of the downstream complement cascade including C3 following retinal ischemia, our results suggest C1q may be acting in a cascade-independent role.

Activation of the complement system in the CNS during times of injury and pathogenesis has been well documented [36, 37]. Increased expression of C1q has been specifically observed to colocalize with hallmark pathological changes observed in several neurodegenerative diseases including Alzheimer's disease (AD), Parkinson's disease (PD), and glaucoma [19, 38]. Furthermore, C1q is known to directly bind to the membrane of neurons, which have a poor capacity to regulate activation of downstream complement cascade factors [39]. Our studies demonstrate significant upregulation of C1q at both local and distal sites in the visual system following I/R injury. As such, C1q has been identified as a potential prime therapeutic target. Although not indicated for treatment of chronic neurodegenerative disease, previous strategies to modulate C1q have targeted C1r/C1s, which is necessary with C1q to form the C1 complex, using recombinant C1-INH as well as soluble CR1 [40]. In animal models of brain ischemia, administration of C1-INH was observed to reduce infarct volume and neurological deficits [26, 41]. Similar to our findings of cell rescue and retinal morphology preservation, deletion of C1q has been identified as a protective mechanism in various other disease models. Recent *in vitro* data suggested C1q promoted neurite progression by modulating expression of genes necessary

for outgrowth [42]. These findings were later supported, and extended *in vivo,* demonstrating axon regeneration and improved guidance following spinal cord injury [43]. In both studies however, downstream C3 and C5 had non-growth promoting effects, suggesting distinct mechanistic roles for different complement components. AD mice deficient for *C1q* ($APPQ^{-/-}$) significantly preserved functional neurons and increased dendritic staining in the hippocampus compared to Aβ pathological (APP) mice [44]. Accumulation of C1q during normal brain aging has been implicated in cognitive decline; age-matched *C1qa*-deficient mice were observed to perform significantly better in a series of learning and memory behavioral tests compared to WT mice [23]. Further, in the DBA/2J spontaneous glaucoma model, *C1qa* was identified to be differentially expressed in the retina and ONH preceding phenotypic glaucomatous damage. Deletion of *C1qa* significantly delayed RGC axonal damage [20, 21].

In our current study, we identified for the first time a temporal response pattern for microglia and astrocyte activation in the retina and SC after retinal I/R injury. Furthermore, we demonstrated the significant increase in microglial activation and cell density resulted from accumulation of C1q in the injured tissue. In the CNS, astrocytes, microglia, and neurons have been identified as the primary producers of complement proteins [45, 38]. Our data support previous reports that disturbances to the retina from injury and inflammation results in a dynamic response of microglia, known to phagocytose dying neurons [46-48]. Evidence suggests the increased cell density may result from infiltrating microglia through compromised blood-retinal barriers [49]; however, our methodology was unable to differentiate resident and migratory microglia. Further studies utilizing fluorescently-labeled transplanted cells will be needed to identify whether our observed changes were due to infiltration, proliferation, or a combination of both. Given the implication of chronic reactive microglia in neurodegenerative disease as well

as recently discovered developmental roles [50, 51], several approaches have been made to abate microglial activation. Some methodologies such as modulation of fractalkine receptor CX_3CR1 have been met with mixed results [27], while others have effectively returned microglia to their resting quiescent state and significantly protected against microglial-mediated neurodegeneration [52, 53, 46].

Despite our *C1q*-dependent modulation of activated microglia and observed morphological protection in the retina, we were unable to totally rescue I/R induced loss of retinal function as assessed through scotopic ERG. Coinciding with this finding, mice deficient in *C1qa* displayed increased levels of GFAP similar to WT animals following retinal I/R. This supports previous results that microglia are the primary synthesizers of complement proteins, specifically C1q, leading to pathogenesis from prolonged inflammatory responses [7, 54]. This suggests following ischemic episodes in the retina, prolonged astrocyte and Müller cell activation is stimulated by proinflammatory factors different from microglia. Reactive astrogliosis is known to be triggered by cytokines such as TNFα, CNTF, IL-1β, and IL-6 [55]. Further, these macroglial cells facilitate a certain degree of neurodegeneration independent from microglia, which may explain our findings of visual deficits. Similar to microglia, astrocytes posses the machinery for synaptic engulfment; however, this appears to be a C1q-independent process [56]. GFAP represents an essential intermediate filament of reactive astrocytes necessary for the many astroglial functions following injury [57]. Genetic deletion of GFAP has provided mixed results of protection and exacerbation that appear to be dependent on the nature of the injury [58-60]. Astrocytes, both neighboring and tissue-specific, have been identified as a highly heterogenous population in their gene expression patterns, morphology, and proliferative responses to injury, which are further complicated by their proximity to the trauma [14].

Therefore, it is likely that retinal astrocytes would react much differently to retinal I/R injury compared to astrocytes in the SC. Therefore, we find it unsurprising that elimination of *C1q* had no significant effect on controlling this gliotic response in the SC. Combinatorial therapies have had recent success in improving pathological endpoints in models of injury and disease [61]; therefore, targeting multiple proinflammatory proteins may further suppress the glial response to I/R injury, thereby providing enhanced neuroprotection.

Conclusions

In summary, we have identified the temporal expression patterns of C1q and the subsequent glial response to retinal I/R injury to neurons in both the retina and SC. Further, we demonstrate that retinal I/R induced neurodegeneration requires of C1q expression, and that genetic ablation of C1q completely inhibited the reactive microglial response leading to preservation of retinal morphology and significant protection of RGCs compared with WT mice. However, retinal astrocyte and Müller cell activation persisted causing only transient functional retinal protection. Our results are the first to identify a relationship between C1q and microglia following retinal injury, which we hypothesize to be directly related to their roles in synaptic maturation in the developing visual system [51]. Greater understanding of the similarities between developmental and neurodegenerative signaling represents exciting new avenues for therapeutic intervention and enhanced neuroprotection of the visual axis

Methods

Animals

Male and female transgenic mice for *C1qa* (B6.129P2-C1qa<tmlmjw>/Sj) that were backcrossed 10 generations onto a pure C57BL/6J background and (hereafter referred to as either *C1qa*$^{+/-}$ or *C1qa*$^{-/-}$), were generously provided from the Simon John laboratory (Jackson Laboratory; Bar Harbor, ME). Female C57BL/6J (Jackson Laboratory) and male and female *C1qa* mice (3-4 months of age) were used for transient retinal I/R studies. Animals were maintained in 12-h:12-h/light:dark cycle. All studies and animal care were performed as approved by the Institutional Animal Care and Use Committee at the University of North Texas Health Science Center and followed the Association for Research in Vision and Ophthalmology (ARVO) Statement for the Use of Animals in Ophthalmic and Vision Research.

Retinal I/R

Retinal I/R was induced as described previously [24]. Briefly, mice were anesthetized with a ketamine/xylazine/acepromazine cocktail (100/10/3 mg/kg), and the left eyes were dilated (2.5% Phenylephrine HCl; Paragon BioTeck, Inc.) followed by cannulation of the anterior chamber with a 30-gauge needle connected to a reservoir containing sterile PBS. The reservoir was elevated to generate an intraocular pressure of 120 mmHg for 1 h to induce retinal ischemia. Afterwards, the cannula was removed and blood was allowed to naturally reperfuse the retina.

Body temperature was maintained on a digitally controlled heating pad for the duration of the procedure and recovery.

Immunofluorescence of the retina and SC

Following euthanasia of the mice, ischemic and contralateral control eyes were gently removed and placed in 4% paraformaldehyde (PFA) for 4h followed by a 20% sucrose solution overnight. Whole brains were delicately excised and fixed in 4% PFA for 6-8h, after which a 3mm region was cut to include the superior colliculus (SC) using a mouse brain block. The SC-containing brain section was also embedded in a 20% sucrose solution overnight. Eyes and brains were placed in Tissue-Tek OCT compound (Sakura Finetek USA, Torrance, CA) and frozen over dry ice before being stored at -80°C. Eyes and brains were frozen sectioned at 12mm and placed on Superfrost Plus slides (VWR, Radnor PA). Slides were triple washed in PBS, blocked and permeabilized for 1h in blocking buffer (PBS with 10% fetal bovine serum and 0.15% Triton X-100) before incubation with primary antibodies overnight at 4°C. For retinal sections anti-C1q (A201, 1:1000) from Quidel (San Diego, CA) was used; however excessive non-specific labeling was observed with this antibody in SC sections, therefore anti-C1q (ab182451, 1:200) from Abcam (Cambridge, MA) developed by Stephan and colleagues was used [23]. For glial cell analysis, antibodies to Iba1 (019-19741, 1:500) from Wako Chemicals (Richmond, VA) and GFAP (ab7260, 1:300) from Abcam were used. RGC counts were performed using the specific marker Rbpms (GTX118619; 1:200) from GeneTex (Irvine, CA). Tissues were incubated in secondary antibodies conjugated with Alexaflour 488 and Alexaflour 592 (1:250; Invitrogen/Molecular Probes, Carlsbad, CA) for 1h at room temperature. Slides were

mounted with cover slips using ProlongGold anti-fade reagent with DAPI (Molecular Probes, Life Technologies, Grand Island, NY). Images were taken using a Nikon Eclipse Ti inverted microscope (Nikon; Melville, NY) and CRi Nuance FX multispectral imaging system (Caliper Life Sciences; Hopkinton, MA). Autofluorescence was subtracted using Nuance 3.0 software (Caliper Life Sciences).

Cell density analysis

Density of astrocytes, Müller cells and microglia in the retina and SC was calculated using thresholding analysis in ImageJ (NIH; Bethesda, MD). Briefly, images were separated by color channel into an RGB stack, after which a region of interest (ROI) was drawn around the entire tissue. A threshold was set to positively select only $Iba1^+$ or $GFAP^+$ cells, and this threshold was maintained for all images analyzed. Measurements were limited to this threshold and the percent area occupied of the section was determined. A minimum of three images per section and three slides spanning the depth of the tissue were analyzed and averaged per animal. A similar methodology was used to assess fluorescence intensity of C1q in retina and SC sections.

Histological assessment of the retina

Whole globes were immersion fixed in 4% PFA overnight at 4°C, followed by paraffin processing. Eyes were sectioned at 5mm and stained with hematoxylin and eosin (H&E). Entire retinas were imaged, ora serrata to ora serrata through the optic nerve head, and thickness was

measured using calibrated calipers in ImageJ from the nerve fiber layer (NFL) through the outer nuclear layer (ONL) at two peripheral and two central locations of the retina. Three slides were selected per retina and the four cross sectional measurements from each retina were averaged together. Nuclei in the H&E ganglion cell layer (GCL), including RGCs and displaced amacrine cells, were counted from each retina and averaged.

Scotopic flash electroretinography (ERG)

All animals were dark adapted overnight; mice were anesthetized with isoflurane and connected to the HMsERG system (Ocuscience; Rolla, MO). Body temperature was maintained at 37°C. A ground electrode was placed subcutaneously by the tail and reference electrodes inserted under each eye. Silver-thread electrodes were placed across the apex of the cornea and held in place with a Gonak (Akorn; Lake Forest, IL) coated contact lens. Eyes were exposed to a series of light flashes at increasing intensities (0.1, 0.3, 1, 3, 10, and 25 cd.s/m^2). Amplitudes and implicit times of waveforms were measured and analyzed.

Statistics

Statistical analysis was performed using SigmaPlot 12 (Systat; San Jose, CA). Student's paired t-test was used to compare experimental groups within animals, ischemic versus contralateral control. One-way ANOVA was used to compare among three or more groups, such as comparing between time points for experimental groups. Holm-Sidak *post hoc* analysis was

used for multiple comparisons. All data are expressed as mean ± standard error mean (SEM), and p-values less 0.05 were considered statistically significant.

Authors' Contributions: AFC, RJW, GRH, and SWMJ conceived of the study, participated in the design and interpretation of results. SMS and BJK performed all *in vivo* procedures. SMS and JM performed immunoassays and histological assessment. SMS and AFC outlined, prepared, and edited the manuscript. All authors read an approved the final manuscript

Acknowledgements

The authors would like to thank Sandra Neubauer (histological technician, NTERI) for providing tissue sections and H&E stained slides, Neal Olarte (TCOM student, Ft Worth TX) for help in masked morphological analysis studies. Grant support generously provided by the Department of Defense (W81XWH-10-2-003), NIA Training grant (T32 AG020494), and a Sigma Xi GiAR.

Figure Legends

Figure 1. Retinal I/R injury significantly increases C1q expression in the retina.

C57BL/6J mice were subjected to unilateral I/R injury and sacrificed at the indicated time points post I/R. Contralateral control eyes **(A)** displayed basal deposits of C1q in the GCL; however, ischemic eyes **(B – F)** had significantly greater expression of C1q as early as day 3 **(B)** and sustained to the end of the time course on day 28 **(F)**. Positive labeling was only observed in the GCL and IPL. **(G)** Fluorescence intensity quantification revealed statistically significant upregulation of C1q ($p<0.01$) at all time points in ischemic versus uninjured retinas. Peak intensity in ischemic eyes was observed on day 21 post injury ($p<0.05$). Mean ± SEM, n=7 per group. **$p<0.01$ determined by student's paired t-test, #$p<0.05$ tested using One-way ANOVA followed by Holm-Sidak post test. GCL = Ganglion Cell Layer, IPL = Inner Plexiform Layer. Scale bars = 50μm

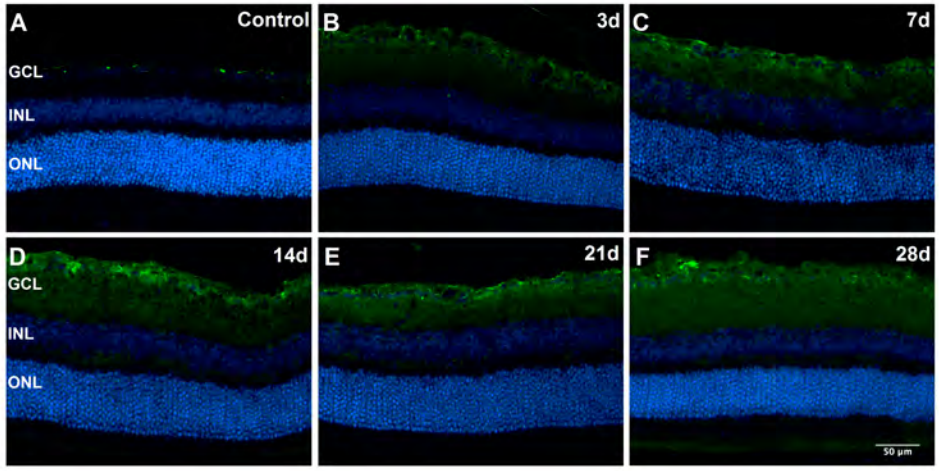
A
Control
GCL
INL
ONL
B
3d
C
7d
D
14d
GCL
INL
ONL
E
21d
F
28d
50 µm

G

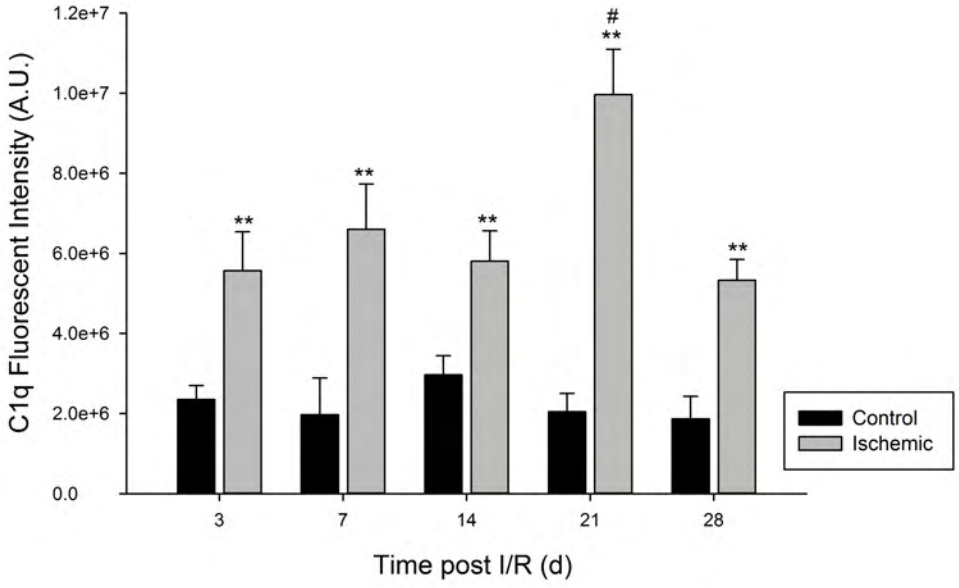
1.2e+7
1.0e+7
8.0e+6
6.0e+6
4.0e+6
2.0e+6
0.0
C1q Fluorescent Intensity (A.U.)
**
**
**
#
**
**
3
7
14
21
28
Time post I/R (d)
Control
Ischemic

Figure 2. Local ischemic injury in the retina increases expression of C1q in the superior colliculus.

(A) Representative images displaying differences in C1q expression between hemispheres of the SC 7 days following retinal I/R. Yellow outline indicates area of SC measured, scale = 20x. **(B)** Quantification of fluorescence intensity indicated significant differences between ipsilateral (uninjured) and contralateral (ischemic) hemispheres on days 7 and 28 ($p<0.01$). C1q expression was greatest on day 28 in both hemispheres of the SC, and significantly different versus all time points assessed. Mean ± SEM, n = 7 per time point. **$p<0.01$ using student's paired t-test, #$p<0.05$ ##$p<0.01$ compared across time points within a group determined via One-way ANOVA followed by Holm-Sidak post test. Scale bars = 100μm.

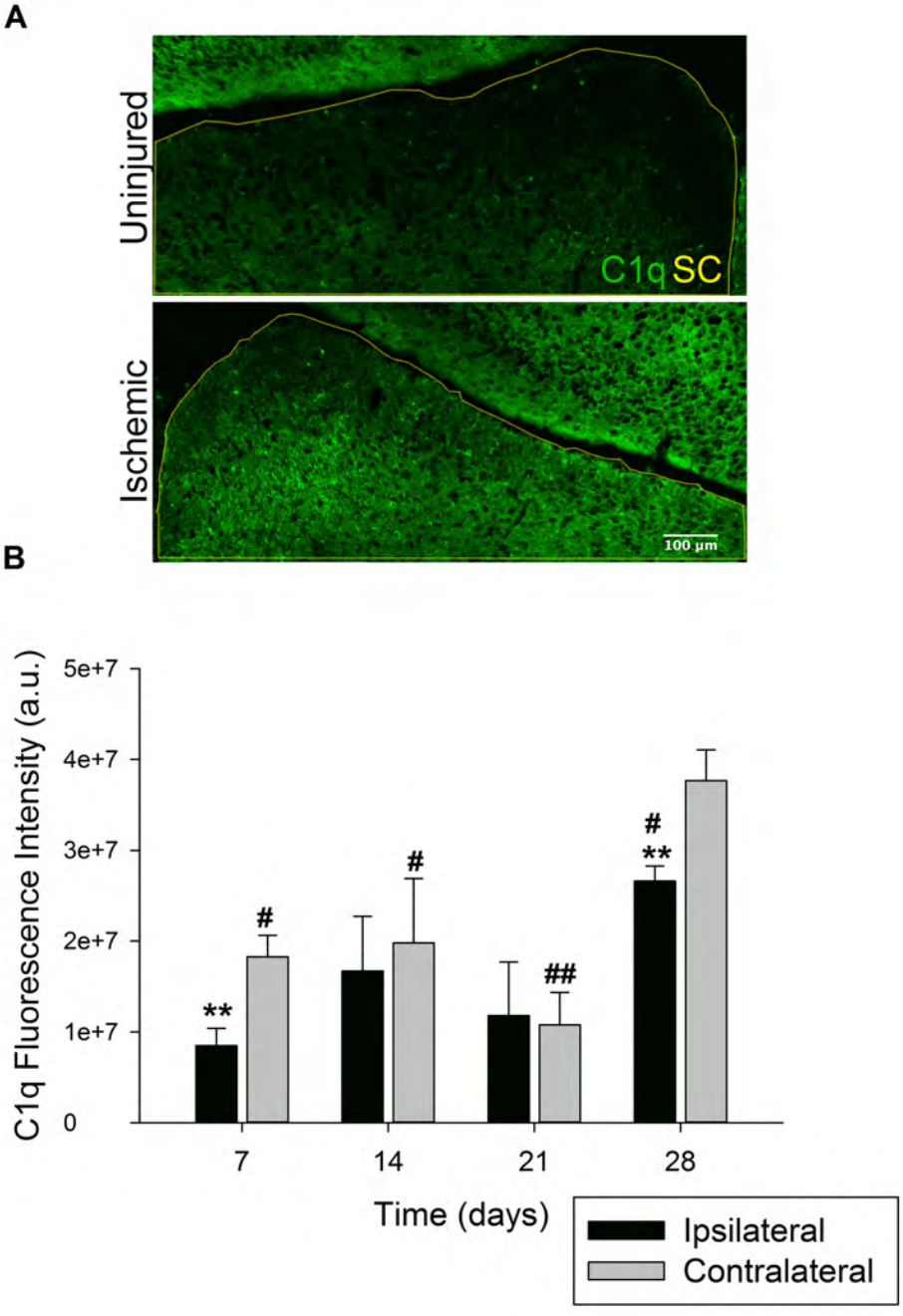
A
Uninjured
C1q SC
Ischemic
100 µm
B
C1q Fluorescence Intensity (a.u.)
5e+7
4e+7
3e+7
2e+7
1e+7
0
**
#
#
##
#
**
7
14
21
28
Time (days)
Ipsilateral
Contralateral

Figure 3. Activation and increased cell populations of macroglia and microglia in the retina post I/R.

Representative images of Iba1- and GFAP-positive cells in uninjured **(A,C)** and ischemic **(B,D)** retinas. **(A,B)** Yellow inset boxes of selected $Iba1^+$ microglia demonstrate morphological differences between senescent **(i)** and activated **(ii)** cellular states. **(C,D)** Morphological differences observed in $GFAP^+$ cells following ischemia. Astrocytes and Müller cells display elongated processes extending through the layers of the retina in addition to thickened cell bodies present in the GCL and NFL. **(E-F)** Thresholding analysis based upon percent area of retina occupied was applied to determine changes in cell density. Microglial density **(E)** was significantly increased in ischemic retinas at all time points quantified compared with uninjured controls. Density of macroglia **(F)** trended upward on day 3 and was statistically significant at all time points measured thereafter. Mean ± SEM, n = 7 per group. *$p<0.05$ **$p<0.01$ ***$p<0.001$ using students paired t-test between control and ischemic groups. GCL = Ganglion Cell layer, NFL = Nerve Fiber Layer.

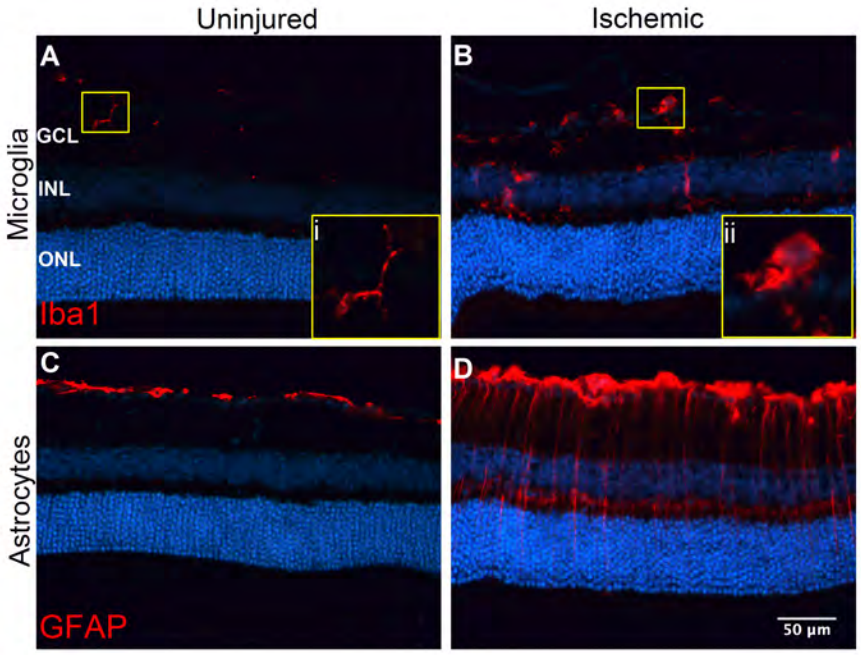
Uninjured
Ischemic
A
B
Microglia
GCL
INL
ONL
Iba1
i
ii
C
D
Astrocytes
GFAP
50 µm

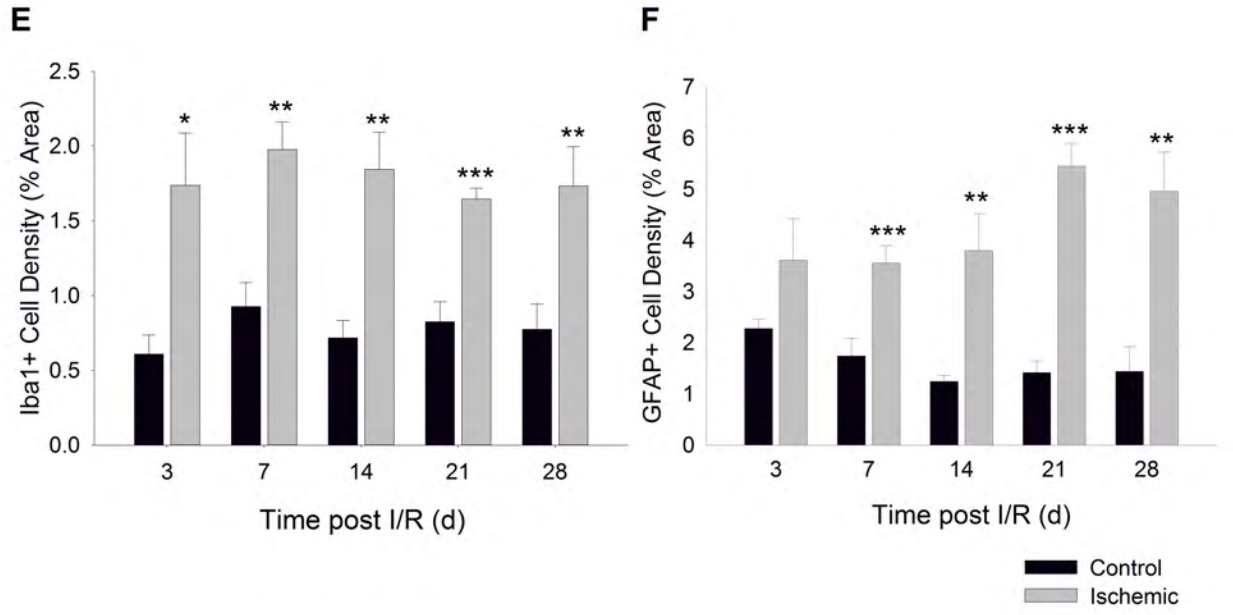
E
Iba1+ Cell Density (% Area)
2.5
2.0
1.5
1.0
0.5
0.0
*
**
**
***
**
3
7
14
21
28
Time post I/R (d)
F
GFAP+ Cell Density (% Area)
7
6
5
4
3
2
1
0
***
**
***
**
3
7
14
21
28
Time post I/R (d)
Control
Ischemic

Figure 4. Retinal I/R activates and increases glial cell populations in the SC.

Representative images demonstrate differences observed in astrocytes **(A,B)** and microglia **(C,D)** between uninjured ipsilateral and I/R-receiving contralateral hemispheres of the SC. **(E)** Quantification of microglial density was observed to be significantly different between hemispheres on days 7 and 14 ($p<0.01$) following I/R. No differences were detected between hemispheres by 21 days post injury. However, a statistically significant difference was determined in the uninjured ipsilateral hemisphere when days 21 ($p<0.01$) and 28 ($p<0.001$) were compared to earlier time points. **(F)** Density of $GFAP^+$ astrocytes was quantified; however, no significant differences could be determined between SC hemispheres at any time point following retinal I/R. However, statistical differences ($p<0.05$) were observed in both ipsilateral and contralateral hemispheres when day 28 was compared against astrocyte density on days 14 and 21. Mean ± SEM, n = 7 per group. **$p<0.01$ using students paired t-test between ipsilateral and contralateral hemispheres, #$p<0.05$ ##$p<0.01$ ###$p<0.001$ determined by One-way ANOVA followed by Holm-Sidak post test.

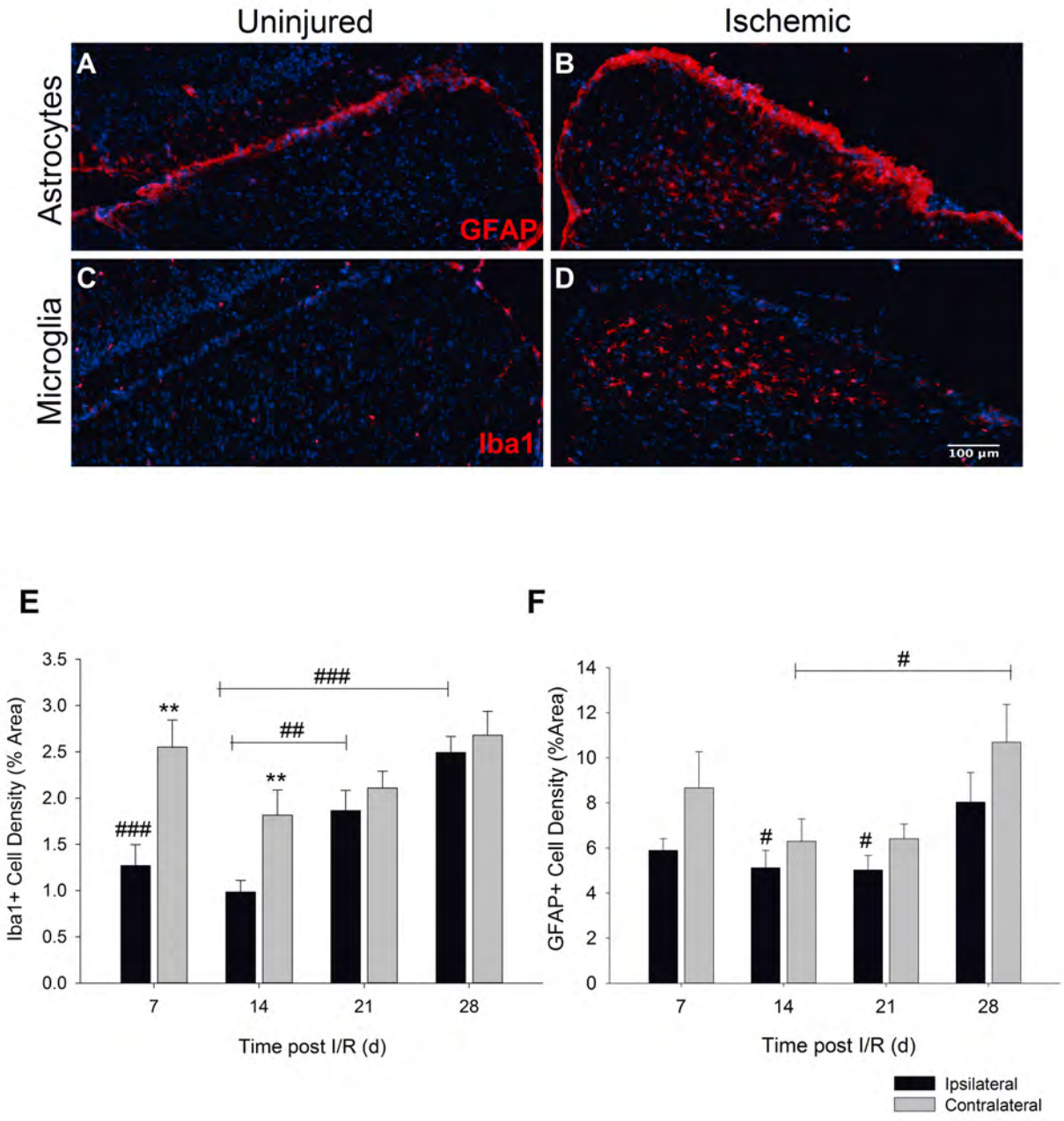
Uninjured
Ischemic
Astrocytes
Microglia
A
B
C
D
GFAP
Iba1
100 µm
E
F
Iba1+ Cell Density (% Area)
GFAP+ Cell Density (%Area)
Time post I/R (d)
Time post I/R (d)
###
##
**
**
###
#
#
#
Ipsilateral
Contralateral

Figure 5. *C1qa*-deficiency protects against retinal thinning resulting from ischemic injury.

(A) Representative H&E stained retinal cross-section images demonstrating the differences in retinal morphology observed in animals receiving retinal I/R injury compared with an uninjured retina. Retinas from WT mice were observed to have significant thinning of the IPL and INL, as well as dramatic loss of the NFL. However, retinas from $C1qa^{+/-}$ and $C1qa^{-/-}$ showed no visible changes in thickness. **(B)** Retinal layer thickness analysis of the whole retinal, the inner plexiform layer (IPL), inner nuclear layer (INL), and outer nuclear layer (ONL). A significant difference was determined between control and WT retinas ($p<0.01$) in all layers measured except for the ONL. This difference was not observed in $C1qa^{+/-}$ and $C1qa^{-/-}$ retinas. Further, a significant rescue of retinal thickness could be seen between WT and transgenic animals in the whole retina ($p<0.01$), the INL ($p<0.01$), and the IPL ($p<0.05$). Mean ± SEM, n = 7 per group. **$p<0.01$, ***$p<0.001$ compared to control and #$p<0.05$, ##$p<0.01$, ###$p<0.001$ compared to WT – I/R determined by One-way ANOVA followed by Holm-Sidak post test. Scale bars = 50μm

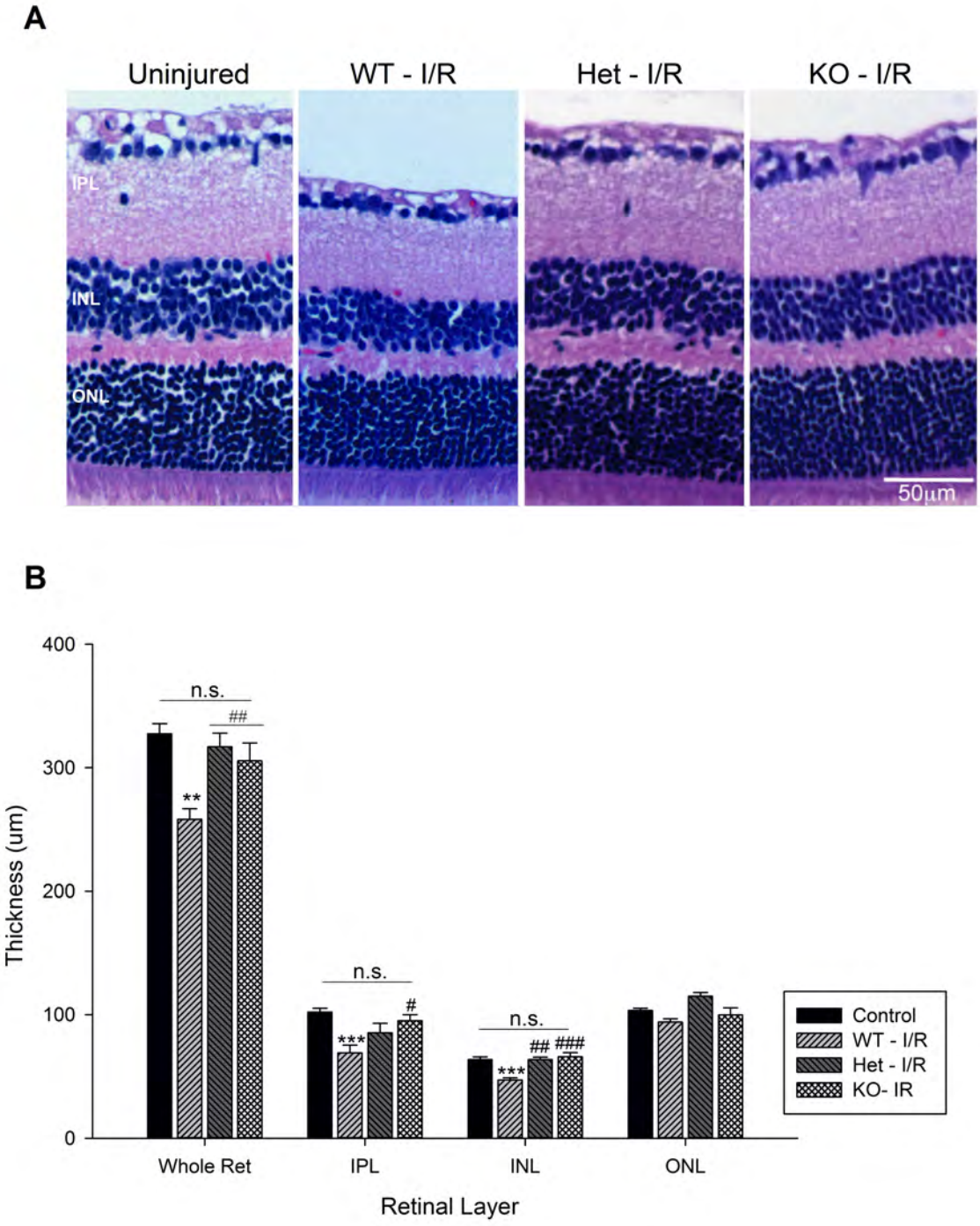
A
Uninjured
WT - I/R
Het - I/R
KO - I/R
IPL
INL
ONL
50μm
B
Thickness (um)
400
300
200
100
0
n.s.
##
**
n.s.
***
#
n.s.
***
##
###
Whole Ret
IPL
INL
ONL
Retinal Layer
Control
WT - I/R
Het - I/R
KO- IR

Figure 6. *C1qa*-deficiency mitigates loss of RGCs using two independent assays of cell counts 28 days following retinal I/R.

(A) H&E stained and **(C)** Rbpms-immunolabeled retinal cross sections used to assess RGC loss between uninjured controls and three *C1qa* genetic backgrounds receiving ischemic injury. **(B)** Quantification of nuclei counted in the GCL determined there was a significant loss of cells ($p<0.01$) in WT retinas but not in the *C1qa*-deficient retinas compared to control. **(D)** Counts of $Rbpms^{+}$ RGCs displayed a statistically significant loss ($p<0.01$) in ischemic eyes of WT mice compared to controls. No statistical differences were determined in ischemic retinas of $C1qa^{+/-}$ or $C1qa^{-/-}$ animals. However, a stastical difference ($p<0.01$) was measured when $C1qa^{-/-}$ retinas were compared to WT. Mean ± SEM, n = 7 per group. **$p<0.01$ compared to control and ##$p<0.01$ compared to WT – I/R determined by One-way ANOVA followed by Holm-Sidak post test. Scale bars = 50μm.

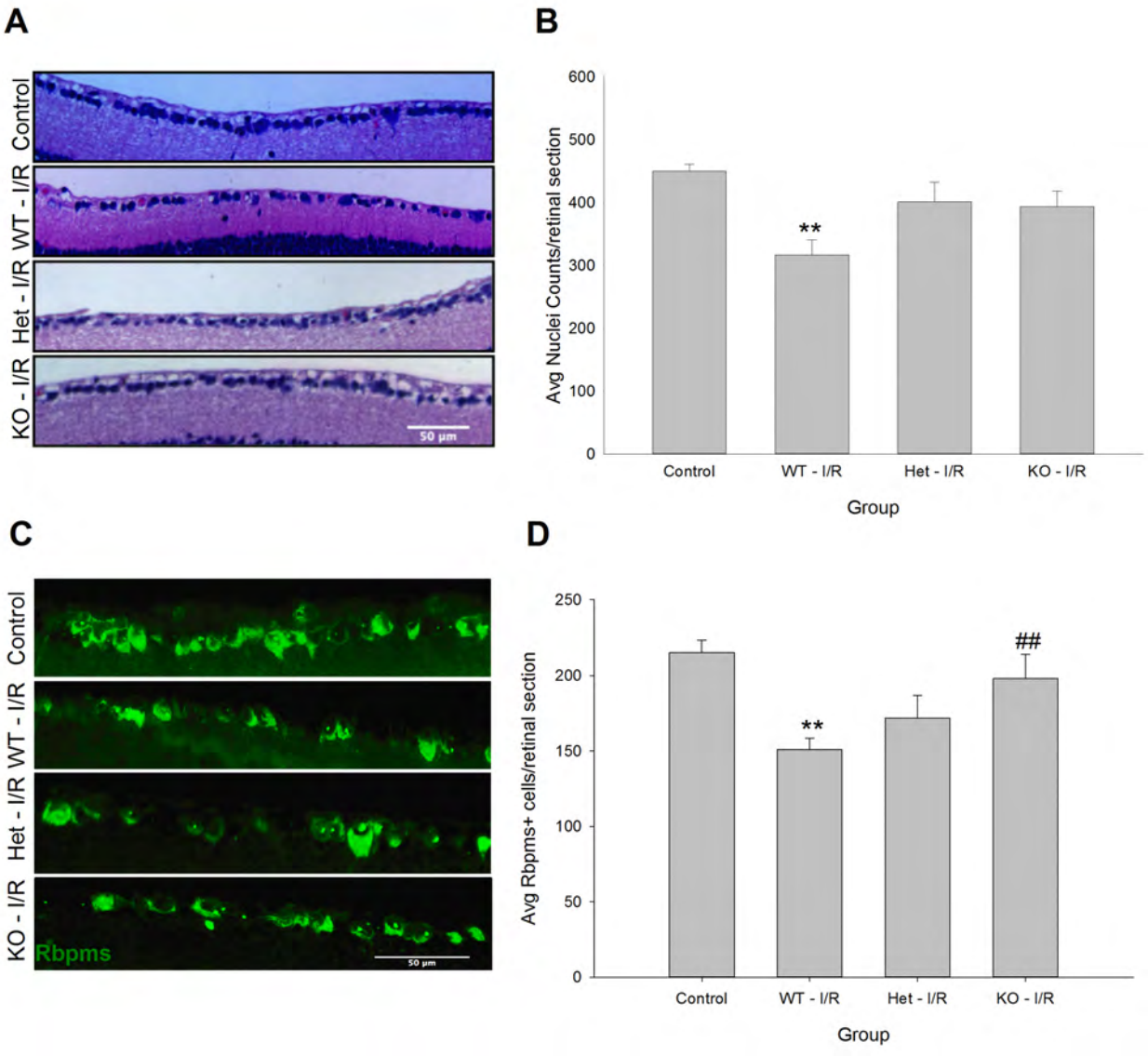
A
Control
WT - I/R
Het - I/R
KO - I/R
50 µm
B
Avg Nuclei Counts/retinal section
600
500
400
300
200
100
0
**
Control
WT - I/R
Het - I/R
KO - I/R
Group
C
Control
WT - I/R
Het - I/R
KO - I/R
Rbpms
50 µm
D
Avg Rbpms+ cells/retinal section
250
200
150
100
50
0
**
##
Control
WT - I/R
Het - I/R
KO - I/R
Group

Figure 7. *C1q*-deficiency delays loss of visual function due to retinal I/R.

(A) Representative ERG traces observed in WT mice comparing waveforms from ischemic and uninjured eyes across a series of flash intensities tested 28 days post injury. **(B)** Comparison of b-wave amplitudes over a 28 day time course at an intensity of 3000mcd.s/m^2. A statistically significant loss of b-wave response was observed in WT ($p<0.01$) and Het ($p<0.05$) ischemic eyes compared to uninjured controls at all time points. However, following initial b-wave suppression, KO ischemic eyes displayed a significant rescue ($p<0.05$) on day 14. This rescue was transient as a slight decline was observed over the remaining two time points; by the end no statistical differences were observed between any animals receiving ischemic injury. Mean ± SEM, n = 8 per group. *$p<0.05$ **$p<0.01$ ***$p<0.001$ compared to control #$p<0.05$ comared to WT – I/R determined by One-way ANOVA followed by Holm-Sidak post test.

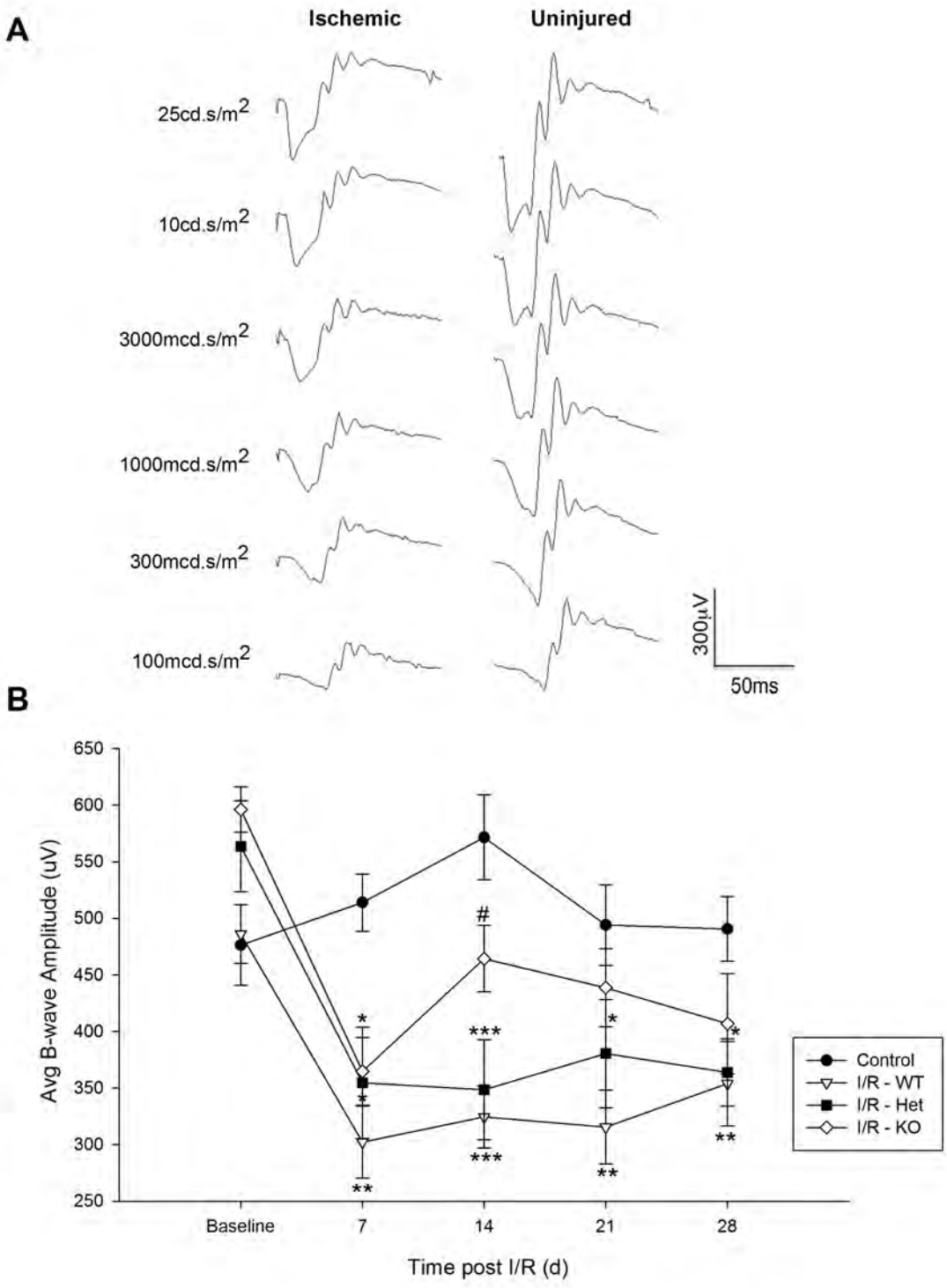
A
Ischemic
Uninjured
25cd.s/m2
10cd.s/m2
3000mcd.s/m2
1000mcd.s/m2
300mcd.s/m2
100mcd.s/m2
300µV
50ms
B
Avg B-wave Amplitude (uV)
650
600
550
500
450
400
350
300
250
Baseline
7
14
21
28
Time post I/R (d)
Control
I/R - WT
I/R - Het
I/R - KO

Figure 8. *C1qa*-deficiency modulates the reactive microglial but not astrocyte response in the retina and SC.

(A,B) Bar graphs display density of $Iba1^+$ microglia **(A)** or $GFAP^+$ **(B)** cells in the retina at both 7 and 28 days post injury. No statistical changes between uninjured or injured $C1qa^{+/-}$ or $C1qa^{-/-}$ mice were observed in microglia density at any time point measured; however, there was a statistically significant decrease compared with WT retinal microglia ($p<0.001$). On day 28 there was significant difference in $GFAP^+$ cell density ($p<0.05$) between ischemic and uninjured retinas of $C1qa^{+/-}$ and $C1qa^{-/-}$ mice. **(C,D)** Bar graphs demonstrating glial cell density in the SC of *C1qa*-deficient mice. **(C)** Microglial density was unchanged in both the ischemic-receiving and uninjured ipsilateral hemisphere at both 7 and 28 days, and $C1qa^{-/-}$ displayed significant decrease compared to peak microglial density at day 28 ($p<0.05$). **(D)** No differences were determined between hemispheres on day 7 or 28 in astrocyte density, but there was a significant increase in density on day 28 when compared to day 7 in $C1qa^{+/-}$ ($p<0.01$) and $C1qa^{-/-}$ ($p<0.05$) mice. No statistical differences were measured when *C1qa*-deficicient were compared to peak WT astrogliosis density. Horizontal reference lines in all bar graphs represent peak cell density observed in WT mice. Mean ± SEM, n = 6 per group. *$p<0.05$ **$p<0.01$ compared to uninjured control determined by student's paired t-test. +$p<0.05$ ++$p<0.01$ compared across time points determined by student's t-test. #$p<0.05$, ###$p<0.001$ compared to glial cell density of I/R injured retinas of WT mice, determined by One-way ANOVA followed by Holm-Sidak post test.

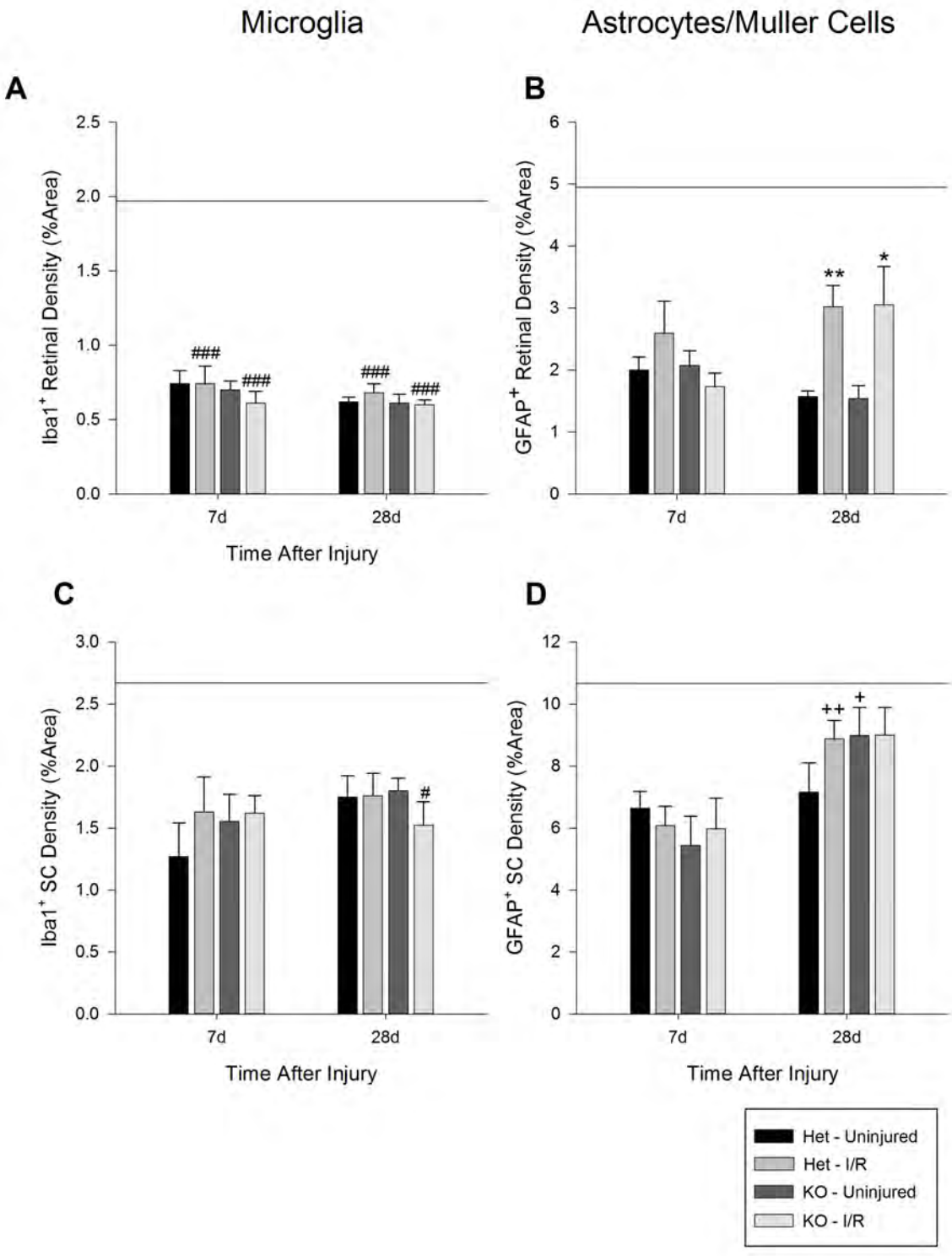
Microglia
Astrocytes/Muller Cells
A
B
C
D
Iba1+ Retinal Density (%Area)
GFAP+ Retinal Density (%Area)
Iba1+ SC Density (%Area)
GFAP+ SC Density (%Area)
7d
28d
Time After Injury
###
**
*
#
++
+
Het - Uninjured
Het - I/R
KO - Uninjured
KO - I/R

References

1. Kaur C, Foulds WS, Ling EA. Blood-retinal barrier in hypoxic ischaemic conditions: basic concepts, clinical features and management. Progress in retinal and eye research. 2008;27(6):622-47. doi:10.1016/j.preteyeres.2008.09.003.

2. D'Onofrio PM, Koeberle PD. What can we learn about stroke from retinal ischemia models? Acta pharmacologica Sinica. 2013;34(1):91-103. doi:10.1038/aps.2012.165.

3. Kuehn MH, Kim CY, Jiang B, Dumitrescu AV, Kwon YH. Disruption of the complement cascade delays retinal ganglion cell death following retinal ischemia-reperfusion. Experimental eye research. 2008;87(2):89-95. doi:10.1016/j.exer.2008.04.012.

4. Osborne NN, Casson RJ, Wood JP, Chidlow G, Graham M, Melena J. Retinal ischemia: mechanisms of damage and potential therapeutic strategies. Progress in retinal and eye research. 2004;23(1):91-147. doi:10.1016/j.preteyeres.2003.12.001.

5. Soto I, Howell GR. The complex role of neuroinflammation in glaucoma. Cold Spring Harbor perspectives in medicine. 2014;4(8). doi:10.1101/cshperspect.a017269.

6. Pekny M, Wilhelmsson U, Pekna M. The dual role of astrocyte activation and reactive gliosis. Neuroscience letters. 2014;565:30-8. doi:10.1016/j.neulet.2013.12.071.

7. Harvey H, Durant S. The role of glial cells and the complement system in retinal diseases and Alzheimer's disease: common neural degeneration mechanisms. Experimental brain research. 2014;232(11):3363-77. doi:10.1007/s00221-014-4078-7.

8. Nimmerjahn A, Kirchhoff F, Helmchen F. Resting microglial cells are highly dynamic surveillants of brain parenchyma in vivo. Science. 2005;308(5726):1314-8. doi:10.1126/science.1110647.

9. Streit WJ, Mrak RE, Griffin WS. Microglia and neuroinflammation: a pathological perspective. Journal of neuroinflammation. 2004;1(1):14. doi:10.1186/1742-2094-1-14.

10. Aguzzi A, Barres BA, Bennett ML. Microglia: scapegoat, saboteur, or something else? Science. 2013;339(6116):156-61. doi:10.1126/science.1227901.

11. Hu X, Li P, Guo Y, Wang H, Leak RK, Chen S et al. Microglia/macrophage polarization dynamics reveal novel mechanism of injury expansion after focal cerebral ischemia. Stroke; a journal of cerebral circulation. 2012;43(11):3063-70. doi:10.1161/STROKEAHA.112.659656.

12. Qu J, Jakobs TC. The Time Course of Gene Expression during Reactive Gliosis in the Optic Nerve. PloS one. 2013;8(6):e67094. doi:10.1371/journal.pone.0067094.

13. Zamanian JL, Xu L, Foo LC, Nouri N, Zhou L, Giffard RG et al. Genomic analysis of reactive astrogliosis. The Journal of neuroscience : the official journal of the Society for Neuroscience. 2012;32(18):6391-410. doi:10.1523/JNEUROSCI.6221-11.2012.

14. Anderson MA, Ao Y, Sofroniew MV. Heterogeneity of reactive astrocytes. Neuroscience letters. 2014;565:23-9. doi:10.1016/j.neulet.2013.12.030.

15. Ransohoff RM, Brown MA. Innate immunity in the central nervous system. The Journal of clinical investigation. 2012;122(4):1164-71. doi:10.1172/JCI58644.

16. Saijo K, Glass CK. Microglial cell origin and phenotypes in health and disease. Nature reviews Immunology. 2011;11(11):775-87. doi:10.1038/nri3086.

17. Kishore U, Reid KB. C1q: structure, function, and receptors. Immunopharmacology. 2000;49(1-2):159-70.

18. Nicholson-Weller A, Klickstein LB. C1q-binding proteins and C1q receptors. Current opinion in immunology. 1999;11(1):42-6.

19. Bonifati DM, Kishore U. Role of complement in neurodegeneration and neuroinflammation. Molecular immunology. 2007;44(5):999-1010. doi:10.1016/j.molimm.2006.03.007.

20. Howell GR, Macalinao DG, Sousa GL, Walden M, Soto I, Kneeland SC et al. Molecular clustering identifies complement and endothelin induction as early events in a mouse model of glaucoma. The Journal of clinical investigation. 2011;121(4):1429-44. doi:10.1172/JCI44646.

21. Stevens B, Allen NJ, Vazquez LE, Howell GR, Christopherson KS, Nouri N et al. The classical complement cascade mediates CNS synapse elimination. Cell. 2007;131(6):1164-78. doi:10.1016/j.cell.2007.10.036.

22. Fourgeaud L, Boulanger LM. Synapse remodeling, compliments of the complement system. Cell. 2007;131(6):1034-6. doi:10.1016/j.cell.2007.11.031.

23. Stephan AH, Madison DV, Mateos JM, Fraser DA, Lovelett EA, Coutellier L et al. A dramatic increase of C1q protein in the CNS during normal aging. The Journal of neuroscience : the official journal of the Society for Neuroscience. 2013;33(33):13460-74. doi:10.1523/JNEUROSCI.1333-13.2013.

24. Kim BJ, Braun TA, Wordinger RJ, Clark AF. Progressive morphological changes and impaired retinal function associated with temporal regulation of gene expression after retinal ischemia/reperfusion injury in mice. Molecular neurodegeneration. 2013;8:21. doi:10.1186/1750-1326-8-21.

25. Hofbauer A, Drager UC. Depth segregation of retinal ganglion cells projecting to mouse superior colliculus. The Journal of comparative neurology. 1985;234(4):465-74. doi:10.1002/cne.902340405.

26. De Simoni MG, Storini C, Barba M, Catapano L, Arabia AM, Rossi E et al. Neuroprotection by complement (C1) inhibitor in mouse transient brain ischemia. Journal of cerebral blood flow

and metabolism : official journal of the International Society of Cerebral Blood Flow and Metabolism. 2003;23(2):232-9.

27. Sheridan GK, Murphy KJ. Neuron-glia crosstalk in health and disease: fractalkine and CX3CR1 take centre stage. Open biology. 2013;3(12):130181. doi:10.1098/rsob.130181.

28. Ginsberg MD. Neuroprotection for ischemic stroke: past, present and future. Neuropharmacology. 2008;55(3):363-89. doi:10.1016/j.neuropharm.2007.12.007.

29. Chen Y, Green CR, Wang K, Danesh-Meyer HV, Rupenthal ID. Sustained intravitreal delivery of connexin43 mimetic peptide by poly(d,l-lactide-co-glycolide) acid micro- and nanoparticles - Closing the gap in retinal ischaemia. European journal of pharmaceutics and biopharmaceutics : official journal of Arbeitsgemeinschaft fur Pharmazeutische Verfahrenstechnik eV. 2014. doi:10.1016/j.ejpb.2014.12.005.

30. Chao HM, Chuang MJ, Liu JH, Liu XQ, Ho LK, Pan WH et al. Baicalein protects against retinal ischemia by antioxidation, antiapoptosis, downregulation of HIF-1alpha, VEGF, and MMP-9 and upregulation of HO-1. Journal of ocular pharmacology and therapeutics : the official journal of the Association for Ocular Pharmacology and Therapeutics. 2013;29(6):539-49. doi:10.1089/jop.2012.0179.

31. Shibeeb O, Chidlow G, Han G, Wood JP, Casson RJ. Effect of subconjunctival glucose on retinal ganglion cell survival in experimental retinal ischaemia and contrast sensitivity in human glaucoma. Clinical & experimental ophthalmology. 2015. doi:10.1111/ceo.12581.

32. Kim SJ, Sung MS, Heo H, Lee JH, Park SW. Mangiferin Protects Retinal Ganglion Cells in Ischemic Mouse Retina via SIRT1. Current eye research. 2015:1-12. doi:10.3109/02713683.2015.1050736.

33. Zhang Z, Qin X, Tong N, Zhao X, Gong Y, Shi Y et al. Valproic acid-mediated neuroprotection in retinal ischemia injury via histone deacetylase inhibition and transcriptional activation. Experimental eye research. 2012;94(1):98-108. doi:10.1016/j.exer.2011.11.013.

34. Lee D, Kim KY, Shim MS, Kim SY, Ellisman MH, Weinreb RN et al. Coenzyme Q10 ameliorates oxidative stress and prevents mitochondrial alteration in ischemic retinal injury. Apoptosis : an international journal on programmed cell death. 2014;19(4):603-14. doi:10.1007/s10495-013-0956-x.

35. Andreeva K, Zhang M, Fan W, Li X, Chen Y, Rebolledo-Mendez JD et al. Time-dependent Gene Profiling Indicates the Presence of Different Phases for Ischemia/Reperfusion Injury in Retina. Ophthalmology and eye diseases. 2014;6:43-54. doi:10.4137/OED.S17671.

36. Orsini F, De Blasio D, Zangari R, Zanier ER, De Simoni MG. Versatility of the complement system in neuroinflammation, neurodegeneration and brain homeostasis. Frontiers in cellular neuroscience. 2014;8:380. doi:10.3389/fncel.2014.00380.

37. van Beek J, Elward K, Gasque P. Activation of complement in the central nervous system: roles in neurodegeneration and neuroprotection. Annals of the New York Academy of Sciences. 2003;992:56-71.

38. Veerhuis R, Nielsen HM, Tenner AJ. Complement in the brain. Molecular immunology. 2011;48(14):1592-603. doi:10.1016/j.molimm.2011.04.003.

39. Singhrao SK, Neal JW, Morgan BP, Gasque P. Increased complement biosynthesis by microglia and complement activation on neurons in Huntington's disease. Experimental neurology. 1999;159(2):362-76. doi:10.1006/exnr.1999.7170.

40. Ricklin D, Lambris JD. Complement-targeted therapeutics. Nature biotechnology. 2007;25(11):1265-75. doi:10.1038/nbt1342.

41. Heydenreich N, Nolte MW, Gob E, Langhauser F, Hofmeister M, Kraft P et al. C1-inhibitor protects from brain ischemia-reperfusion injury by combined antiinflammatory and antithrombotic mechanisms. Stroke; a journal of cerebral circulation. 2012;43(9):2457-67. doi:10.1161/STROKEAHA.112.660340.

42. Benoit ME, Tenner AJ. Complement protein C1q-mediated neuroprotection is correlated with regulation of neuronal gene and microRNA expression. The Journal of neuroscience : the official journal of the Society for Neuroscience. 2011;31(9):3459-69. doi:10.1523/JNEUROSCI.3932-10.2011.

43. Peterson SL, Nguyen HX, Mendez OA, Anderson AJ. Complement protein C1q modulates neurite outgrowth in vitro and spinal cord axon regeneration in vivo. The Journal of neuroscience : the official journal of the Society for Neuroscience. 2015;35(10):4332-49. doi:10.1523/JNEUROSCI.4473-12.2015.

44. Fonseca MI, Zhou J, Botto M, Tenner AJ. Absence of C1q leads to less neuropathology in transgenic mouse models of Alzheimer's disease. The Journal of neuroscience : the official journal of the Society for Neuroscience. 2004;24(29):6457-65. doi:10.1523/JNEUROSCI.0901-04.2004.

45. Levi-Strauss M, Mallat M. Primary cultures of murine astrocytes produce C3 and factor B, two components of the alternative pathway of complement activation. Journal of immunology. 1987;139(7):2361-6.

46. Li L, Eter N, Heiduschka P. The microglia in healthy and diseased retina. Experimental eye research. 2015;136:116-30. doi:10.1016/j.exer.2015.04.020.

47. Thanos S, Richter W. The migratory potential of vitally labelled microglial cells within the retina of rats with hereditary photoreceptor dystrophy. International journal of developmental

neuroscience : the official journal of the International Society for Developmental Neuroscience. 1993;11(5):671-80.

48. Zhang C, Tso MO. Characterization of activated retinal microglia following optic axotomy. Journal of neuroscience research. 2003;73(6):840-5. doi:10.1002/jnr.10713.

49. Tanaka R, Komine-Kobayashi M, Mochizuki H, Yamada M, Furuya T, Migita M et al. Migration of enhanced green fluorescent protein expressing bone marrow-derived microglia/macrophage into the mouse brain following permanent focal ischemia. Neuroscience. 2003;117(3):531-9.

50. Ransohoff RM, Perry VH. Microglial physiology: unique stimuli, specialized responses. Annual review of immunology. 2009;27:119-45. doi:10.1146/annurev.immunol.021908.132528.

51. Schafer DP, Lehrman EK, Kautzman AG, Koyama R, Mardinly AR, Yamasaki R et al. Microglia sculpt postnatal neural circuits in an activity and complement-dependent manner. Neuron. 2012;74(4):691-705. doi:10.1016/j.neuron.2012.03.026.

52. Bosco A, Crish SD, Steele MR, Romero CO, Inman DM, Horner PJ et al. Early reduction of microglia activation by irradiation in a model of chronic glaucoma. PloS one. 2012;7(8):e43602. doi:10.1371/journal.pone.0043602.

53. Wang M, Wang X, Zhao L, Ma W, Rodriguez IR, Fariss RN et al. Macroglia-microglia interactions via TSPO signaling regulates microglial activation in the mouse retina. The Journal of neuroscience : the official journal of the Society for Neuroscience. 2014;34(10):3793-806. doi:10.1523/JNEUROSCI.3153-13.2014.

54. Schafer MK, Schwaeble WJ, Post C, Salvati P, Calabresi M, Sim RB et al. Complement C1q is dramatically up-regulated in brain microglia in response to transient global cerebral ischemia. Journal of immunology. 2000;164(10):5446-52.

55. Ridet JL, Malhotra SK, Privat A, Gage FH. Reactive astrocytes: cellular and molecular cues to biological function. Trends in neurosciences. 1997;20(12):570-7.

56. Chung WS, Clarke LE, Wang GX, Stafford BK, Sher A, Chakraborty C et al. Astrocytes mediate synapse elimination through MEGF10 and MERTK pathways. Nature. 2013;504(7480):394-400. doi:10.1038/nature12776.

57. Hol EM, Pekny M. Glial fibrillary acidic protein (GFAP) and the astrocyte intermediate filament system in diseases of the central nervous system. Current opinion in cell biology. 2015;32:121-30. doi:10.1016/j.ceb.2015.02.004.

58. Cho KS, Yang L, Lu B, Feng Ma H, Huang X, Pekny M et al. Re-establishing the regenerative potential of central nervous system axons in postnatal mice. Journal of cell science. 2005;118(Pt 5):863-72. doi:10.1242/jcs.01658.

59. Li L, Lundkvist A, Andersson D, Wilhelmsson U, Nagai N, Pardo AC et al. Protective role of reactive astrocytes in brain ischemia. Journal of cerebral blood flow and metabolism : official journal of the International Society of Cerebral Blood Flow and Metabolism. 2008;28(3):468-81. doi:10.1038/sj.jcbfm.9600546.

60. Menet V, Prieto M, Privat A, Gimenez y Ribotta M. Axonal plasticity and functional recovery after spinal cord injury in mice deficient in both glial fibrillary acidic protein and vimentin genes. Proceedings of the National Academy of Sciences of the United States of America. 2003;100(15):8999-9004. doi:10.1073/pnas.1533187100.

61. Kurimoto T, Yin Y, Omura K, Gilbert HY, Kim D, Cen LP et al. Long-distance axon regeneration in the mature optic nerve: contributions of oncomodulin, cAMP, and pten gene deletion. The Journal of neuroscience : the official journal of the Society for Neuroscience. 2010;30(46):15654-63. doi:10.1523/JNEUROSCI.4340-10.2010.

CHAPTER III

EARLY DETECTION AND ELIMINATION OF SUPEROXIDE FOLLOWING RETINAL INJURY IS NEUROPROTECTIVE

Sean M Silverman, Ning Fan, Danli Liu, Yang Liu, Lu Liu, Byung-Jin Kim, Liping Tang, Abbot F. Clark, Xuyang Liu, Iok-Hou Pang

Abstract

Retinal injures such as ischemia/reperfusion (I/R) and optic nerve crush (ONC) lead to increased generation of reactive oxygen species (ROS). This significant increase in ROS is associated with mediating permanent morphological damage and retinal neurons, as well as impaired visual function. Identifying these changes in the retina has in the past been limited to the use of *ex vivo* assays requiring sacrifice of animals. Here we turn to the chemilluminescent probe L-012, previously demonstrated to noninvasively detect subcutaneous increases in ROS in mice. We show for the first time L-012 produces significant luminescent signal specifically in eyes receiving either retinal I/R injury or ONC. Histological examination determined L-012 was safe and non-toxic to the retina. Additionally, we tested two superoxide inhibitors, Apocynin and TEMPOL, to demonstrate the selectivity of L-012 and to effectively reduce the levels of luminescence due to retinal injury. Both inhibitors were tested as well for neuroprotective potential following retinal I/R injury. TEMPOL treatment provided mild protection against inner retinal thinning and decreased electroretinography (ERG) b-wave amplitudes associated with visual function in comparison with vehicle treated mice. However, Apocynin significantly rescued b-wave amplitudes and completely preserved retinal morphology. Together, our data demonstrates the potential for early detection of ROS in the eye using L-012 creating a therapeutic window for successful neuroprotection.

Key Words:

Retinal ischemia, optic nerve crush, reactive oxygen species, L-012, neuroprotection

Introduction

Mitochondrial respiration is primarily responsible for production of reactive oxygen species (ROS), including superoxide. Ordinarily the endogenous antioxidant enzymes degrade these highly reactive molecules. However, accumulating levels of ROS overwhelm the intrinsic defense mechanisms leading to damage including oxidative and nitrative modifications to cellular proteins, lipid peroxidation, DNA damage, and ultimately neuronal death [1, 2]. Mitochondrial dysfunction and increased ROS generation have been linked to numerous neurodegenerative diseases including ALS, Parkinson, Alzheimers disease, glaucoma, and even normal brain aging [3]. In addition to their pathogenic role however, researchers are beginning to understand a role for ROS in biological processes regulating cell fate, stress response, vascular tone and wound healing. In the retina, it remains to be determined the precise role ROS plays in physiology and pathophysiology.

Retinal neurons are particularly susceptible to oxidative stress because of the high levels of oxygen consumption, glucose oxidation, and polyunsaturated fatty acids in the retina [4]. Unsurprisingly, ROS has an integral role in several retinopathies and optic neuropathies, such as age-related macular degeneration [5], retinopathy of prematurity and diabetic retinopathy [6], retinal ischemia [7], optic nerve trauma [8], and glaucoma [9]. However, their role as a causative or secondary mediator of damage remains unclear. Generation of free radicals following ischemic injury, more specifically occurring during reperfusion [10], is amongst the earliest pathogenic changes leading to breakdown of blood barriers, immune cell infiltration, and apoptosis [11]. Therefore, superoxide represents a prime therapeutic target against the deficits caused by retinal ischemia. While several strategies for inhibition or removal of ROS have been developed, advances in detection methods of ROS have remained relatively inadequate.

In vivo monitoring of ROS is technically challenging due to the rapid turnover of ROS and

the limited sensitivity and specificity of ROS probes. Current detection methods include fluorescent probes such as dihydroethidium (DHE), spectrophotometric measurements, electron spin resonance spectroscopy, spin traps, and markers for oxidation and nitration of proteins, lipids, and DNA. These are all useful for assessment of oxidative stress in cultured cells, *ex vivo* biopsy, or *post mortem* tissue samples [12]. However, there remains an unmet need for a sensitive and reliable method of non-invasive *in vivo* ROS detection. Recent studies have demonstrated that L-012 (8-amino-5-chloro-7-phenylpyrrido [3,4-*d*]-pyridazine-1, 4 (2*H,*3*H*) dione), a highly sensitive chemiluminescent probe [13], can be used to detect subcutaneous ROS activity by *in vivo* luminescent imaging [14, 15].

Because of the ability for light to penetrate through the transparent refracting media of the eye and reach the retina, we hypothesized that L-012 chemiluminescence could be detected by non-invasive in vivo imaging in mouse models of ocular injury. In the present study we, characterize and optimize the use of L-012 as the first non-invasive *in vivo* method to assess temporal accumulation of ROS in the mouse retina following retinal ischemia/reperfusion (I/R) and optic nerve crush (ONC) injuries. Furthermore, we demonstrate the selectivity of L-012 through real-time modulation of luminescence, and the neuroprotective potential of early detection using two selective inhibitors of superoxide.

Material and methods

Animals

9- to 12-week old female C57BL/6J mice were purchased from Jackson Laboratory (Bar Harbor, ME, USA) and Guangdong animal experimental center (Guangzhou, China). All animals were maintained and handled in accordance with the ARVO statement for the Use of Animals in Ophthalmic and Vision Research. The University of North Texas Health

Center Animal Care and Use Committee approved the research protocol prior to initiation of the study.

Mouse models of injury

Retinal I/R was induced as described previously [16]. Briefly, mice were anesthetized with a ketamine/xylazine/acepromazine cocktail (100/10/3mg/kg) followed by cannulation of the anterior chamber with a 30-gauge needle connected to a reservoir containing sterile PBS. The reservoir was elevated to generate an intraocular pressure of 120 mmHg for 1 h to induce retinal ischemia. Afterwards, the cannula was removed and blood was allowed to naturally reperfuse the retina.

For ONC, mice were anesthetized by intraperitoneal (IP) injection of ketamine and xylazine (100 and 10 mg/kg, respectively) and supplemented by topical ophthalmic anesthesia (0.5% proparacaine hydrochloride ophthalmic solution, Alcaine. SA Alcon-Couvreur NV, Puurs, Belgium) in the left eye. The left optic nerve of mice in the crush group was exposed intraorbitally through a small window made between the surrounding muscles and vascular plexus, and crushed approximately 1mm posterior to the globe with a self-closing forceps for 10 seconds. In the sham surgery group the left optic nerve was exposed but not crushed. Bacitracin Zinc with polymixin B sulfate ophthalmic ointment (Akorn Inc., Lake forest, USA) was topically administered post surgery to prevent ocular infection.

L-012 and in vivo imaging of mice

ROS detection by the chemiluminescent probe L-012 was captured using the small animal *in vivo* imaging system (IVIS Lumina XR, Caliper Life Sciences, MA, USA), which

consisted of a dark chamber equipped with a cooled CCD camera and an internal heating pad. L-012 was purchased from Wako Pure Chemical Industries (Osaka, Japan) and dissolved in Millipore water. L-012 was administered intraperitoneally (ip) at a dose of 75mg/kg in a volume of 100µl. Animals were anesthetized by isoflurane inhalation (2%, Bulter Schein Animal Health, Dublin, OH) during the recording procedure. Prior to imaging, pupils were dilated by 1% Tropicamide ophthalmic solution (Bausch & Lomb Pharmaceuticals Inc., Claremont, CA, USA), the cornea was moistened with Artificial Tears™ ointment (Rugby, Rockville Center, NY), and their body temperature was maintained at 37ºC. Mice were examined for acceptability into the study prior to imaging defined by a set of inclusion criteria containing pupil dilation, absence of congestion and edema of the conjunctiva, and a cataract score less than 1. We defined 6 cataract grades according to the degree of lens opacification; no lenticular opacification (grade 0), very small discrete lenticular opacification (barely visible, grade 0.5), small discrete lenticular opacification (grade 1), larger lenticular opacification but still not involving entire lens (grade 2), lenticular opacification involving entire lens (grade 3) and severe lenticular opacification involving entire lens (grade 4). Mice were placed on their right side with the injured eye oriented towards the camera. Images of chemiluminescence were acquired sequentially in 5 minute exposure intervals, from 15 min up to 60 minutes after L-012 injection. Data was analyzed using the Living Image Software (PerkinElmer, Waltham, MA). Light emission from the left eye was quantified as photons/second/cm^2/steradian.

Retinal detection of superoxide

Validation of superoxide detection in the retina by L-012 was confirmed with dihydroethidium (DHE) (Thermo Fisher Scientific, Waltham, MA). After enucleation of

whole globes, eyes without fixation were submerged in Tissue-Tek OCT (Sakura Finetek USA, Torrance, CA) and snap frozen in methylbutane placed in liquid nitrogen. Eyes were cryosectioned at a thickness of 10μm and allowed to dry at room temperature for 1 hr. Slides were gently washed in PBS followed by incubation with 5μM DHE at 37°C for 25 minutes. Slides then were washed once more in PBS and mounted with ProlongGold anti-fade reagent with DAPI (Molecular Probes, Life Technologies, Grand Island, NY). Images were taken using a Nikon Eclipse Ti inverted microscope (Nikon, Melville, NY) containing the CRi Nuance FX multispectral imaging system (Caliper Life Sciences, Hopkinton, MA). Immunofluorescence was quantified using ImageJ (NIH, Bethesda, MD).

Experimental manipulation of ROS production in mice

Inhibitors of ROS were tested to observe modulation of L-012 chemiluminescence in our models of ocular injury. TEMPOL (4-hydroxy-2,2,6,6-tetramethylpiperidine-N-oxyl, Sigma-Aldrich, St. Louis, MO, USA), previously shown to reduce ROS levels in various tissues (Thiemermann, 2003; Thaler et al., 2011), was dissolved in PBS, and administered ip (100mg/kg in 100μl) 15 min prior to L-012 injection. Apocynin (4-hydroxy-3-methoxyacetophenone, Sigma-Aldrich, St. Louis, MO,USA), a selective reversible NADPH-oxidase inhibitor, that efficiently reduced ROS production in many experimental models (Stefanska and Pawliczak, 2008; Haruta at al., 2009), was dissolved in PBS and 0.7% DMSO at a concentration of 50mg/kg in 100μl, also administered ip 15 min prior to L-012 injection. Live imaging was performed at peak ROS production times after L-012 injection.

Protection against loss of visual function with ROS inhibitors

The abilities of TEMPOL and Apocynin to protect against visual deficits resulting from retinal I/R were determined. Mice were pretreated with either vehicle (PBS), TEMPOL, or Apocynin 30 mins prior to injury, and daily administration for one week after I/R. Visual function was measured using scotopic flash electroretinography (ERG) once weekly over a 4 week time course [16]. Animals were dark adapted overnight; mice were anesthetized with 2% isoflurane and connected to the HMsERG system (Ocuscience; Rolla, MO). Body temperature was maintained at 37°C. A ground electrode was placed subcutaneously by the tail and reference electrodes were inserted under each eye. Both eyes were dilated using 1% Tropicamide, and corneas were anesthetized topically with 0.5% Proparacaine. Silver-thread electrodes were placed across the apex of the cornea and held in place with Gonak (Akorn; Lake Forest, IL) coated contact lenses. Eyes were exposed to a series of light flashes at increasing intensities (0.1, 0.3, 1, 3, 10, and 25 cd.s/m^2). Amplitude and implicit times of waveforms were measured and analyzed in ERGView v4.380R (Ocuscience; Rolla, MO).

Histology evaluation and retinal layer thickness analysis

To evaluate toxicity of L-012, mice were euthanized immediately following their final live imaging session at the end of their respective time courses. Eyes were gently enucleated and fixed in 4% paraformaldehyde (PFA) at 4°C overnight. Eyes then were paraffin embedded and cross sectioned at a thickness of 5μm, followed by H&E staining for morphological observation of the retina. For assessment of retinal protection following treatment with ROS inhibitors, eyes were collected and processed similarly 28 days post retinal I/R. Retinas were imaged from ora serata to ora serata through the optic nerve and

thicknesses of the whole retina, the inner plexiform layer (IPL), inner nuclear layer (INL), and outer nuclear layer (ONL) were quantified in ImageJ at two peripheral and two central locations as previously described [16].

Statistical analysis

Data were analyzed using Prism software (Graphpad, San Diego, CA, USA). A one-way ANOVA followed by Bonferroni's test for multiple comparisons was used to compare the difference among multiple groups. Unpaired Student's *t*-test was used for comparison between two groups. The mean ± SEM was presented for all the data. A value of $P<0.05$ was regarded as statistically significant.

Results

ROS accumulation in the retina identified by L-012 chemiluminescence

L-012 has recently been identified as a highly sensitive method for non-invasive *in vivo* detection for ROS following LPS injection in the gut [14, 15]. We tested the sensitivity of this compound in the eye following transient retinal I/R injury. While the eye presents as a more accessible tissue target than the gut, it is protected by a series of blood ocular barriers that may restrict L-012 bioavailability following systemic administration. However, a single ip injection of L-012 24 hours post retinal I/R produced a significant chemiluminescent signal only in the ischemic eye, while no signal was detected in the contralateral uninjured control (Fig 1A). For all quantification purposes, mice were oriented with their injured eye facing towards the camera. Chemiluminescent intensity was measured by creating a region of

interest (ROI) around the injured eye and subtracting from all background noise for a corrected average intensity (Fig 1B). To further identify if ROS was being detected in the retina, we also utilized the optic nerve crush (ONC) model as an additional model of retinal injury. One day post ONC, we also identified chemiluminescent signals emanating only from the injured eye (Fig 1C). No signal was observed in sham control eyes (data not shown).

Sustainability and toxicity of L-012 following ocular injury

Following positive detection of chemiluminescence in the eye, we sought to determine how long a single injection could provide a detectable signal, as well as a time course of ROS detection post injury. In our model of retinal ischemia, we identified day 1 post injury as the optimal window of ROS detection via L-012. During this peak window, we observed a single injection produced a significant intensity ($p<0.01$) for at least 60 minutes (Fig 2A). On days 3 through 14, little to no detectable signals were measured. Similarly, following ONC the peak window for detection was on day 1. Interestingly, chemiluminescence following ONC was not as sustainable as that seen in ischemic eyes. While the initial readings produced a much greater intensity than was observed in I/R treated animals, there was a significant downward trend 20 minutes after L-012 injection. A more stable time-dependent measurement was recorded on day 3 (Fig 2B).

Previous reports identify L-012 as being non-toxic both *in vitro* and *in vivo [17, 18];* however, L-012 chemiluminescence was not previously tested in the eye. Therefore, we deemed it critical to observe the health of retinal tissue following the conclusion of our time course study. Examination of H&E stained tissue revealed no evidence of toxicity following multiple administrations of L-012 (Fig 3B-E). Additionally, no histological evidence of immune response was observed between contralateral (Fig 3B&D) and injured (Fig 3C&E)

tissue when compared with naïve retinal sections (Fig 3A). Morphological differences between control and injured tissue included expected loss of retinal ganglion cells (RGCs) in ONC retinas (Fig 3E) and early signs of retinal I/R-induced thinning (Fig 3C).

Validation of retinal superoxide

Unfortunately, imaging using the small animal IVIS only allows for us to view chemiluminescent signal from the whole eye. Therefore, we utilized the *ex vivo* DHE assay to verify the presence of superoxide in the retina. Representative images of ischemic retinas from 24 to 72 hours post ischemia demonstrate an increase in DHE labeling compared to the uninjured control retinas (Fig 4A-D). The most dramatic changes appeared to be in the ganglion cell layer (GCL) and outer nuclear layer (ONL). Fluorescent intensity was quantified in all nucleated layers of the retina to further identify the increases in superoxide levels. These were very statistically significant increases ($p<0.001$) as early as 24 hours post injury in both the GCL (Fig 4E) ($1.55x10^6 \pm 1.71x10^5$) and the ONL (Fig 4G) ($1.83x10^7 \pm 1.04x10^6$) in comparison to uninjured retinas ($8.16x10^5 \pm 2.52x10^4$ and $1.21x10^7 \pm 8.77x10^5$, respectively). Levels of superoxide in these layers remained significantly increased at all time points observed. In the inner nuclear layer (INL) however, significant increases ($p<0.05$) were only observed 72 hours after injury (Fig 4F).

Modulation of chemiluminescence following superoxide inhibtion

TEMPOL, a superoxide scavenger, and Apocynin, a selective reversible NADPH-oxidase inhibitor, have both effectively been shown to significantly reduce levels of superoxide following injury *in vivo* [19-21]. Either TEMPOL (100mg/kg) or Apocynin

(50mg/kg) were administered intraperitoneally (ip) 15 minutes prior to L-012 injection and live imaging. 24 hours post I/R, TEMPOL significantly ($p<0.01$) suppressed chemiluminescent signals in the eye as early as 25 minutes post injection (13.2 ± 7.45%) compared to animals receiving L-012 and vehicle. During the window of peak intensity from 25-35 minutes, TEMPOL significantly quenched all measurements (Fig 5A). Similarly, Apocynin treatment also dramatically reduced L-012 activity ($p<0.01$) during this same window. No statistical differences were determined between treatments with the two inhibitors. We also tested the efficacy of both inhibitors 48 hours post injury. Again, while there were no statistical differences between the extents of inhibition with either compound, both significantly ($p<0.05$) reduced chemiluminescent measurement compared to vehicle (Fig 5B). We tested the same inhibitors in animals subjected to ONC injury. Using a similar protocol, either TEMPOL or Apocynin was administered ip 30 minutes prior to live imaging 1 day post ONC. We calculated the average radiance from 15 min to 25 min of imaging, and both inhibitors significantly reduced chemiluminescence ($p<0.05$). No differences in efficacy were seen between these two inhibitors (Fig 5C).

Neuroprotection against ischemic injury

Given the dramatic reduction in L-012 signals following superoxide inhibition, we hypothesized that early treatments targeting ROS would protect animals against visual and morphological deficits resulting from retinal I/R injury. Mice were pretreated with either TEMPOL or Apocynin 30 minutes prior to ischemia, as well as a daily administration for seven days post injury. Scotopic flash ERG readings were taken weekly over the next 28 days. On day 28, mice receiving vehicle treatment displayed a statistically significant loss in ERG b-wave amplitudes ($p<0.01$) in ischemic eyes compared to the uninjured contralateral eyes.

Interestingly, while TEMPOL treatment moderately improved b-wave amplitudes compared to vehicle, animals receiving Apocynin recorded b-wave amplitudes matching that of uninjured control eyes ($p<0.05$ compared to vehicle, Fig 6A). We also measured b-waves from contralateral eyes of mice receiving these ROS inhibitors, and did not observe any suppression in ERG amplitudes due to treatment compared to vehicle controls (Fig 6B). Selecting a representative flash intensity of 3000mcd.s/m^2, in a time course study over a 28 day period, TEMPOL was only mildly effective in restoring visual function, while Apocynin significantly ($p<0.05$) protected b-wave amplitudes following retinal I/R injury (Fig 6C).

We hypothesized with the significant protection observed in retinal function, morphological losses we have previously characterized [16] such as thinning of the inner neural retina might be protected against as well. Eyes were harvested following day 28 ERG measurements for H&E staining and assessment of retinal layer thickness. As expected, there was significant I/R-induced thinning ($p<0.001$) of the whole retina (269.5 ± 5.8μm) in the vehicle treated group compared to uninjured eyes (325.3 ± 6.9μm). These losses were specifically seen in the IPL and INL (Fig 7A). Retinal I/R does not damage cells in the ONL, as these cells are supplied by blood flow from the choriocapillaris not the central retinal artery [7]. While treatment with TEMPOL mildly rescued loss of thickness in all layers quantified, Apocynin completely preserved retinal morphology compared to vehicle treated animals ($p<0.001$), making them indistinguishable from uninjured control retinas. Additionally, contralateral retinas from TEMPOL and Apocynin treated mice were examined for drug-induced toxicity; however, there were no significant differences observed compared to vehicle controls (Fig 7B).

Discussion

We have successfully demonstrated a method of non-invasive *in vivo* imaging of temporal ROS production in the eyes of mice following retinal I/R and ONC injuries using L-012 chemiluminescence. We confirmed that L-012 detects superoxide in the retina through the use of *ex vivo* assays and real-time modulation of luminescence with two separate superoxide inhibitors. Finally, we showed that treatment with Apocynin is a viable neuroprotective strategy, capable of significantly rescuing against functional and morphological deficits resulting from retinal I/R and ONC injuries.

Numerous studies have previously established the significance of L-012 in the detection of ROS in cell culture [13, 22, 23]. However, only recently has the sensitivity of this luminol derivative been tested for the subcutaneous detection of reactive oxygen and nitrogen species. Injection of inflammatory stimulants such as LPS, ethanol, PLA microspheres, PEG particles, and c48/80 were all identified *in vivo* to increase ROS through L-012 luminescent properties [14, 15, 24]. Additionally, L-012 was used to demonstrate generation of ROS in the distal colon in a mouse model of genetic colitis [17]. Given these successes, we aimed to test this sensitivity in a previously unstudied tissue, the retina, using injury models known to increase ROS. Only eyes receiving injury produced a detectable luminescent signal following systemic administration of L-012. From this we can conclude that L-012 is capable of crossing the blood-retinal barrier, previously unknown prior to our studies. This finding opens the possibility for observation of superoxide in the brain using models of focal or global ischemia. While other barriers to detection exist, primarily the skull, the ability to cross blood barriers presents for the first time a noninvasive *in vivo* method of superoxide measurement in the CNS. Interestingly, we observed a sustainable signal lasting at least 60 minutes from a single dose, whereas previous studies demonstrated a much more transient signal at a similar concentration [14]. This difference is most likely due to the nature

of the injury. ONC and retinal I/R are severe insults resulting in progressive and permanent damage to the morphology and function of the retina and visual centers in the brain [25, 26]. Whereas administration of LPS into the gut stimulates an inflammatory response that can be cleared by the innate immune response causing only temporary disturbances in homeostasis.

To confirm the detection of superoxide in the retina, we additionally relied on DHE fluorescence in retinal cross sections (Fig 4A). Accumulation of ROS including superoxide has been well established following ischemic injury in many different tissues [7, 27, 28]. Several of these studies have measured superoxide *in situ* using DHE. Likewise, in the retina, DHE has been used to visualize increased superoxide in mouse models of diabetic retinopathy, retinopathy of prematurity, uveitis, and retinal ischemia [29-32]. As expected, we observed a significant increase in DHE staining between control and ischemic eyes as early as 24 hours post injury, corresponding to our findings with L-012. However, DHE assessment revealed significant levels of superoxide at 72 hours in contrast to our *in vivo* findings. However, DHE can result in misleading interpretations of the presence of ROS including oxidation by cytochrome c, oxidation products formed from non-specific peroxidases, high concentrations of DHE leading to saturation of nucleic acid binding sites, and the formation of multiple fluorescent end products to name a few [33-36]. Many of these may potentially explain differences observed between the two methods. HPLC remains the most accurate method to quantify the reaction between DHE and superoxide [37], and future experiments will be needed to more appropriately correlate our findings using L-012.

To further identify the signal being detected during live imaging was due to accumulating superoxide generation, we tested the inhibitors Apocynin and TEMPOL. These studies answered two questions. First, L-012 shows selective activity with superoxide and secondly, live imaging detected superoxide through significantly quenched levels of ROS-induced luminescence in mice treated with Apocynin or TEMPOL compared to animals

receiving a vehicle treatment plus L-012. Both compounds were previously identified to reduce L-012 chemiluminescence following LPS treatment [14], and as expected both significantly suppressed luminescence detected in injured eyes. Recently it was proposed L-012 does not directly react with superoxide, but rather forms an endoperoxide which then becomes excited, suggesting peroxidases like Apocynin inhibit luminescence from this end-product rather than suppressing superoxide [38]. However, Kielland et al [14] observed that the NOS inhibitor L-NAME almost completely eliminated L-012 luminescence when compared to Apocynin, contradicting the alternatively proposed peroxide reaction. Along with superoxide, L-012 is known to strongly react with peroxynitrite in cell culture [22]. While we have not identified the presence of RNS following retinal injury, L-NAME has previously been shown to preserve retinal morphology but fails to rescue ERG b-wave amplitudes after retinal ischemia [39, 40]. In comparison, we found both TEMPOL and Apocynin eliminated as much as 85% of the L-012 luminescence detected during peak activity *in vivo*. It is likely any remaining signal may be due to the reaction of L-012 with RNS. Thus LPS injury may generate a greater NOS response than retinal I/R or ONC injuries, explaining the differences in observed effectiveness with Apocynin treatment between models. Future studies could look to a combined therapy of Nox and NOS inhibition for a greater reduction of superoxide levels after ocular injury.

Following these findings, we determined whether either compound provided neuroprotection against ischemic-induced damages. Despite the effectiveness of TEMPOL to modulate L-012 activity, only Apocynin preserved visual function and retinal integrity. This finding surprised us, as TEMPOL has been shown to increase neuronal survival, reduce glutamate release, decrease markers of apoptosis, and improve neuromotor score following cerebral ischemia [21, 41, 42]. Expression of NAD(P)H oxidase 1 (Nox1) was significantly increased in RGCs following retinal ischemia, increasing their susceptibility to apoptosis [43].

Further, genetic deletion of different Nox genes protects the retina from neovascularization, microglial activation and infiltration, and neuronal death [44-46]. Apocynin has previously been shown to reduce DHE fluorescence after retinal ischemia [46, 47]. More importantly, reduced neovascularization and blood-retinal barrier permeability were observed to be reduced following Apocynin treatment [48, 49]. However, to our knowledge ours is the first study to demonstrate both functional and morphological protection from retinal ischemia using a Nox inhibitor.

Conclusions

In conclusion we demonstrate the sensitivity and safety of the chemiluminescent compound L-012 for non-invasive *in vivo* measurement of superoxide generation following retinal injury. Using this early detection as a window for treatment, we are able to significantly rescue loss of visual function and preserve retinal morphology against ischemic and axonopathy injuries with the Nox inhibitor Apocynin. We propose L-012 as a viable tool for diagnostic detection of superoxide in other animal models of injury, including cerebral ischemic events given its ability to cross blood barriers. This method has the potential to reduce cost and number of animals necessary for studies of temporal ROS changes associated with injury and treatment regiments without the need for sacrifice. Clinically, this may prove to be a useful tool for examining and diagnosing patients following transient ischemic attacks to prevent or reduce tissue loss due to oxidative stress.

Acknowledgments

Research supported by NEI R21EY02463 grant and a grant from the National Natural Science Foundation of China (NNSF #81200688)

Figure Legends

Figure 1. L-012 chemiluminescence in the eye following ocular injury.

C57BL/6J mice were subjected to either retinal I/R or ONC followed by systemic injection of L-012 24 hours post injury. Chemiluminescence was only detected in left injured eyes following I/R **(A)** or ONC **(C). (B)** For quantification purposes animals were positioned with their injured eyes towards the camera for optimal detection. Region of interests (ROI) were placed around the injured tissue and were subtracted from background values detected in animal skin and fur for a corrected average chemiluminescence.

Figure 1

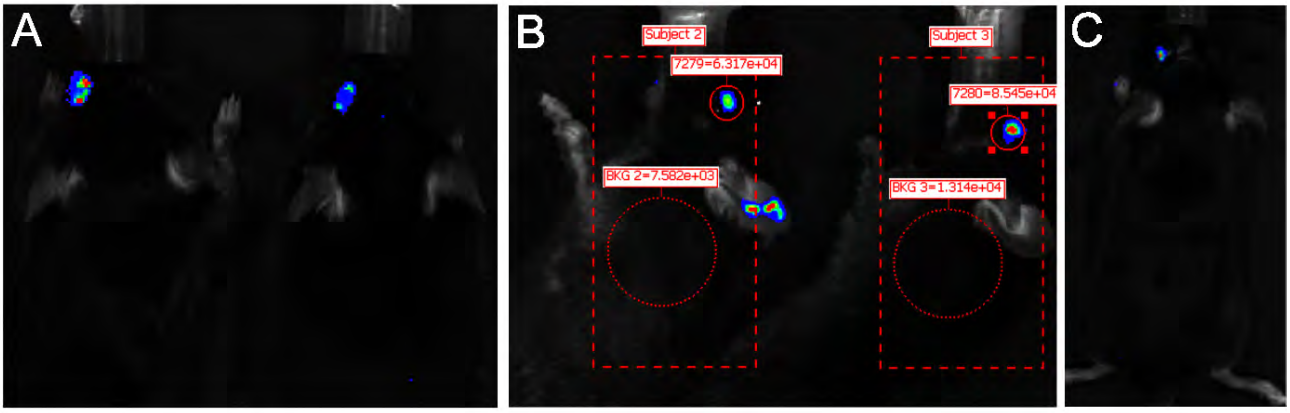
A
B
Subject 2
7279=6.317e+04
BKG 2=7.582e+03
Subject 3
7280=8.545e+04
BKG 3=1.314e+04
C

Figure 2. Time course of measurable L-012 activity after injury.

(A) A single treatment with L-012 produced detectable levels of chemiluminescence for at least 60 minutes after retinal I/R compared to uninjured eyes ($p<0.001$). However, from 72 hours to 14 days post injury only negligible activity was measured. **(B)** 24 hours after ONC, a significant increase in luminescence was measured ($p<0.05$) compared to sham operated animals. Time for ROS detection was much more transient in ONC animals, showing a dramatic decline in chemiluminescent activity after 20 minutes and a loss of statistical difference by 30 minutes. Mean ± SEM, n=5 (ONC) or 7 (I/R). *$p<0.05$ **$p<0.01$ ***$p<0.001$ compared between time points using one-way ANOVA followed by Bonferonni *post hoc* test

Figure 2

A

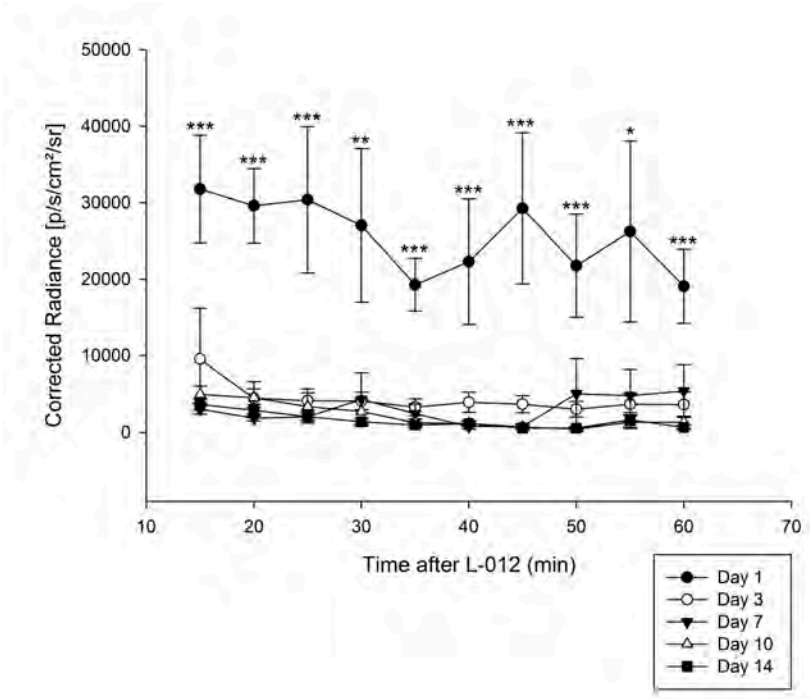
Corrected Radiance [p/s/cm²/sr]
50000
40000
30000
20000
10000
0
10
20
30
40
50
60
70
Time after L-012 (min)
Day 1
Day 3
Day 7
Day 10
Day 14

B

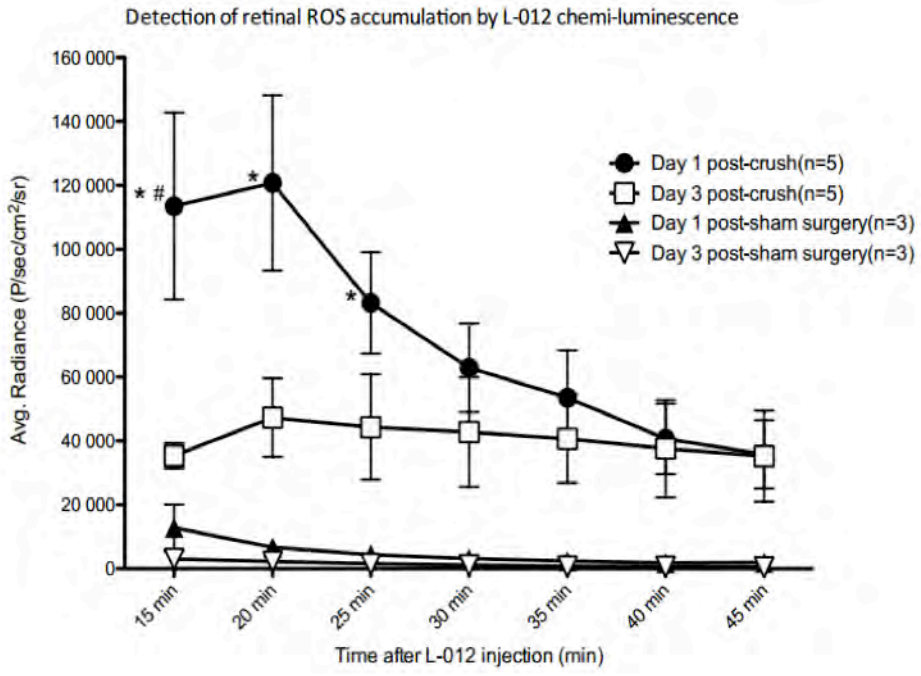
Detection of retinal ROS accumulation by L-012 chemi-luminescence
Avg. Radiance (P/sec/cm²/sr)
160 000
140 000
120 000
100 000
80 000
60 000
40 000
20 000
0
15 min
20 min
25 min
30 min
35 min
40 min
45 min
Time after L-012 injection (min)
Day 1 post-crush(n=5)
Day 3 post-crush(n=5)
Day 1 post-sham surgery(n=3)
Day 3 post-sham surgery(n=3)

Figure 3. Multiple doses of L-012 are non-toxic to the retina.

Representative images demonstrate the effects of L-012 administration to the morphology of the retina **(B-E)**. After completing the time course assessment of ROS activity post retinal I/R injury, no discernable differences were observed between animals receving L-012 in injured **(C)** or uninjured **(B)** retinas when compared with naïve samples **(A)**. Early signs of I/R-induced retinal thinning were observed between control and inured samples. Likewise, mice subjected to ONC followed by L-012 administration showed no signs of toxicity in injured **(E)** or uninjured **(D)** sections observed compared to naïve retinas **(A)**. The only difference observed between ONC **(E)** and control **(D)** eyes was the anticipated ONC-induced loss of RGCs. n=5 (ONC) or 7 (I/R).

Figure 3

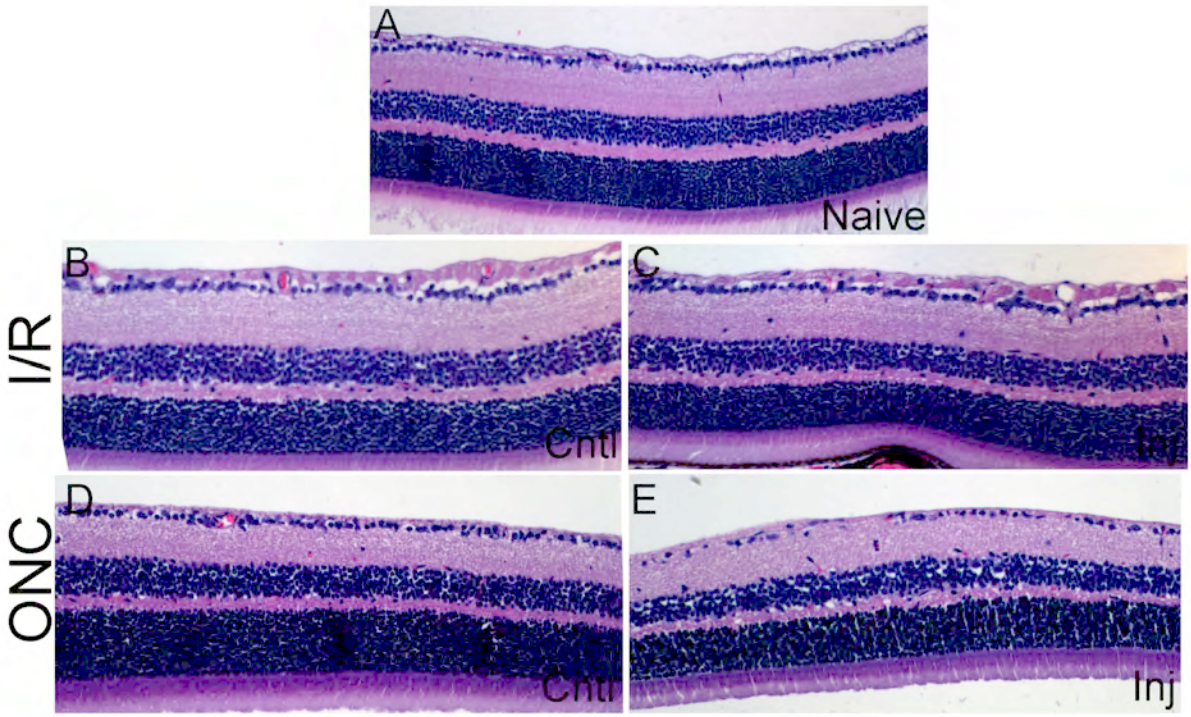

Figure 4. Visualization and validation of retinal superoxide with DHE.

Representative images from control **(A)** and ischemic retinas treated with DHE 24 **(B),** 48 **(C)**, and 72 **(D)** hours after injury demonstrating increased levels of superoxide. Differences in fluorescent intensity were quantified in the three nucleated layers of the retina. As early as 24 hours after injury, and at all time points measured, superoxide was observed to be significantly increased in the GCL **(E)**. In the INL **(F)**, there was a gradual increase in superoxide levels over time, showing signficant difference from control by 72 hours. Similar to the GCL, the ONL **(G)** was observed to have a statistically significant increase 24 hours after injury compared to control retinas. Mean ± SEM, n=4. *$p<0.05$ **$p<0.01$ ***$p<0.001$ compared between time points using one-way ANOVA followed by Bonferonni *post hoc* test.

Figure 4

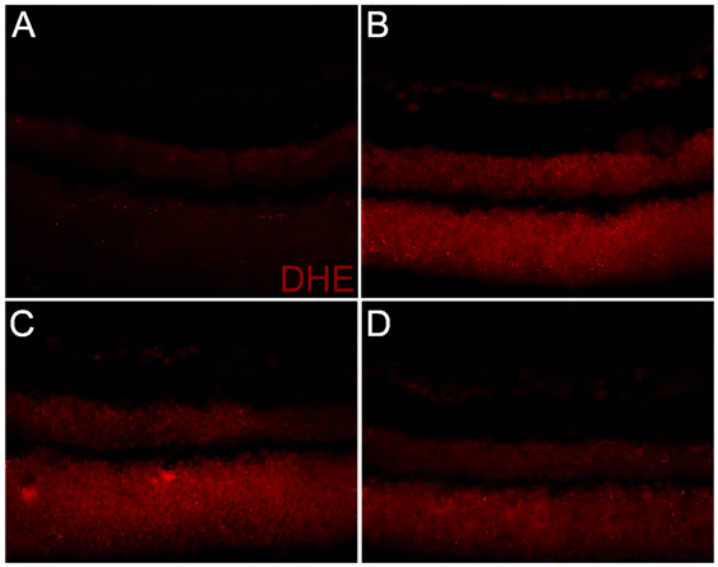
A
B
DHE
C
D

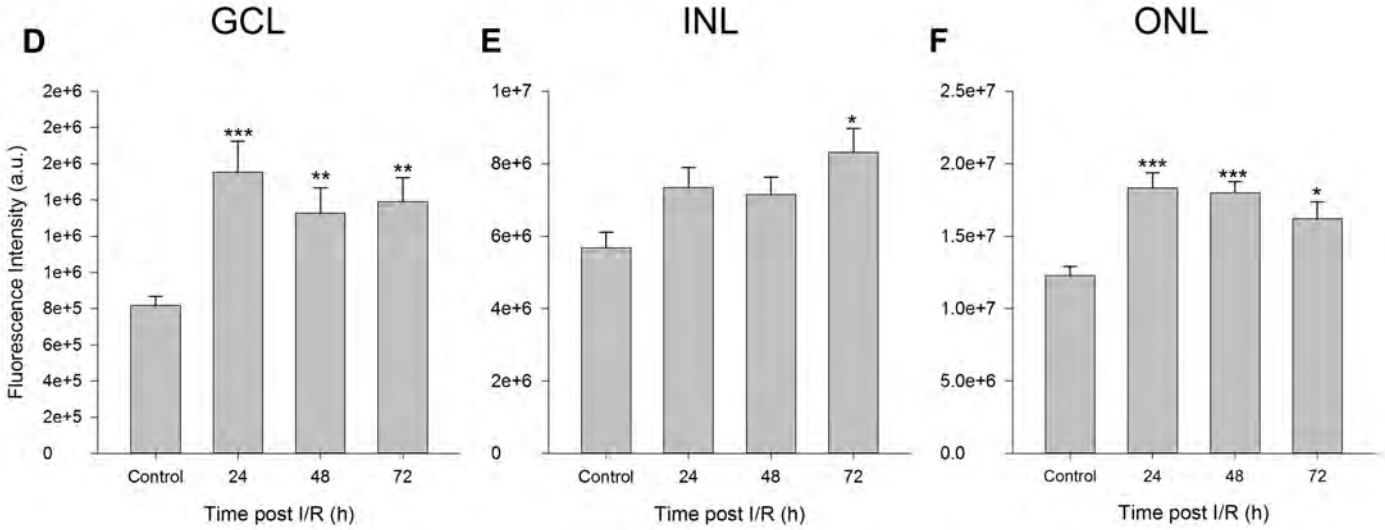
D
GCL
Fluorescence Intensity (a.u.)
2e+6
2e+6
2e+6
1e+6
1e+6
1e+6
8e+5
6e+5
4e+5
2e+5
0
***
**
**
Control
24
48
72
Time post I/R (h)
E
INL
1e+7
8e+6
6e+6
4e+6
2e+6
0
*
Control
24
48
72
Time post I/R (h)
F
ONL
2.5e+7
2.0e+7
1.5e+7
1.0e+7
5.0e+6
0.0
***
***
*
Control
24
48
72
Time post I/R (h)

Figure 5. In vivo modulation of retinal superoxide.

Selectivity of L-012 for superoxide was determined by treating mice with two known inhibitors, Apocynin and TEMPOL. **(A)** 24 and **(B)** 48 hours post I/R, both superoxide inhibitors significantly reduced L-012 chemiluminescence during the time of peak activity. No differences in efficacy were determined when comparing inhibitors. **(C)** Animals receiving ONC also showed significant reduction of superoxide activity with TEMPOL and Apocynin. Mean ± SEM, n=5. *p<0.05 **p<0.01 ***p<0.001 compared to L-012 and vehicle treated animals using one-way ANOVA followed by Bonferonni *post hoc* test.

Figure 5

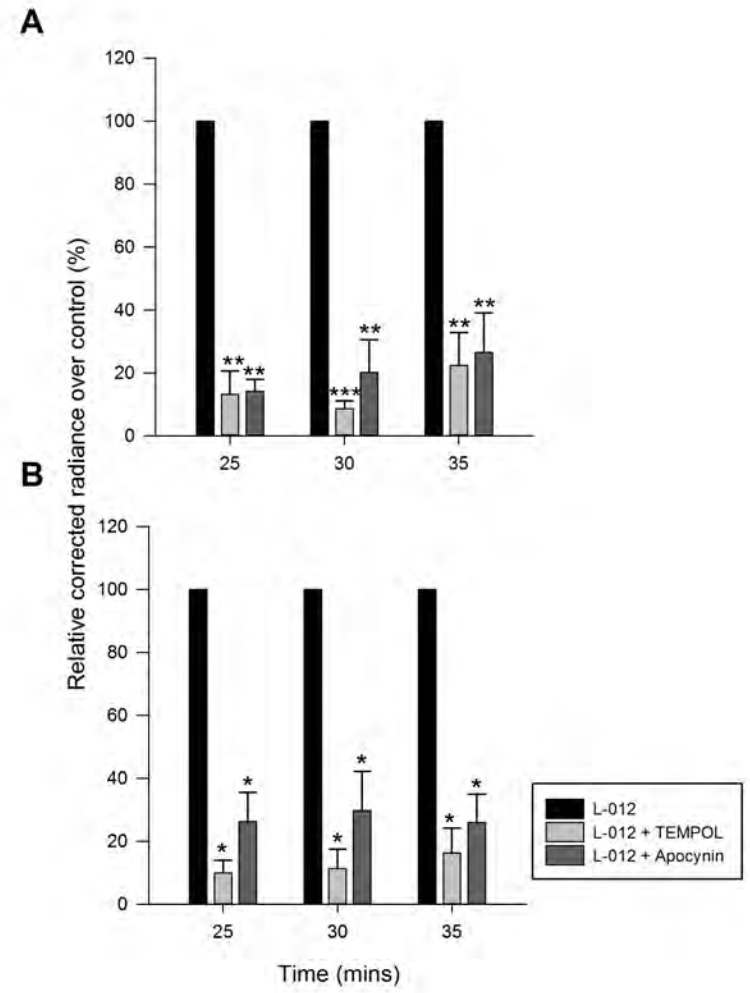
A
B
Relative corrected radiance over control (%)
120
100
80
60
40
20
0
25
30
35
Time (mins)
L-012
L-012 + TEMPOL
L-012 + Apocynin

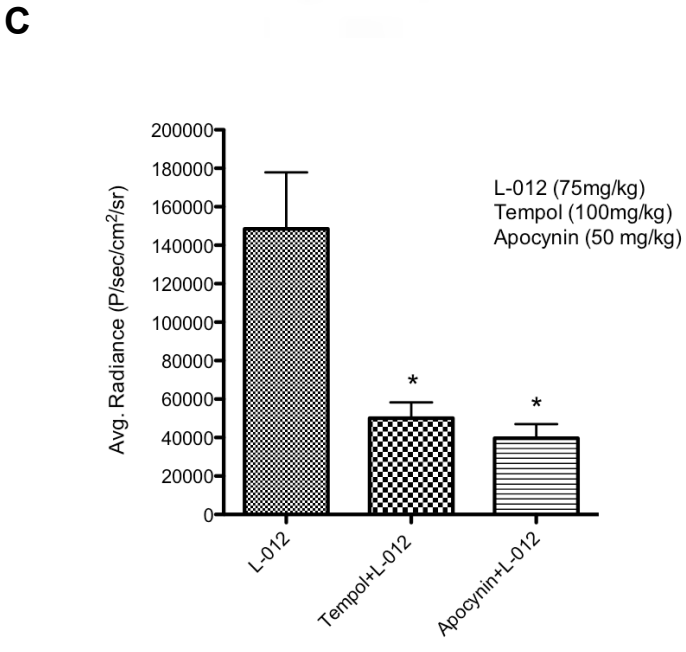
C
Avg. Radiance (P/sec/cm2/sr)
200000
180000
160000
140000
120000
100000
80000
60000
40000
20000
0
L-012 (75mg/kg)
Tempol (100mg/kg)
Apocynin (50 mg/kg)
L-012
Tempol+L-012
Apocynin+L-012

Figure 6. Inhibition of superoxide is protective against loss of visual function.

Scotopic flash ERG was measured weekly following retinal I/R and 7 days treatment with vehicle, TEMPOL, or Apocynin. **(A)** On day 28 vehicle treated animals had significantly suppressed ERG b-wave amplitudes compared with uninjured control eyes. While TEMPOL provided mild improvement, Apocynin treatment sigificantly protected against visual deficits resulting from injury. **(B)** Contralateral uninjured eyes displayed no changes in b-wave amplitudes resulting from treatment with either inihibitor. **(C)** Time course plot at a representative intensity of 3,000mcd.s/m^2 displaying changes in b-wave amplitudes in each treatment group. While all three treatment groups displayed signifcant loss of b-wave amplitudes as early as day 7, Apocynin rescued activity by day 14 and was significantly increased compared to vehicle thereafter. TEMPOL treatment was able to mildly improve b-wave amplitudes after day 14 as well, showing no difference from control eyes by day 28. Mean ± SEM, n=6/7. *$p<0.05$ **$p<0.01$ compared to control and #$p<0.05$ compared to vehicle using one-way ANOVA followed by Bonferonni *post hoc* test.

Figure 6

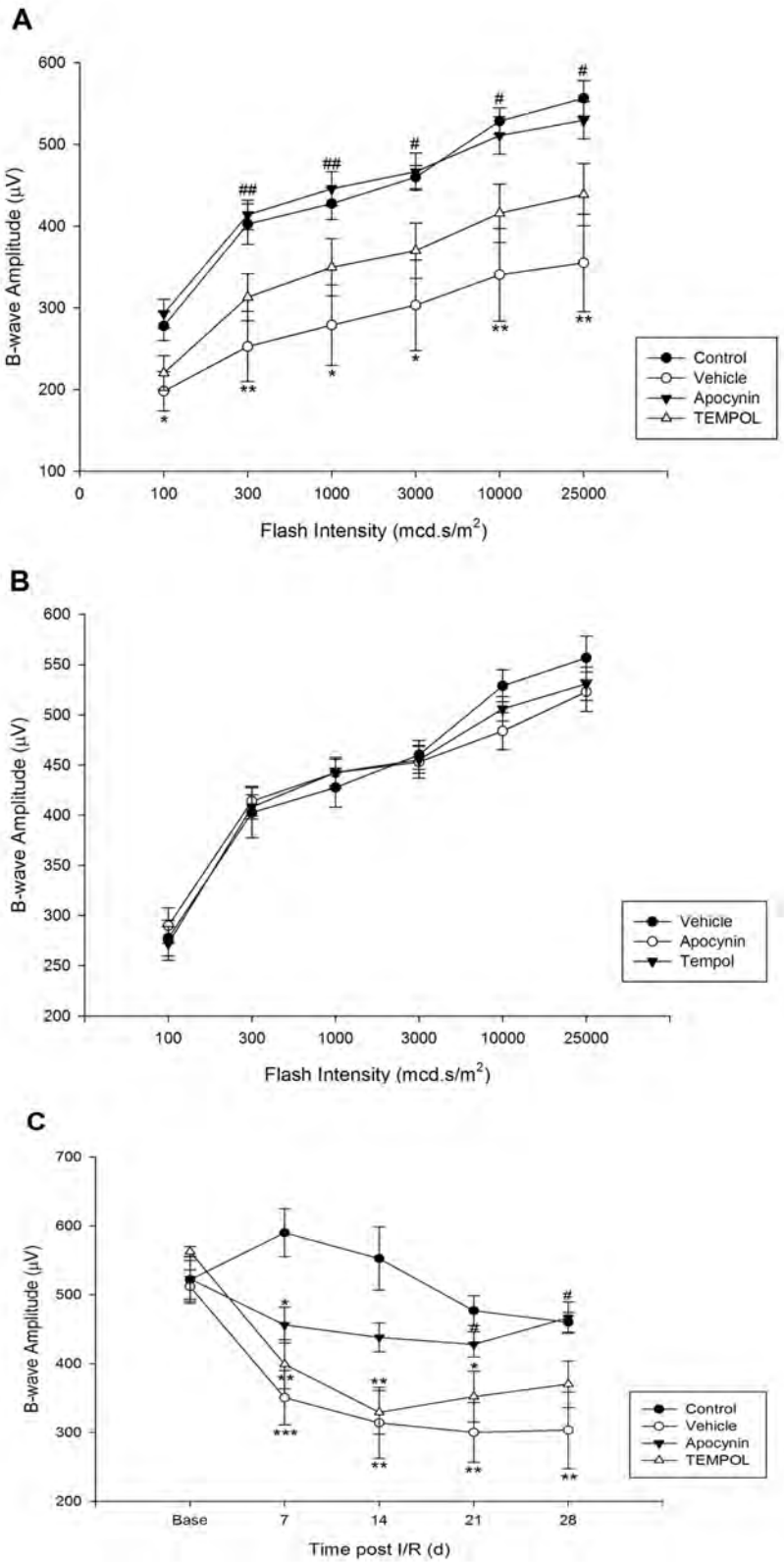
A
B-wave Amplitude (μV)
Flash Intensity (mcd.s/m²)
Control
Vehicle
Apocynin
TEMPOL
B
B-wave Amplitude (μV)
Flash Intensity (mcd.s/m²)
Vehicle
Apocynin
Tempol
C
B-wave Amplitude (μV)
Base
7
14
21
28
Time post I/R (d)
Control
Vehicle
Apocynin
TEMPOL

Figure 7. Superoxide inhibitors are neuroprotective for retinal morphology.

Retinal thicknesses were measured from H&E stained control and ischemic retinas 28 days after injury. **(A)** Vehicle treated mice had significantly decreased thickness in all quantified layers except the ONL. Treatment with TEMPOL displayed mild rescue but was still significantly reduced when compared to control retinas. Apocynin treatment significantly protected against ischemic induced changes in the retina, showing no difference to uninjured eyes. **(B)** Contralateral uninjured eyes of animals receiving either inhibitor displayed no significant difference in thickness compared to control retinas. Mean ± SEM, n=6/7. **p<0.01 ***p<0.001 compared to control and #p<0.05 ##p<0.01 ###p<0.001 compared to vehicle using one-way ANOVA followed by Bonferonni *post hoc* test.

Figure 7

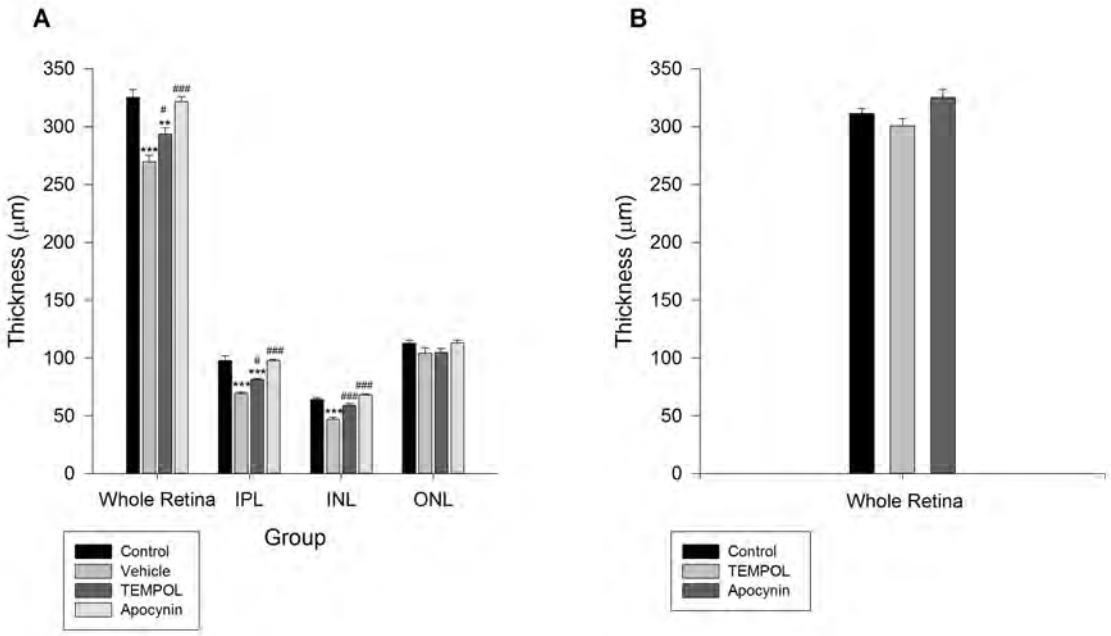
A
Thickness (μm)
350
300
250
200
150
100
50
0
Whole Retina
IPL
INL
ONL
Group
Control
Vehicle
TEMPOL
Apocynin
B
Thickness (μm)
350
300
250
200
150
100
50
0
Whole Retina
Control
TEMPOL
Apocynin

References

[1] Manzanero, S.; Santro, T.; Arumugam, T. V. Neuronal oxidative stress in acute ischemic stroke: sources and contribution to cell injury. *Neurochemistry international* **62:**712-718; 2013.

[2] Bryan, N.; Ahswin, H.; Smart, N.; Bayon, Y.; Wohlert, S.; Hunt, J. A. Reactive oxygen species (ROS)--a family of fate deciding molecules pivotal in constructive inflammation and wound healing. *European cells & materials* **24:**249-265; 2012.

[3] Emerit, J.; Edeas, M.; Bricaire, F. Neurodegenerative diseases and oxidative stress. *Biomedicine & pharmacotherapy = Biomedecine & pharmacotherapie* **58:**39-46; 2004.

[4] Arden, G. B.; Sivaprasad, S. Hypoxia and oxidative stress in the causation of diabetic retinopathy. *Current diabetes reviews* **7:**291-304; 2011.

[5] Winkler, B. S.; Boulton, M. E.; Gottsch, J. D.; Sternberg, P. Oxidative damage and age-related macular degeneration. *Molecular vision* **5:**32; 1999.

[6] Wilkinson-Berka, J. L.; Rana, I.; Armani, R.; Agrotis, A. Reactive oxygen species, Nox and angiotensin II in angiogenesis: implications for retinopathy. *Clinical science* **124:**597-615; 2013.

[7] Osborne, N. N.; Casson, R. J.; Wood, J. P.; Chidlow, G.; Graham, M.; Melena, J. Retinal ischemia: mechanisms of damage and potential therapeutic strategies. *Progress in retinal and eye research* **23:**91-147; 2004.

[8] Kanamori, A.; Catrinescu, M. M.; Kanamori, N.; Mears, K. A.; Beaubien, R.; Levin, L. A. Superoxide is an associated signal for apoptosis in axonal injury. *Brain : a journal of neurology* **133:**2612-2625; 2010.

[9] Aslan, M.; Cort, A.; Yucel, I. Oxidative and nitrative stress markers in glaucoma. *Free radical biology & medicine* **45:**367-376; 2008.

[10] Kuriyama, H.; Waki, M.; Nakagawa, M.; Tsuda, M. Involvement of oxygen free radicals in experimental retinal ischemia and the selective vulnerability of retinal damage. *Ophthalmic research* **33:**196-202; 2001.

[11] Bonne, C.; Muller, A.; Villain, M. Free radicals in retinal ischemia. *General pharmacology* **30:**275-280; 1998.

[12] Halliwell, B.; Whiteman, M. Measuring reactive species and oxidative damage in vivo and in cell culture: how should you do it and what do the results mean? *British journal of pharmacology* **142:**231-255; 2004.

[13] Nishinaka, Y.; Aramaki, Y.; Yoshida, H.; Masuya, H.; Sugawara, T.; Ichimori, Y. A new sensitive chemiluminescence probe, L-012, for measuring the production of superoxide anion by cells. *Biochemical and biophysical research communications* **193:**554-559; 1993.

[14] Kielland, A.; Blom, T.; Nandakumar, K. S.; Holmdahl, R.; Blomhoff, R.; Carlsen, H. In vivo imaging of reactive oxygen and nitrogen species in inflammation using the luminescent probe L-012. *Free radical biology & medicine* **47:**760-766; 2009.

[15] Zhou, J.; Tsai, Y. T.; Weng, H.; Tang, L. Noninvasive assessment of localized inflammatory responses. *Free radical biology & medicine* **52:**218-226; 2012.

[16] Kim, B. J.; Braun, T. A.; Wordinger, R. J.; Clark, A. F. Progressive morphological changes and impaired retinal function associated with temporal regulation of gene expression after retinal ischemia/reperfusion injury in mice. *Molecular neurodegeneration* **8:**21; 2013.

[17] Asghar, M. N.; Emani, R.; Alam, C.; Helenius, T. O.; Gronroos, T. J.; Sareila, O.; Din, M. U.; Holmdahl, R.; Hanninen, A.; Toivola, D. M. In vivo imaging of reactive oxygen and nitrogen species in murine colitis. *Inflammatory bowel diseases* **20:**1435-1447; 2014.

[18] Wassmann, S.; Stumpf, M.; Strehlow, K.; Schmid, A.; Schieffer, B.; Bohm, M.; Nickenig, G. Interleukin-6 induces oxidative stress and endothelial dysfunction by overexpression of the angiotensin II type 1 receptor. *Circulation research* **94:**534-541; 2004.

[19] Lu, Q.; Yang, Y.; Villar, V. A.; Asico, L.; Jones, J. E.; Yu, P.; Li, H.; Weinman, E. J.; Eisner, G. M.; Jose, P. A. D5 dopamine receptor decreases NADPH oxidase, reactive oxygen species and blood pressure via heme oxygenase-1. *Hypertension research : official journal of the Japanese Society of Hypertension* **36:**684-690; 2013.

[20] Zhang, Q. G.; Laird, M. D.; Han, D.; Nguyen, K.; Scott, E.; Dong, Y.; Dhandapani, K. M.; Brann, D. W. Critical role of NADPH oxidase in neuronal oxidative damage and microglia activation following traumatic brain injury. *PloS one* **7:**e34504; 2012.

[21] Dohare, P.; Hyzinski-Garcia, M. C.; Vipani, A.; Bowens, N. H.; Nalwalk, J. W.; Feustel, P. J.; Keller, R. W., Jr.; Jourd'heuil, D.; Mongin, A. A. The neuroprotective properties of the superoxide dismutase mimetic tempol correlate with its ability to reduce pathological glutamate release in a rodent model of stroke. *Free radical biology & medicine* **77:**168-182; 2014.

[22] Daiber, A.; Oelze, M.; August, M.; Wendt, M.; Sydow, K.; Wieboldt, H.; Kleschyov, A. L.; Munzel, T. Detection of superoxide and peroxynitrite in model systems and mitochondria by the luminol analogue L-012. *Free radical research* **38:**259-269; 2004.

[23] Sohn, H. Y.; Gloe, T.; Keller, M.; Schoenafinger, K.; Pohl, U. Sensitive superoxide detection in vascular cells by the new chemiluminescence dye L-012. *Journal of vascular research* **36:**456-464; 1999.

[24] Hu, X. T.; Ding, C.; Zhou, N.; Xu, C. Quercetin protects gastric epithelial cell from oxidative damage in vitro and in vivo. *European journal of pharmacology* **754:**115-124; 2015.

[25] Liu, Y.; McDowell, C. M.; Zhang, Z.; Tebow, H. E.; Wordinger, R. J.; Clark, A. F. Monitoring retinal morphologic and functional changes in mice following optic nerve crush. *Investigative ophthalmology & visual science* **55:**3766-3774; 2014.

[26] Kim, B. J.; Siverman, S. M.; Liu, Y.; Wordinger, R. J.; Pang, I. H.; Clark, A. F. In vitro and in vivo protective effects of cJun N-terminal kinase inhibitors on retinal ganglion cells. *Mol Neurodegener (submitted)*; 2015.

[27] Mehta, S. L.; Manhas, N.; Raghubir, R. Molecular targets in cerebral ischemia for developing novel therapeutics. *Brain research reviews* **54:**34-66; 2007.

[28] Fraser, P. A. The role of free radical generation in increasing cerebrovascular permeability. *Free radical biology & medicine* **51:**967-977; 2011.

[29] Du, Y.; Veenstra, A.; Palczewski, K.; Kern, T. S. Photoreceptor cells are major contributors to diabetes-induced oxidative stress and local inflammation in the retina. *Proceedings of the National Academy of Sciences of the United States of America* **110:**16586-16591; 2013.

[30] Sasaki, M.; Ozawa, Y.; Kurihara, T.; Noda, K.; Imamura, Y.; Kobayashi, S.; Ishida, S.; Tsubota, K. Neuroprotective effect of an antioxidant, lutein, during retinal inflammation. *Investigative ophthalmology & visual science* **50:**1433-1439; 2009.

[31] Stevenson, L.; Matesanz, N.; Colhoun, L.; Edgar, K.; Devine, A.; Gardiner, T. A.; McDonald, D. M. Reduced nitro-oxidative stress and neural cell death suggests a protective role for microglial cells in TNFalpha-/- mice in ischemic retinopathy. *Investigative ophthalmology & visual science* **51:**3291-3299; 2010.

[32] Edgar, K. S.; Matesanz, N.; Gardiner, T. A.; Katusic, Z. S.; McDonald, D. M. Hyperoxia depletes (6R)-5,6,7,8-tetrahydrobiopterin levels in the neonatal retina: implications for nitric oxide synthase function in retinopathy. *The American journal of pathology* **185:**1769-1782; 2015.

[33] Fernandes, D. C.; Wosniak, J., Jr.; Pescatore, L. A.; Bertoline, M. A.; Liberman, M.; Laurindo, F. R.; Santos, C. X. Analysis of DHE-derived oxidation products by HPLC in the

assessment of superoxide production and NADPH oxidase activity in vascular systems. *American journal of physiology. Cell physiology* **292:**C413-422; 2007.

[34] Gomes, A.; Fernandes, E.; Lima, J. L. Fluorescence probes used for detection of reactive oxygen species. *Journal of biochemical and biophysical methods* **65:**45-80; 2005.

[35] Kalyanaraman, B.; Darley-Usmar, V.; Davies, K. J.; Dennery, P. A.; Forman, H. J.; Grisham, M. B.; Mann, G. E.; Moore, K.; Roberts, L. J., 2nd; Ischiropoulos, H. Measuring reactive oxygen and nitrogen species with fluorescent probes: challenges and limitations. *Free radical biology & medicine* **52:**1-6; 2012.

[36] Yazdani, M. Concerns in the application of fluorescent probes DCDHF-DA, DHR 123 and DHE to measure reactive oxygen species in vitro. *Toxicology in vitro : an international journal published in association with BIBRA*; 2015.

[37] Zhao, H.; Joseph, J.; Fales, H. M.; Sokoloski, E. A.; Levine, R. L.; Vasquez-Vivar, J.; Kalyanaraman, B. Detection and characterization of the product of hydroethidine and intracellular superoxide by HPLC and limitations of fluorescence. *Proceedings of the National Academy of Sciences of the United States of America* **102:**5727-5732; 2005.

[38] Zielonka, J.; Lambeth, J. D.; Kalyanaraman, B. On the use of L-012, a luminol-based chemiluminescent probe, for detecting superoxide and identifying inhibitors of NADPH oxidase: a reevaluation. *Free radical biology & medicine* **65:**1310-1314; 2013.

[39] Ju, W. K.; Kim, K. Y.; Park, S. J.; Park, D. K.; Park, C. B.; Oh, S. J.; Chung, J. W.; Chun, M. H. Nitric oxide is involved in sustained and delayed cell death of rat retina following transient ischemia. *Brain research* **881:**231-236; 2000.

[40] Ostwald, P.; Goldstein, I. M.; Pachnanda, A.; Roth, S. Effect of nitric oxide synthase inhibition on blood flow after retinal ischemia in cats. *Investigative ophthalmology & visual science* **36:**2396-2403; 1995.

[41] Chiarotto, G. B.; Drummond, L.; Cavarretto, G.; Bombeiro, A. L.; de Oliveira, A. L. Neuroprotective effect of tempol (4 hydroxy-tempo) on neuronal death induced by sciatic nerve transection in neonatal rats. *Brain research bulletin* **106:**1-8; 2014.

[42] Deng-Bryant, Y.; Singh, I. N.; Carrico, K. M.; Hall, E. D. Neuroprotective effects of tempol, a catalytic scavenger of peroxynitrite-derived free radicals, in a mouse traumatic brain injury model. *Journal of cerebral blood flow and metabolism : official journal of the International Society of Cerebral Blood Flow and Metabolism* **28:**1114-1126; 2008.

[43] Dvoriantchikova, G.; Grant, J.; Santos, A. R.; Hernandez, E.; Ivanov, D. Neuronal NAD(P)H oxidases contribute to ROS production and mediate RGC death after ischemia. *Investigative ophthalmology & visual science* **53:**2823-2830; 2012.

[44] Wilkinson-Berka, J. L.; Deliyanti, D.; Rana, I.; Miller, A. G.; Agrotis, A.; Armani, R.; Szyndralewiez, C.; Wingler, K.; Touyz, R. M.; Cooper, M. E.; Jandeleit-Dahm, K. A.; Schmidt, H. H. NADPH oxidase, NOX1, mediates vascular injury in ischemic retinopathy. *Antioxidants & redox signaling* **20:**2726-2740; 2014.

[45] Chan, E. C.; van Wijngaarden, P.; Liu, G. S.; Jiang, F.; Peshavariya, H.; Dusting, G. J. Involvement of Nox2 NADPH oxidase in retinal neovascularization. *Investigative ophthalmology & visual science* **54:**7061-7067; 2013.

[46] Yokota, H.; Narayanan, S. P.; Zhang, W.; Liu, H.; Rojas, M.; Xu, Z.; Lemtalsi, T.; Nagaoka, T.; Yoshida, A.; Brooks, S. E.; Caldwell, R. W.; Caldwell, R. B. Neuroprotection from retinal ischemia/reperfusion injury by NOX2 NADPH oxidase deletion. *Investigative ophthalmology & visual science* **52:**8123-8131; 2011.

[47] Fujita, T.; Hirooka, K.; Nakamura, T.; Itano, T.; Nishiyama, A.; Nagai, Y.; Shiraga, F. Neuroprotective effects of angiotensin II type 1 receptor (AT1-R) blocker via modulating AT1-R signaling and decreased extracellular glutamate levels. *Investigative ophthalmology & visual science* **53:**4099-4110; 2012.

[48] Al-Shabrawey, M.; Bartoli, M.; El-Remessy, A. B.; Platt, D. H.; Matragoon, S.; Behzadian, M. A.; Caldwell, R. W.; Caldwell, R. B. Inhibition of NAD(P)H oxidase activity blocks vascular endothelial growth factor overexpression and neovascularization during ischemic retinopathy. *The American journal of pathology* **167:**599-607; 2005.

[49] Al-Shabrawey, M.; Rojas, M.; Sanders, T.; Behzadian, A.; El-Remessy, A.; Bartoli, M.; Parpia, A. K.; Liou, G.; Caldwell, R. B. Role of NADPH oxidase in retinal vascular inflammation. *Investigative ophthalmology & visual science* **49:**3239-3244; 2008.

CHAPTER IV

DISCUSSION

Retinal ischemia and subsequent reperfusion induces a cascade of pathological mechanisms resulting in permanent tissue damage and irreversible loss of vision to patients as well as in experimental animal models (Osborne et al. 2004). While not ignoring the other biological processes simultaneously occurring, we have focused our efforts in understanding a more precise role for the neuroinflammatory response and accumulation of deleterious ROS, including superoxide. Each of these responses to injury has been implicated in a vast range of chronic neurodegenerative diseases and disorders throughout the CNS, including but not limited to Alzheimers, Parkinsons, ALS, Multiple Sclerosis, and glaucoma (Lipton 1999; Lyman et al. 2014; Orsini et al. 2014; Soto and Howell 2014). Neuroinflammation is a complex reaction comprised of both an early innate response, primarily by activation and increased populations of resident microglia, followed by chronic prolonged macroglial activation. These activities result in increased production of a host of chemokines, cytokines, complement cascade components, and other pro-inflammatory factors (Block and Hong 2005; Pekny and Pekna 2014). Oxidative stress results in an abundance of ROS or RNS that overwhelms the endogenous enzymes designed to protect cells and tissues against of protein and lipid modifications and ultimately cell death (Bonne et al. 1998). Collectively, our work displays the spatiotemporal changes of these two mechanisms of damage to the visual axis resulting from retinal I/R injury. For the first, time we have characterized the changes in C1q expression, activity of the microglia, astrocytes and Müller cells, and increases in superoxide and ROS production.

We separately targeted both of these responses to observe how modulation may be protective against the morphological and functional deficits of retinal I/R injury (Kim et al. 2013). Utilizing *C1qa*-deficient mice, we were successfully able to rescue morphological changes; however, functional losses persisted. We attributed these results from our functional studies to the lack of effect the absence of *C1qa* had on the reactive astroglial response. Developmental studies have demonstrated astrocytes play a key role in synaptogenesis (Chung et al. 2013). As opposed to microglia, astrocytes make direct contact and communicate with neurons. Through secretion of soluble factors, including thrombospondins (TSPs), astrocytes significantly increase the number of synapses and induce proper synapse structural formation in cultured RGCs (Christopherson et al. 2005; Ullian et al. 2001). Further, astrocytic processes have been observed in live imaging studies to extend specifically into sites of synaptic activity in the early postnatal mouse brain (Allen and Barres 2005; Hirrlinger et al. 2004). Further signaling studies implicated ephrins and their appropriate receptors to mediate these interactions (Murai et al. 2003).

Given their role in synaptic formation, it comes as no surprise astrocytes are also involved in synaptic elimination. While microglia are predominantly identified as the resident phagocytes of the CNS, transcriptome analysis reveals astrocytes also possess the appropriate machinery for phagocytosis (Cahoy et al. 2008). Mice deficient in either MEGF10 or MERTK, both phagocytic receptors, displayed a significant reduction in normal synapse elimination during retinogeniculate development (Chung et al. 2013). Indirectly, astrocytes may also be responsible for TGFβ-mediated C1q synaptic pruning (Chung et al. 2015), implicating a shared role for microglia and astrocytes in synaptic maturation. However, in addition to neuroinflammation, another unifying characteristic of neurodegenerative diseases is the

occurrence of synaptic impairment, often preceding neuronal loss. Synaptic impairment includes complete loss of synaptic function and impaired plasticity, leaving neurons incapable of neurotransmission prior to cell death (Lyman et al. 2014). Pathological hallmarks in diseases such as AD and PD are known to stimulate astrocyte proliferation and reactive gliosis (Pekny et al. 2014). Evidence of synaptic stripping by astrocytes has been observed in the withdrawal of synapses following lesion of the facial nerve (Faissner et al. 2010). Therefore, it remains a possibility that failure to attenuate reactive astrogliosis through elimination of *C1q* may result in astrocyte-mediated synaptic impairment and elimination.

In our own studies, we have demonstrated there is a significant reduction in pre and post-synaptic proteins in the SC following retinal I/R (Kim et al., submitted). However, our current work did not determine whether *C1qa*-deficieincy had any affect on synaptic activity. Future studies using markers such as VGLUT2 and SNAP25 in the retina and SC would be useful for quantifying remaining functional synapses. Array tomography, as demonstrated by Stevens and colleagues (Stevens et al. 2007), is a powerful tool for identifying close apposition of synaptic markers indicating maturation. Synaptic markers used in combination with GFAP may implicate astrocytes in synaptic impairment following retinal I/R. Ultrastructural studies using transmission electron microscopy (TEM) and immuno-gold labeling could further show synaptic elimination by reactive astrocytes. While $GFAP^{-/-}Vim^{-/-}$ mice were observed to have increased infarct sizes following ischemic injury (Pekny and Pekna 2004), it is possible a $C1qa^{-/-}GFAP^{-/-}$ mouse may attenuate the pathogenic activities of both microglia and astrocytes. Thus further improving neuroprotection against retinal I/R, as implicated in our studies there is a shared role in the pathological process of chronic neuroinflammation.

Despite being conducted separately to target two different pathological mechanisms for neuroprotective potential, we have identified a temporal relationship between the onset of ROS generation and accumulation, and the neuroinflammatory response, in the context of retinal I/R injury. With this information, it is tempting to speculate the potential relationship between these two biological processes mediating I/R-induced damage. One possible mechanism to consider is that increased expression of C1q stimulates the production of superoxide and other ROS (Figure 1). We identified significant upregulation of C1q as early as day 3 post I/R (Ch. II, Figure 1B) compared with control retinas. At the same time point DHE labeling also confirmed the accumulation of superoxide (Ch. III, Figure 4D). Of note, L-012 identified peak ROS activity 24 hours post injury, and while we did not observe for C1q increases at this same time, other studies have seen changes in C1q expression within the first 24 hours (Mack et al. 2006; Schafer et al. 2000). Microglia are often the first responders to the site of injury, and as such are likely responsible for any initial changes in C1q expression.

The source of C1q-stimulated ROS may be from infiltrating neutrophils. Within hours of reperfusion following cerebral or retinal ischemia, there is increased permeability of blood-brain and blood-retinal barriers respectively, leading to significant accumulation of leukocytes (Lipton 1999; Tsujikawa et al. 1999). Further, neutrophils are known to have a unique receptor ($C1qR_{O2-}$) interacting with the collagen-like domain of C1q that specifically triggers superoxide production and does not induce degranulation or phagocytosis (Ruiz et al. 1995; Tenner 1998). Another possibility is C1q-mediated production of ROS from neurons, as they express the appropriate receptors to bind C1q on their surface. *In vitro* studies demonstrate cultured neurons when treated with recombinant C1q results in significant increases of superoxide and ROS (Luo et al. 2003).

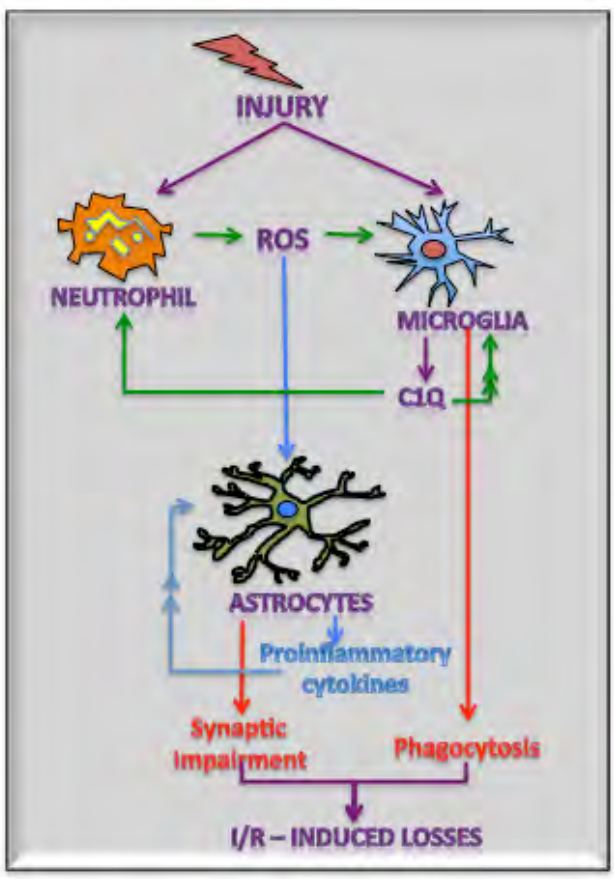

Figure 1. Pathway of C1q-stimulated ROS production. Retinal I/R-induced degeneration in the visual axis is mediated by activated microglia responding to injury that produces C1q, which then binds to infiltrating neutrophils resulting in ROS generation. This ROS activates glial cells to release proinflammatory factors as well as more C1q that results in a feed-forward mechanism of chronic neuroinflammation and permanent retinal damage.

Additionally, mitochondria from brain neurons of *C1qa*-deficient mice following hypoxic-ischemic (HI) injury display a significantly reduced release of ROS compared with WT mice. This reduction was attributed to an overall protection observed in $C1q^{-/-}$ mice after injury (Ten et al. 2010). Changes in ROS, be it from infiltrating neutrophils or resident neurons, likely further

activates resident microglia resulting in a feed-forward loop causing further increases in C1q and other pro-inflammatory factors.

Future studies should quantify the extent of blood-retinal barrier breakdown post retinal I/R injury. This can be performed using Evan's blue dye tissue permeability and calculating the concentration of dye present in the blood and in the retina. Infiltration of leukocytes, including the role of neutrophil-mediated superoxide production, may be observed by immunofluorescence or flow cytometry with cell-specific markers such as CD44, GR1, or CD11b. Another option is perfusion of the mouse using fluorescently-tagged conacavalin A, a lectin known to label adherent leukocytes, followed by counts using high resolution microscopy (Kaji et al. 2007). To test whether C1q is responsible for ROS production following retinal I/R, we would expect to see a dramatic reduction of both L-012 and DHE signal in our *C1qa*$^{-/-}$ mice compared to WT mice. Further, biochemical oxidative stress assays measuring lipid peroxidation and protein oxidation would also confirm a C1q-dependent role for ROS accumulation. *In vitro,* we could isolate either the RGCs or use a mixed retinal culture from *C1qa*$^{-/-}$ mice and measure ROS production under hypoxic conditions in comparison to retinal neurons from WT mice. In our studies, we only investigated ROS in the retina, but it is yet to be determined if and to what extent I/R injury in the eye causes increased free radical production in the SC. Much of our findings in the retina were mirrored in the SC, therefore it is likely DHE analysis would reveal significant production of ROS in the visual centers of the brain. Quantifying the differences in ROS between WT and *C1qa*$^{-/-}$ mice further implicates the role of C1q in superoxide production. L-012 has the ability to cross the blood-retinal barrier, and it may show a similar potential at the blood-brain barrier in animal models of focal ischemia. Whether or not L-012 luminescence can be detected through the skull is yet to be tested. Our time course studies using L-012 did not reveal any *in vivo* ROS

detection in the area of the brain of our mice. Whether this is due to an issue of sensitivity of the signal through the skull and other brain tissues, or the blood-brain barrier remains in tact after retinal I/R remains to be determined.

However, the more likely scenario is increased superoxide and ROS are produced locally by cells in response to injury, causing upregulation of C1q (Figure 2). Given our results that inhibition of ROS was more effective in both long-term morphological and functional preservation compared with deletion of *C1qa*, it is likely ROS acts upstream from increased complement expression.

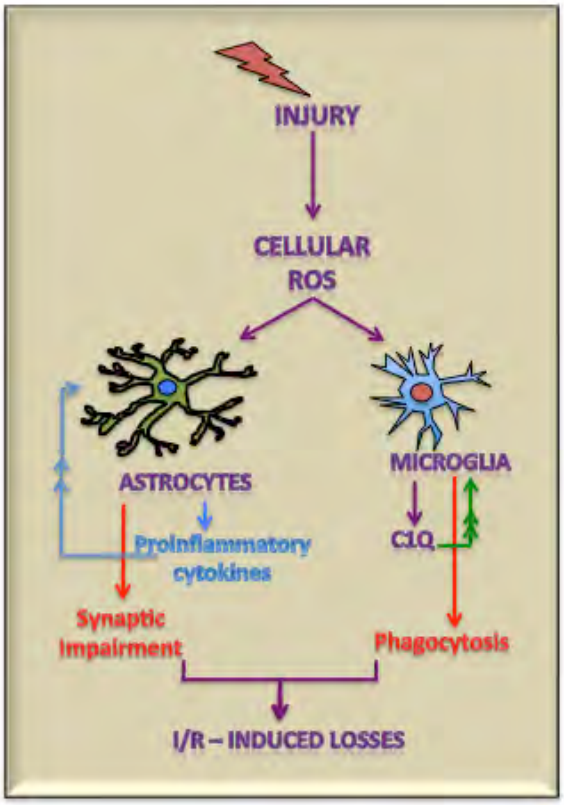

Figure 2. Pathway of cellular ROS stimulation of C1q. Retinal I/R causes glial cells or neurons to generate excess ROS in turn activating other surrounding astrocytes and microglia to produce proinflammatory factors and C1q, similarly resulting in feed-forward mechanism causing degeneration

It is generally believed following I/R injury, a burst of superoxide occurs after degradation of ATP and increases in intracellular calcium in neurons, although activated glial cells also serve as important sources of free radical generation (Osborne et al. 2004). Neuronal superoxide production results primarily from ischemic interruption of the mitochondrial respiratory chain (MRC) and upregulation of NADPH-Oxidase (NOX) shortly after reperfusion (Niatsetskaya et al. 2012; Vallet et al. 2005). A third source of neuronal free radical production following retinal ischemia is linked to the increased production of neuronal nitric oxide synthase (nNOS) (Neufeld et al. 2002). Nitric oxide (NO) is a free radical that serves various important roles in regulating vascular tone in the CNS (Chrissobolis and Faraci 2008). It also reacts with superoxide in the formation of the oxidant peroxynitrite (Manzanero et al. 2013). These sources of neuronal ROS production may catalyze activation of microglia stimulating the increased C1q production.

In addition to neurons, both microglia and astrocytes possess the necessary machinery for synthesis of superoxide. Much like neuronal production, microglia and astrocytes have increased NOX activity in response to a wide host of stimuli including neurodegenerative hallmark proteins such as amyloid beta (Aβ) and α-synuclein, proinflammatory mediators lipopolysaccharide (LPS) and interferon gamma (IFNγ), and ischemic injury (Block and Hong 2005; Nayernia et al. 2014; Qin et al. 2002; Sorce and Krause 2009; Zhang et al. 2005). Interestingly, many neurodegenerative diseases have been identified to share similar activation of the same NOX subunit, NOX2. Profiling studies have revealed that in comparison to neurons and astroglia, NOX2 is most significantly expressed in microglia (Gao et al. 2012; Sorce and Krause 2009). NOX2 is the catalytic subunit of phagocyte NADPH oxidase (PHOX), which represents the primary source of superoxide production in microglia (Block and Hong 2005). It is believed that PHOX activity not only leads to extracellular generation of ROS, but also causes

intracellular ROS responsible for activation of the microglia and production of proinflammatory factors. (Qin et al. 2004; Wang et al. 2004). It is possible the intracellular ROS activation in microglia is the reaction responsible for the increased production of C1q that we and other studies have observed. This increased C1q expression may further activate microglia causing a chronic response of activated microglia producing C1q. Counter intuitively, neurons are capable of producing ROS, but they themselves have a limited antioxidant defense system. However, unlike microglia, astrocytes have direct contact with neurons and may provide protection against oxidative stress (Cabezas et al. 2012). Astrocytes are able to produce the endogenous defense enzymes SOD, glutathione, and catalase (Cabezas et al. 2012). Several studies have also indicated astrocytes provide glutathione support to neurons in the presence of oxidative stress (Barreto et al. 2011; Chen et al. 2001; Shih et al. 2003). Furthermore, mutations in SOD1 are linked to a familial form of ALS, a neurodegenerative motor neuron disease. Knockout of this mutation selectively in astrocytes was shown to significantly slow disease progression, implicating the role of SOD1 in protection (Yamanaka et al. 2008). Therefore, astrocytes may initially represent a defense against neuronal oxidative stress. However, when accumulating ROS leads to injury of astrocytes, this may cause a shift from antioxidant to free radical production.

Future studies will help identify the link between ROS production and accumulation as well as the neuroinflammatory response by glial cells following retinal I/R injury. It is essential for us to identify the primary source of increased C1q expression. Since C1q is a secreted protein, using fluorescent *in situ* hybridization (FISH) we can colocalize increased mRNA synthesis of *C1qa* with cell-specific markers such as Iba1, GFAP, or Rbpms. We expect these experiments will implicate microglia in this increased production. Further, we could also culture microglia under hypoxic conditions to observe if this leads to changes in C1q expression. Our

studies identify the NOX inhibitor Apocynin as a potent neuroprotective compound, capable of rescuing visual function and retinal morphology. If ROS is responsible for stimulating astrocytes and microglia, using activation markers such as GFAP and CD68 respectively, we can identify attenuation of reactive profiles for these glial cells following Apocynin treatment compared to untreated animals. Further, GFAP and Iba1 immunolabeling similar to the staining shown in our studies, will identify changes cell morphologies as well as population density indicating a reactive or resting state. We would expect these findings to be similar to uninjured controls, if ROS is responsible for neuroinflammation. As previously discussed, there is extensive evidence indicating that both microglia and NOX2 are involved in several neurodegenerative conditions. Deletion of *NOX2* was shown to be neuroprotective following retinal I/R as well (Yokota et al. 2011). Therefore, we would expect that Apocynin treatment, which is a selective NOX inhibitor, to significantly reduce NOX2 expression after I/R injury. This could be demonstrated quantitatively in mRNA using qPCR and antibodies against NOX2 on western blots for protein analysis. *In situ* hybridization or use of $Cx3CR1^{GFP/+}$ mice that have fluorescently labeled microglia could also colocalize changes in NOX2 with our previously demonstrated increased population of microglia. Much of our study has focused on the response from retinal and SC glia; however, neurons also are established producers of superoxide. Labeling with DHE nonspecifically displayed upregulation of superoxide within the retina. However, MitoSOX more accurately identifies mitochondrial production. Following retinal I/R injury MitoSOX may demonstrate specific types of neurons responsible for these changes.

In conclusion, we have characterized a spatiotemporal response of ROS and the neuroinflammatory response over a 28 day time course following retinal I/R injury in both the retina and the SC. We built upon these findings by evaluating their impact on pathological,

morphological, and functional deficits through genetic and pharmacological ablative methods. Inhibition of ROS was found to be more efficacious than complete deletion of *C1qa* as determined in our histological and functional neuroprotective assays. With this information, we have constructed two potential pathways for the order of activation of these neurodegenerative mediators following retinal I/R injury (Figure 3). Based on our data, it appears that ROS occurs upstream from both C1q upregulation and glial cell activation.

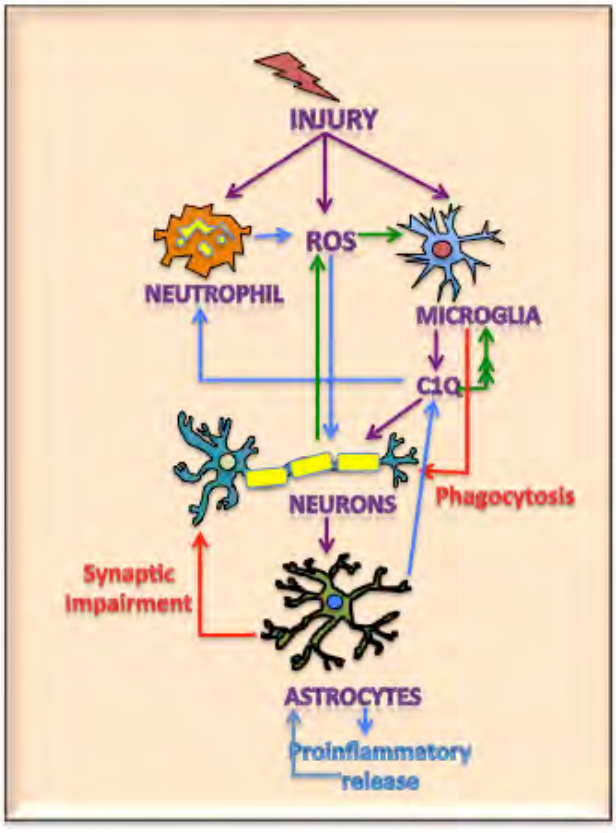

Figure 3. ROS and neuroinflammation mediate neuronal degeneration. A proposed schematic of the intricate and complex relationship that exists between neurons, glial cells, and their individual responses to retinal I/R.

In addition, we also have demonstrated a novel method for noninvasive *in vivo* measurement of superoxide and ROS. With L-012, we were not only able to track these oxidative changes in the retinas of mice over time, but also displayed in real time the effectiveness of two different ROS inhibitors. L-012 has great potential as a diagnostic tool in experimental animal models of injury or disease as several others and we have shown. ROS is a transient event following ischemic injury, and there are other known mediators that may stimulate a chronic neuroinflammatory response in neurodegenerative diseases. We demonstrate here the potential impact that modulation of C1q and ROS would have on disease progression.

References

Allen NJ, Barres BA. 2005. Signaling between glia and neurons: focus on synaptic plasticity. Curr Opin Neurobiol 15:542-8.

Barreto GE, Gonzalez J, Torres Y, Morales L. 2011. Astrocytic-neuronal crosstalk: implications for neuroprotection from brain injury. Neurosci Res 71:107-13.

Block ML, Hong JS. 2005. Microglia and inflammation-mediated neurodegeneration: multiple triggers with a common mechanism. Prog Neurobiol 76:77-98.

Bonne C, Muller A, Villain M. 1998. Free radicals in retinal ischemia. Gen Pharmacol 30:275-80.

Cabezas R, El-Bacha RS, Gonzalez J, Barreto GE. 2012. Mitochondrial functions in astrocytes: neuroprotective implications from oxidative damage by rotenone. Neurosci Res 74:80-90.

Cahoy JD, Emery B, Kaushal A, Foo LC, Zamanian JL, Christopherson KS, Xing Y, Lubischer JL, Krieg PA, Krupenko SA and others. 2008. A transcriptome database for astrocytes, neurons, and oligodendrocytes: a new resource for understanding brain development and function. J Neurosci 28:264-78.

Chen Y, Vartiainen NE, Ying W, Chan PH, Koistinaho J, Swanson RA. 2001. Astrocytes protect neurons from nitric oxide toxicity by a glutathione-dependent mechanism. J Neurochem 77:1601-10.

Chrissobolis S, Faraci FM. 2008. The role of oxidative stress and NADPH oxidase in cerebrovascular disease. Trends Mol Med 14:495-502.

Christopherson KS, Ullian EM, Stokes CC, Mullowney CE, Hell JW, Agah A, Lawler J, Mosher DF, Bornstein P, Barres BA. 2005. Thrombospondins are astrocyte-secreted proteins that promote CNS synaptogenesis. Cell 120:421-33.

Chung WS, Allen NJ, Eroglu C. 2015. Astrocytes Control Synapse Formation, Function, and Elimination. Cold Spring Harb Perspect Biol 7.

Chung WS, Clarke LE, Wang GX, Stafford BK, Sher A, Chakraborty C, Joung J, Foo LC, Thompson A, Chen C and others. 2013. Astrocytes mediate synapse elimination through MEGF10 and MERTK pathways. Nature 504:394-400.

Faissner A, Pyka M, Geissler M, Sobik T, Frischknecht R, Gundelfinger ED, Seidenbecher C. 2010. Contributions of astrocytes to synapse formation and maturation - Potential functions of the perisynaptic extracellular matrix. Brain Res Rev 63:26-38.

Gao HM, Zhou H, Hong JS. 2012. NADPH oxidases: novel therapeutic targets for neurodegenerative diseases. Trends Pharmacol Sci 33:295-303.

Hirrlinger J, Hulsmann S, Kirchhoff F. 2004. Astroglial processes show spontaneous motility at active synaptic terminals in situ. Eur J Neurosci 20:2235-9.

Kaji Y, Usui T, Ishida S, Yamashiro K, Moore TC, Moore J, Yamamoto Y, Yamamoto H, Adamis AP. 2007. Inhibition of diabetic leukostasis and blood-retinal barrier breakdown with a soluble form of a receptor for advanced glycation end products. Invest Ophthalmol Vis Sci 48:858-65.

Kim BJ, Braun TA, Wordinger RJ, Clark AF. 2013. Progressive morphological changes and impaired retinal function associated with temporal regulation of gene expression after retinal ischemia/reperfusion injury in mice. Mol Neurodegener 8:21.

Lipton P. 1999. Ischemic cell death in brain neurons. Physiol Rev 79:1431-568.

Luo X, Weber GA, Zheng J, Gendelman HE, Ikezu T. 2003. C1q-calreticulin induced oxidative neurotoxicity: relevance for the neuropathogenesis of Alzheimer's disease. J Neuroimmunol 135:62-71.

Lyman M, Lloyd DG, Ji X, Vizcaychipi MP, Ma D. 2014. Neuroinflammation: the role and consequences. Neurosci Res 79:1-12.

Mack WJ, Sughrue ME, Ducruet AF, Mocco J, Sosunov SA, Hassid BG, Silverberg JZ, Ten VS, Pinsky DJ, Connolly ES, Jr. 2006. Temporal pattern of C1q deposition after transient focal cerebral ischemia. J Neurosci Res 83:883-9.

Manzanero S, Santro T, Arumugam TV. 2013. Neuronal oxidative stress in acute ischemic stroke: sources and contribution to cell injury. Neurochem Int 62:712-8.

Murai KK, Nguyen LN, Irie F, Yamaguchi Y, Pasquale EB. 2003. Control of hippocampal dendritic spine morphology through ephrin-A3/EphA4 signaling. Nat Neurosci 6:153-60.

Nayernia Z, Jaquet V, Krause KH. 2014. New insights on NOX enzymes in the central nervous system. Antioxid Redox Signal 20:2815-37.

Neufeld AH, Kawai S, Das S, Vora S, Gachie E, Connor JR, Manning PT. 2002. Loss of retinal ganglion cells following retinal ischemia: the role of inducible nitric oxide synthase. Exp Eye Res 75:521-8.

Niatsetskaya ZV, Sosunov SA, Matsiukevich D, Utkina-Sosunova IV, Ratner VI, Starkov AA, Ten VS. 2012. The oxygen free radicals originating from mitochondrial complex I contribute to oxidative brain injury following hypoxia-ischemia in neonatal mice. J Neurosci 32:3235-44.

Orsini F, De Blasio D, Zangari R, Zanier ER, De Simoni MG. 2014. Versatility of the complement system in neuroinflammation, neurodegeneration and brain homeostasis. Front Cell Neurosci 8:380.

Osborne NN, Casson RJ, Wood JP, Chidlow G, Graham M, Melena J. 2004. Retinal ischemia: mechanisms of damage and potential therapeutic strategies. Prog Retin Eye Res 23:91-147.

Pekny M, Pekna M. 2004. Astrocyte intermediate filaments in CNS pathologies and regeneration. J Pathol 204:428-37.

Pekny M, Pekna M. 2014. Astrocyte reactivity and reactive astrogliosis: costs and benefits. Physiol Rev 94:1077-98.

Pekny M, Wilhelmsson U, Pekna M. 2014. The dual role of astrocyte activation and reactive gliosis. Neurosci Lett 565:30-8.

Qin L, Liu Y, Cooper C, Liu B, Wilson B, Hong JS. 2002. Microglia enhance beta-amyloid peptide-induced toxicity in cortical and mesencephalic neurons by producing reactive oxygen species. J Neurochem 83:973-83.

Qin L, Liu Y, Wang T, Wei SJ, Block ML, Wilson B, Liu B, Hong JS. 2004. NADPH oxidase mediates lipopolysaccharide-induced neurotoxicity and proinflammatory gene expression in activated microglia. J Biol Chem 279:1415-21.

Ruiz S, Henschen-Edman AH, Tenner AJ. 1995. Localization of the site on the complement component C1q required for the stimulation of neutrophil superoxide production. J Biol Chem 270:30627-34.

Schafer MK, Schwaeble WJ, Post C, Salvati P, Calabresi M, Sim RB, Petry F, Loos M, Weihe E. 2000. Complement C1q is dramatically up-regulated in brain microglia in response to transient global cerebral ischemia. J Immunol 164:5446-52.

Shih AY, Johnson DA, Wong G, Kraft AD, Jiang L, Erb H, Johnson JA, Murphy TH. 2003. Coordinate regulation of glutathione biosynthesis and release by Nrf2-expressing glia potently protects neurons from oxidative stress. J Neurosci 23:3394-406.

Sorce S, Krause KH. 2009. NOX enzymes in the central nervous system: from signaling to disease. Antioxid Redox Signal 11:2481-504.

Soto I, Howell GR. 2014. The complex role of neuroinflammation in glaucoma. Cold Spring Harb Perspect Med 4.

Stevens B, Allen NJ, Vazquez LE, Howell GR, Christopherson KS, Nouri N, Micheva KD, Mehalow AK, Huberman AD, Stafford B and others. 2007. The classical complement cascade mediates CNS synapse elimination. Cell 131:1164-78.

Ten VS, Yao J, Ratner V, Sosunov S, Fraser DA, Botto M, Sivasankar B, Morgan BP, Silverstein S, Stark R and others. 2010. Complement component c1q mediates mitochondria-driven oxidative stress in neonatal hypoxic-ischemic brain injury. J Neurosci 30:2077-87.

Tenner AJ. 1998. C1q receptors: regulating specific functions of phagocytic cells. Immunobiology 199:250-64.

Tsujikawa A, Ogura Y, Hiroshiba N, Miyamoto K, Kiryu J, Tojo SJ, Miyasaka M, Honda Y. 1999. Retinal ischemia-reperfusion injury attenuated by blocking of adhesion molecules of vascular endothelium. Invest Ophthalmol Vis Sci 40:1183-90.

Ullian EM, Sapperstein SK, Christopherson KS, Barres BA. 2001. Control of synapse number by glia. Science 291:657-61.

Vallet P, Charnay Y, Steger K, Ogier-Denis E, Kovari E, Herrmann F, Michel JP, Szanto I. 2005. Neuronal expression of the NADPH oxidase NOX4, and its regulation in mouse experimental brain ischemia. Neuroscience 132:233-8.

Wang T, Qin L, Liu B, Liu Y, Wilson B, Eling TE, Langenbach R, Taniura S, Hong JS. 2004. Role of reactive oxygen species in LPS-induced production of prostaglandin E2 in microglia. J Neurochem 88:939-47.

Yamanaka K, Chun SJ, Boillee S, Fujimori-Tonou N, Yamashita H, Gutmann DH, Takahashi R, Misawa H, Cleveland DW. 2008. Astrocytes as determinants of disease progression in inherited amyotrophic lateral sclerosis. Nat Neurosci 11:251-3.

Yokota H, Narayanan SP, Zhang W, Liu H, Rojas M, Xu Z, Lemtalsi T, Nagaoka T, Yoshida A, Brooks SE and others. 2011. Neuroprotection from retinal ischemia/reperfusion injury by NOX2 NADPH oxidase deletion. Invest Ophthalmol Vis Sci 52:8123-31.

Zhang W, Wang T, Pei Z, Miller DS, Wu X, Block ML, Wilson B, Zhang W, Zhou Y, Hong JS and others. 2005. Aggregated alpha-synuclein activates microglia: a process leading to disease progression in Parkinson's disease. FASEB J 19:533-42.